# 4. 인플레이션: 우주배경복사

최 기 영

한국천문연구원
Korea Astronomy & Space Science Institute

Open KIAS

Pyeong-Chang Summer Institute 2014

Alpensia Resort, August 24 - 30, 2014

- 우주속 물질 상태의 진화

atom, molecule
neucleus
electron

??????? → Inflation → 매우 뜨거운

쿼크, 글루온, 전자의 플라즈마

열적평형 상태

Quark-hadron transition

양성자, 중성자, 전자의 플라즈마

BBN

매우 차가운 거대 구조 형성

은하,은하단

Gas

Recombination, photon decoupling : CMB

물질지배

복사지배

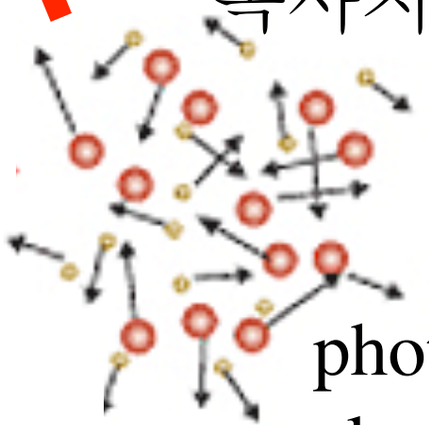

photons, electrons, light nuclei

물질의 상태

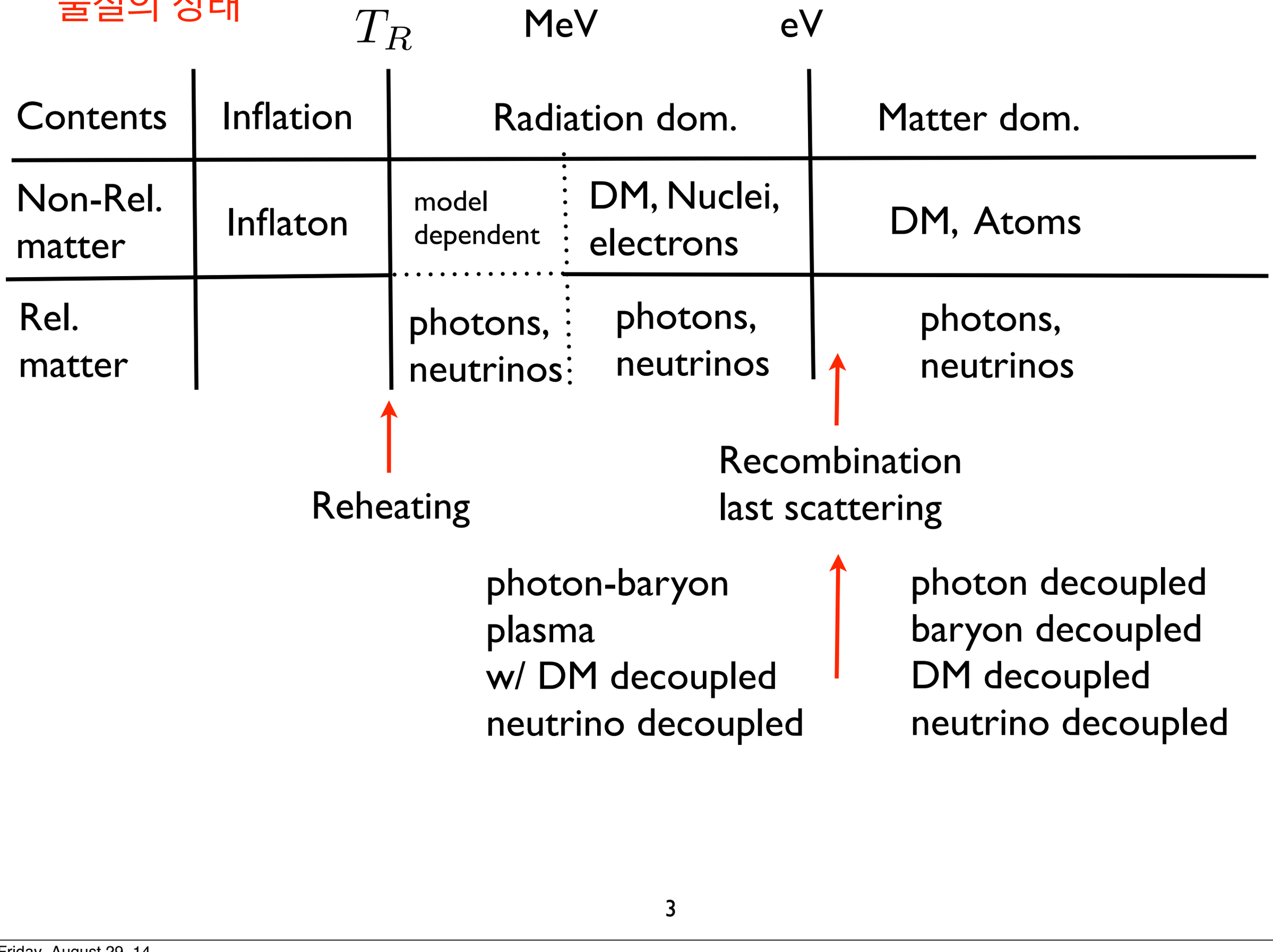
$T_R$
MeV
eV
Contents
Inflation
Radiation dom.
Matter dom.
Non-Rel. matter
Inflaton
model dependent
DM, Nuclei, electrons
DM, Atoms
Rel. matter
photons, neutrinos
photons, neutrinos
photons, neutrinos
Reheating
Recombination
last scattering
photon-baryon plasma w/ DM decoupled neutrino decoupled
photon decoupled baryon decoupled DM decoupled neutrino decoupled

# Evolution in the big bang cosmology

| | Inflation | RD | MD | DE |
|---|---|---|---|---|
| $\rho$ | const | $R^{-4}$ | $R^{-3}$ | const |
| $R(t)$ | $\exp(Ht)$ | $t^{1/2}$ | $t^{2/3}$ | $\exp(Ht)$ |
| $H^{-1}$ | const | $2t$ | $\frac{3}{2}t$ | const |

## Scale

### Comoving scale, Physical scale

$$\lambda \equiv \frac{2\pi}{k}, \quad \lambda_{\rm phys} = R(t)\lambda$$

### Comoving mode, Physical mode

$$k = \frac{2\pi}{\lambda}, \qquad k_{\rm phys} = \frac{2\pi}{\lambda_{\rm phys}} = R^{-1}k$$

## Hubble scale

### Comoving scale, Physical scale

$$R^{-1}H^{-1} \qquad H^{-1}$$

### Comoving mode, Physical mode

$$2\pi(RH) \qquad 2\pi H$$

# Horizon exit and reentry: physical scale

$$\lambda \equiv \frac{2\pi}{k}, \quad \lambda_{\rm phys} = R(t)\lambda$$

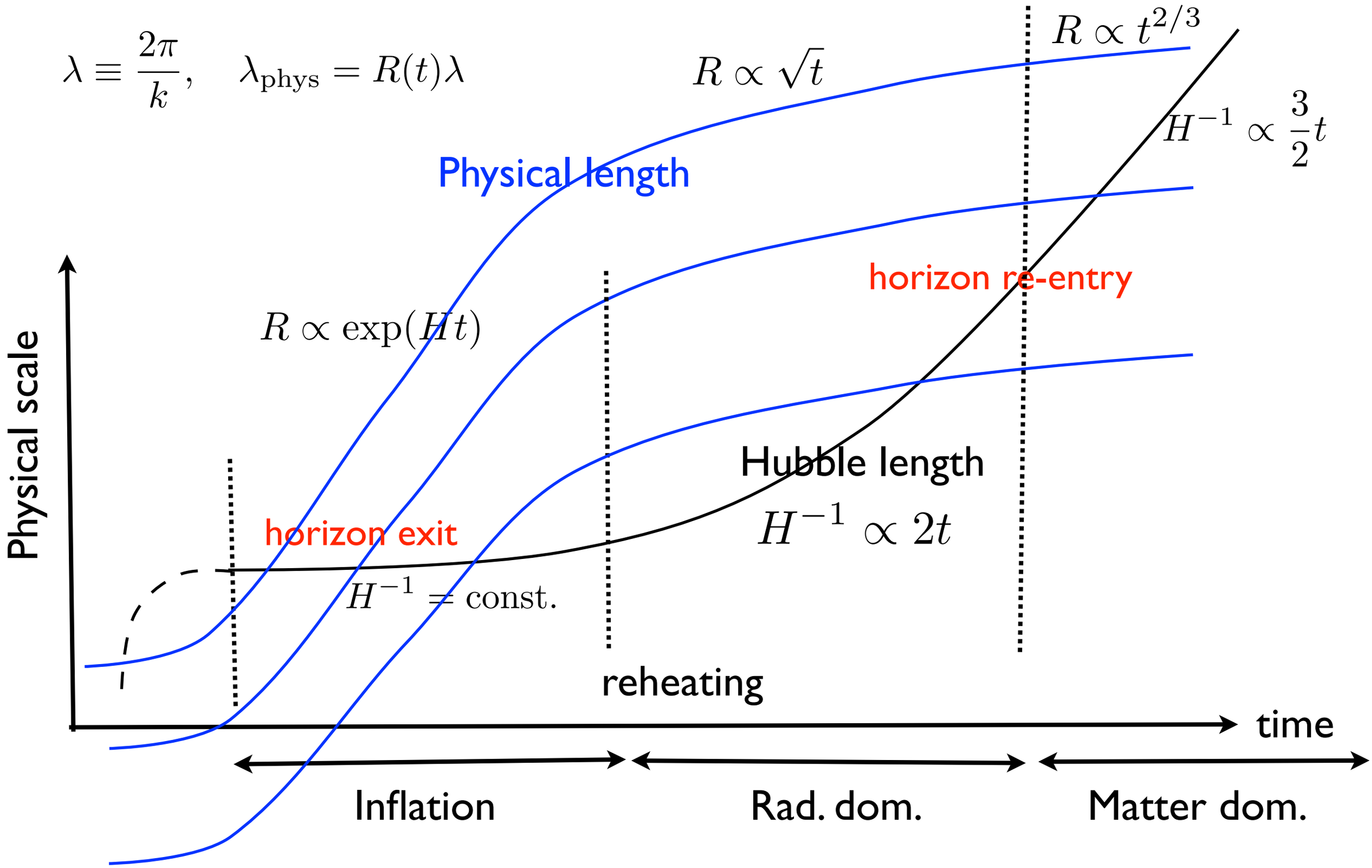

## The scale and the horizon entry

The small scale enters the horizon earlier.

At a given time, a mode in super-horizon

$$\lambda \gg (aH)^{-1} \qquad \lambda_{\rm phys} \gg H^{-1}$$

$$k \ll aH \qquad ka^{-1} \ll H^{-1}$$

At a given time, a mode in sub-horizon

$$k \gg aH \qquad \lambda_{\rm phys} \ll H^{-1}$$

# 왜 인플레이션이 필요한가?

Flatness problem, horizon problem, Monopole problem, …

우주의 급격한 팽창과 재가열에 의하여 위의 모든 것을 설명

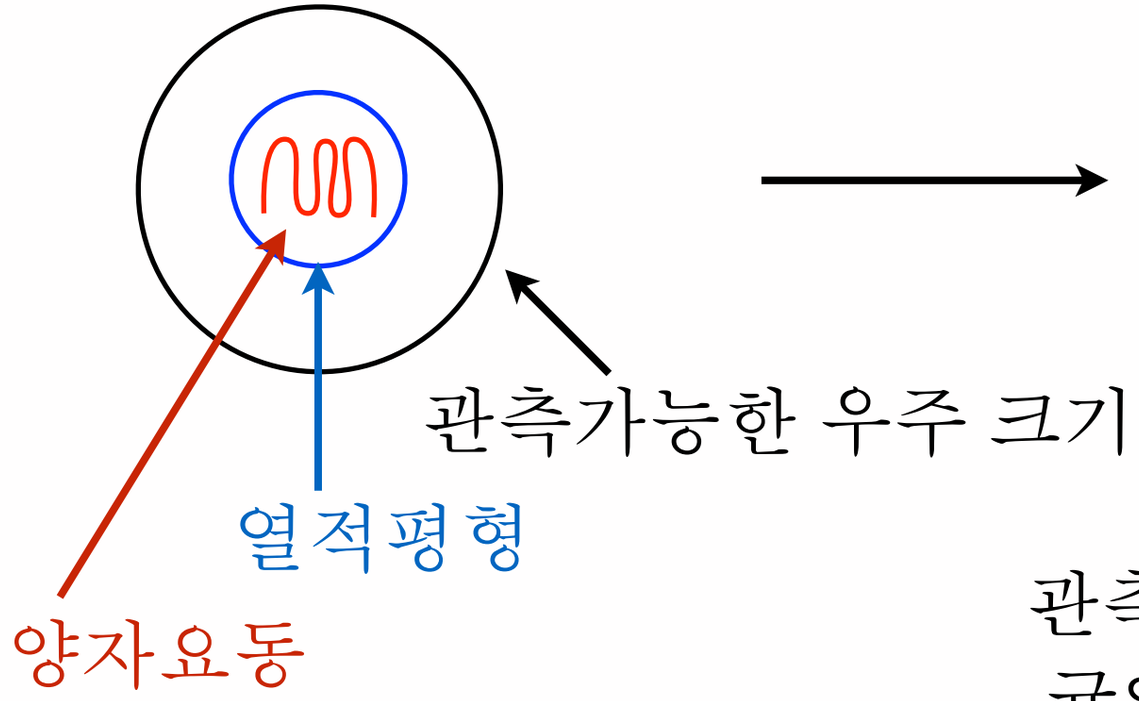


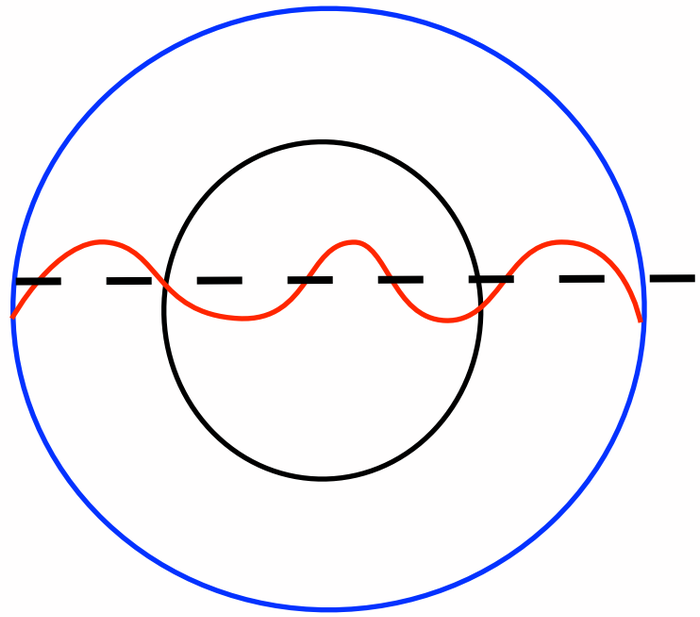

관측가능한 우주내에서 물질의 분포는
균일, 등방적으로 보인다.

하지만 양자요동에 해당하는
비균일한 분포가 존재한다.

- Inflation

The small fluctuation in the density?

Inflation, also can explain the origin of the large scale structure of the Universe. The quantum fluctuations in the microscopic inflationary region is magnified to cosmic size and become the seeds of the growth of structure in the Universe.

A massless scalar field acquires a perturbation and freezes in after horizon exit

$\delta\phi_k = \frac{i}{\sqrt{2k}}\frac{H}{k}$ with almost Gaussian distribution. It gives a power spectrum

$\mathcal{P}_{\delta\phi}(k) = \left(\frac{H_k}{2\pi}\right)^2$ defined by $\langle \delta\phi_{\mathrm{k}} \delta\phi_{\mathrm{k}'} \rangle = \frac{2\pi^2}{k^3}\mathcal{P}_{\delta\phi}(k)\delta^3(\mathbf{k}+\mathbf{k}')$

[Mukhanov, Chibisov, 1981]

Size of the Hubble expansion during inflation

$$h \equiv h^+, h^\times$$

Tensor spectrum : the power spectrum for the two polarization modes

$$\langle h_{\mathbf{k}} h_{\mathbf{k}'} \rangle = (2\pi)^3 \, \delta(\mathbf{k} + \mathbf{k}') \, P_h(k) \,, \qquad \mathcal{P}_h = \frac{k^3}{2\pi^2} P_h(k)$$

We define the tensor power spectrum as the sum of the power spectra for the two polarizations

$$\mathcal{P}_t = 2\mathcal{P}_h \qquad \mathcal{P}_t = \frac{H^2}{M_P^2 \pi^2}$$

Tensor spectral index

$$n_t \equiv \frac{d \ln \mathcal{P}_t}{d \ln k}$$

The tensor power spectrum can be written as

$$\mathcal{P}_t(k) = A_t(k_*) \left( \frac{k}{k_*} \right)^{n_t(k_*)}$$

Curvature perturbation: $\zeta(\mathbf{x}) = \int \zeta_{\mathbf{k}} e^{i\mathbf{kx}} \frac{d^3k}{(2\pi)^{3/2}}$

$\langle \cdots \rangle$
: ensemble average
of fluctuations

Power spectrum : size of perturbation

$$\langle \zeta(\mathbf{k_1})\zeta(\mathbf{k_2}) \rangle = (2\pi)^3 P(k_1)\delta^3(\mathbf{k_1}+\mathbf{k_2})$$

$$= (2\pi)^3 \frac{2\pi^2}{k_1^3}\mathcal{P}(k_1)\delta^3(\mathbf{k_1}+\mathbf{k_2})$$

$$\int \frac{\mathrm{d}^3\mathrm{k}}{(2\pi)^3} P_\zeta(k) = \int \mathcal{P}_\zeta(k)\,\mathrm{d}\,\mathrm{logk}$$

$$\mathcal{P}(k) = \frac{k^3}{2\pi^2}P(k)$$

Scalar spectral index

$$n_s - 1 \equiv \frac{d\ln\mathcal{P}}{d\ln k}$$

$$\mathcal{P}_\zeta = \frac{H^2}{8\pi^2\epsilon M_P^2}$$

Running of spectral index

$$\alpha_s \equiv \frac{dn_\zeta}{d\ln k}$$

Approximation by a power law around pivot scale $k_*$

$$\mathcal{P}(k) = A_s \left(\frac{k}{k_*}\right)^{n_s(k_*)-1+\frac{1}{2}\alpha_s(k_*)\ln(k/k_*)}$$

- Origin of the primordial curvature perturbation : Inflation

Inflation → Radiation dominated era → CMB

$\delta\phi$

quantum fluctuation of a light scalar field

$\zeta$

$$\frac{\Delta T}{T} \sim 10^{-5}$$

anisotropy in CMB

$$\zeta = -\psi - H\frac{\delta\rho}{\dot{\rho}}$$

$$\delta\rho \simeq \frac{dV}{d\phi}\delta\phi$$

curvature perturbation
: conserved outside horizon
if $p = p(\rho)$

[Lyth, Malik, Sasaki, 2005]

$$\frac{\Delta T}{T} = -\frac{1}{5}\zeta \quad \text{(SW limit)}$$

If not, it can be changed
eg, multi-field

[Planck, 2013]

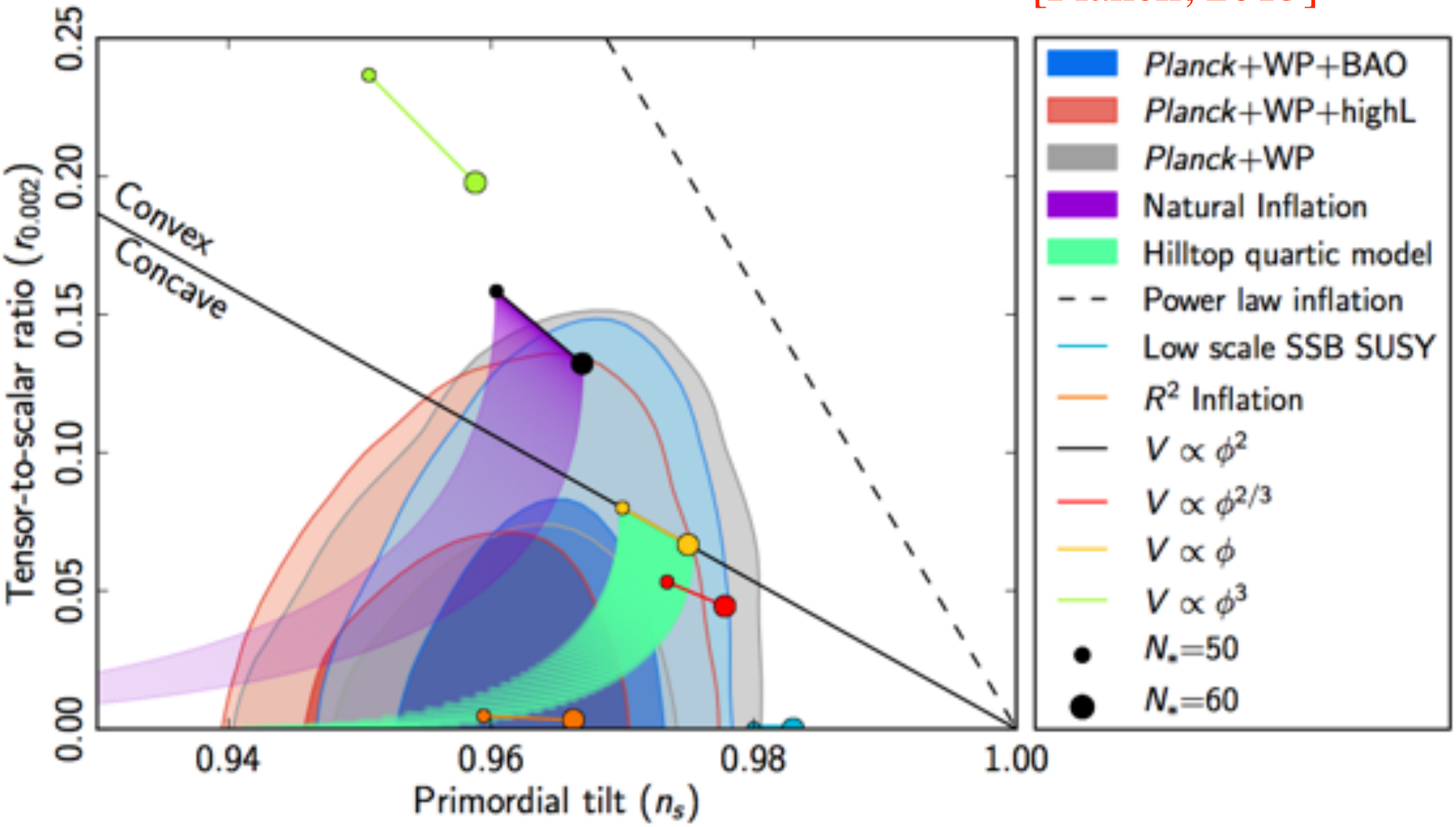
Tensor-to-scalar ratio ($r_{0.002}$)
0.25
0.20
0.15
0.10
0.05
0.00
Convex
Concave
0.94
0.96
0.98
1.00
Primordial tilt ($n_s$)
*Planck*+WP+BAO
*Planck*+WP+highL
*Planck*+WP
Natural Inflation
Hilltop quartic model
Power law inflation
Low scale SSB SUSY
$R^2$ Inflation
$V \propto \phi^2$
$V \propto \phi^{2/3}$
$V \propto \phi$
$V \propto \phi^3$
$N_*$=50
$N_*$=60

# Perturbation equations

아인슈타인 방정식 $G_{\mu\nu} = \frac{8\pi G}{c^4} T_{\mu\nu}$

시공간의 구조와 물질밀도를 연결시키는 방정식

인플레이션기간동안 인플라톤 입자의 양자요동은 시공간의 요동을 일으킨다. (스칼라, 텐서 요동)

Metric perturbation

$$ds^2 = (1+2\phi)dt^2 - a^2[(1-2\psi)\delta_{ij} - h_{ij}]dx^i dx^j$$

스칼라 요동

밀도 섭동

$\delta\rho(t, \mathbf{x})$

텐서 요동

traceless, transverse $h^i_i = 0, \quad h^i_{j,i} = 0,$

중력파 생성

Then the linear order Einstein equation $\overline{\delta G}^{\alpha}_{\beta} = 8\pi G \overline{\delta T}^{\alpha}_{\beta}$. gives perturbation equations.

Scalar perturbations

$$\Delta\Psi - 3\mathcal{H}\left(\Psi' + \mathcal{H}\Phi\right) = 4\pi G a^2 \overline{\delta T}^{0}_{0},$$

$$\left(\Psi' + \mathcal{H}\Phi\right)_{,i} = 4\pi G a^2 \overline{\delta T}^{0}_{i},$$

$$\left[\Psi'' + \mathcal{H}(2\Psi + \Phi)' + \left(2\mathcal{H}' + \mathcal{H}^2\right)\Phi + \tfrac{1}{2}\Delta(\Phi - \Psi)\right]\delta_{ij} - \tfrac{1}{2}(\Phi - \Psi)_{,ij} = -4\pi G a^2 \overline{\delta T}^{i}_{j}.$$

Vector perturbations

$$\Delta \overline{V}_i = 16\pi G a^2 \overline{\delta T}^{0}_{i(V)},$$

$$\left(\overline{V}_{i,j} + \overline{V}_{j,i}\right)' + 2\mathcal{H}\left(\overline{V}_{i,j} + \overline{V}_{j,i}\right) = -16\pi G a^2 \overline{\delta T}^{i}_{j(V)},$$

Tensor perturbations

$$\left(h''_{ij} + 2\mathcal{H}h'_{ij} - \Delta h_{ij}\right) = 16\pi G a^2 \overline{\delta T}^{i}_{j(T)},$$

We want to solve the equations for

$$\Psi,\ \Phi,\ h,\ \delta\rho,\ \delta p$$

photon, baryon, DM, neutrino

Initial conditions

given by the value from inflation at around the horizon exit.
They are constant on superhorizon scale and evolve when the scale enters the horizon.

## Tensor perturbations

$$\left(h''_{ij} + 2\mathcal{H}h'_{ij} - \Delta h_{ij}\right) = 16\pi G a^2 \overline{\delta T}^{i}_{j(T)}, \qquad = 0$$

for a perfect fluid

With Fourier transform, for each mode,

with $h_{ij} = \frac{v}{a} e_{ij}$, we can solve $v'' + \left(k^2 - \frac{a''}{a}\right) v = 0.$

then the solution is for RD $a \propto \eta$, and $v \propto \exp(\pm i k \eta)$

$$h_{ij} = \frac{1}{\eta}(C_1 \sin(k\eta) + C_2 \cos(k\eta))\, e_{ij}$$

In superhorizon, $(k\eta \ll 1)$ the amplitude is constant, determined by the value fixed at around horizon exit. $h \propto \frac{v}{a} \sim \frac{e^{-ik\eta} H}{k^{3/2}}$

In the subhorizon, it decreases inverse proportional to the scale factor.

This is in general true independent on the equation of state.

# Scalar perturbation

The growth of the primordial density perturbation in the expanding universe depends on the scale, type of matter and background matter.

Outside horizon : density perturbation $\frac{\delta\rho}{\rho}$ is constant
with adiabatic condition $p = p(\rho)$

Inside horizon : density perturbation grows for larger than Jeans scale and oscillate for smaller scales.

| $\frac{\delta\rho}{\rho} \propto$ | Radiation dom. | Matter dom. |
|---|---|---|
| Non-Rel. matter | $\log a \propto \log t$ | $a \propto t^{2/3}$ |
| Rel. matter | oscillating | oscillating |

$$\zeta = -\Phi - H\frac{\delta\rho}{\rho} \qquad \delta\rho = -2\Phi$$ superhorizon

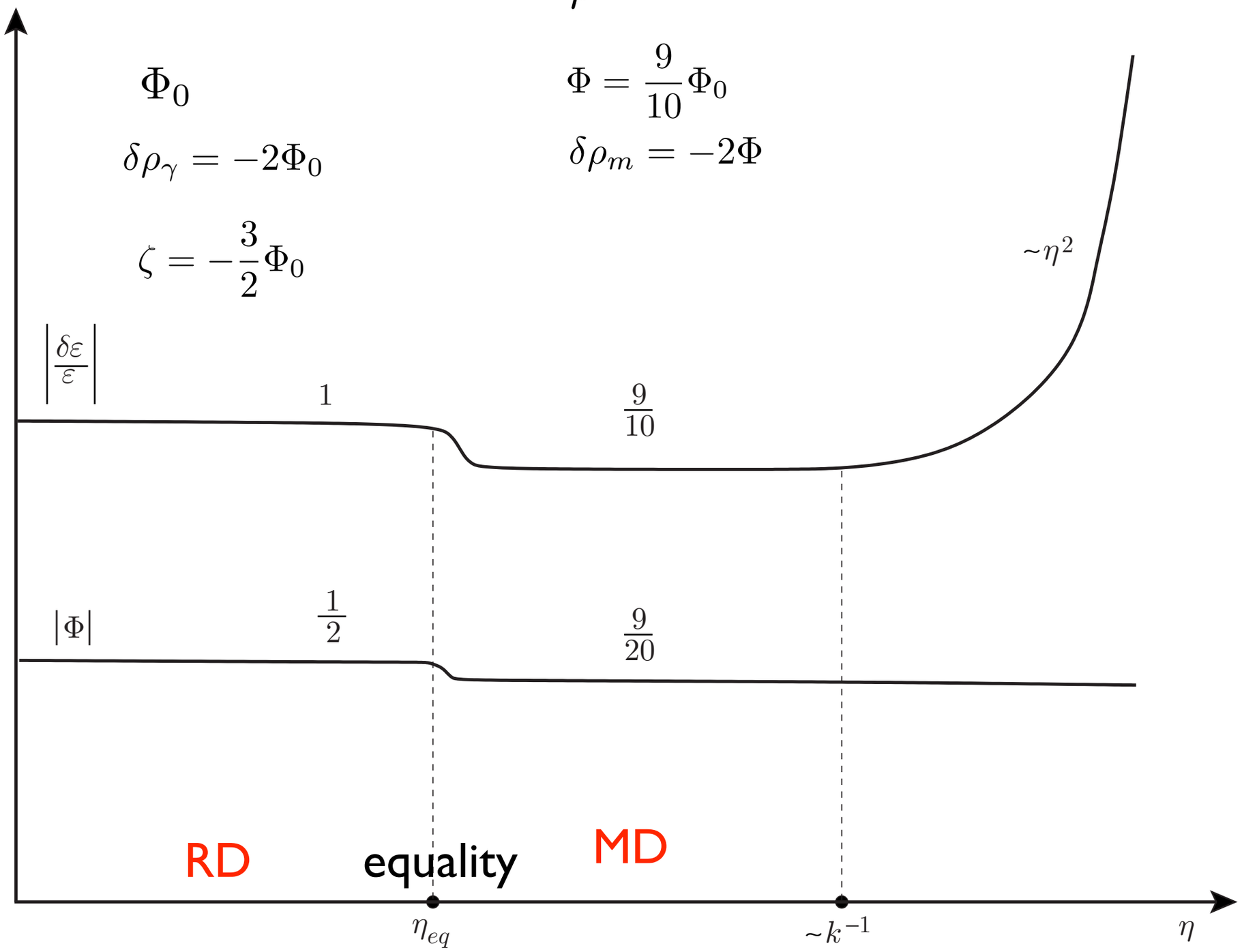


[Mukhanov]

## Baryon-radiation plasma and cold dark matter and CMB anisotropy

Before recombination, baryons are strongly coupled to radiation and the baryon and radiation can be treated as a single fluid.

The other component, dark matter, which is non-relativistic and interact only gravitationally with the baryon-photon plasma.

We assume the perturbation of dark matter and radiation are initially same : adiabatic perturbation.

Evolution of density contrast for a given k mode

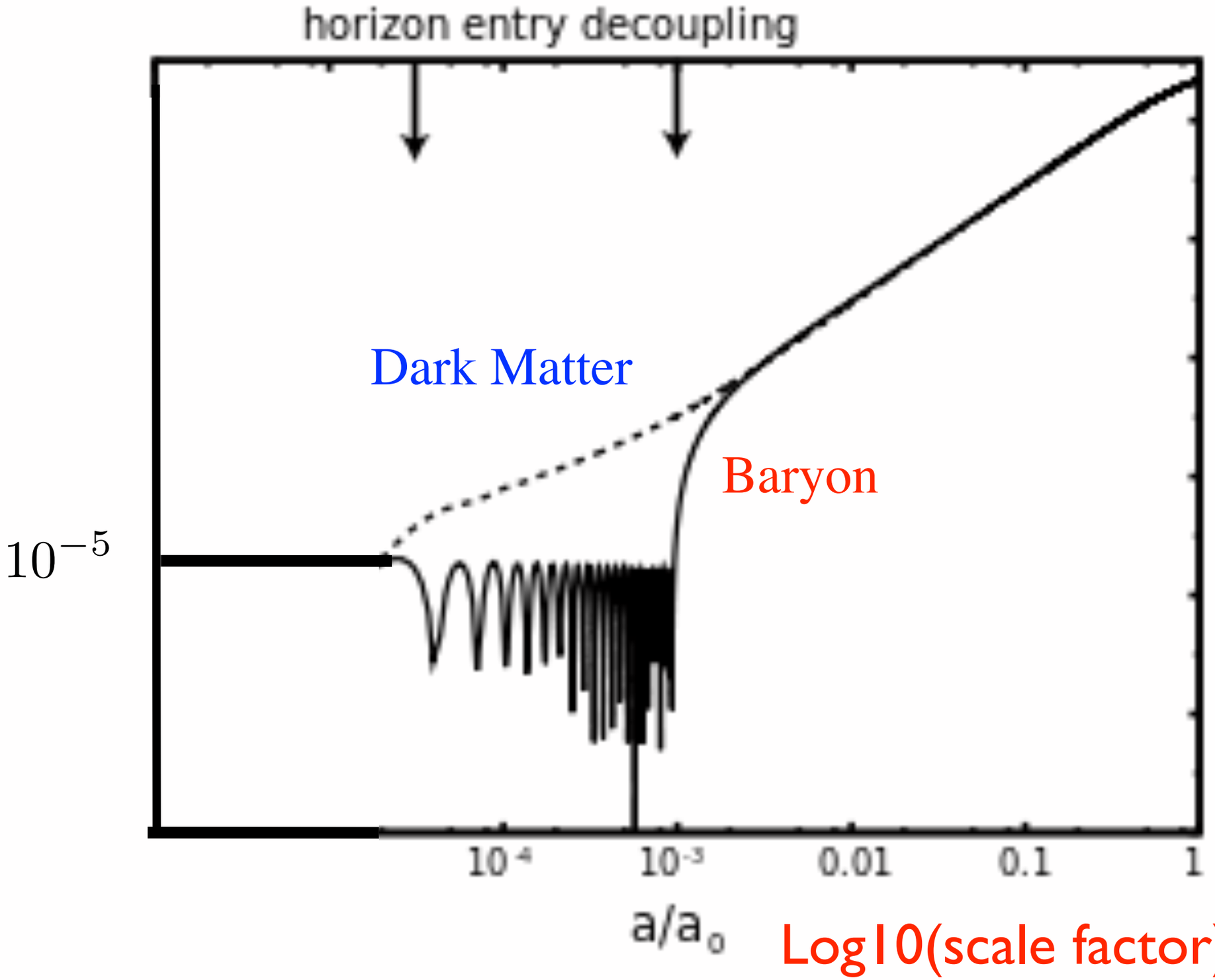

- 물질의 진화 : 우주거대구조의 형성

43Mpc box

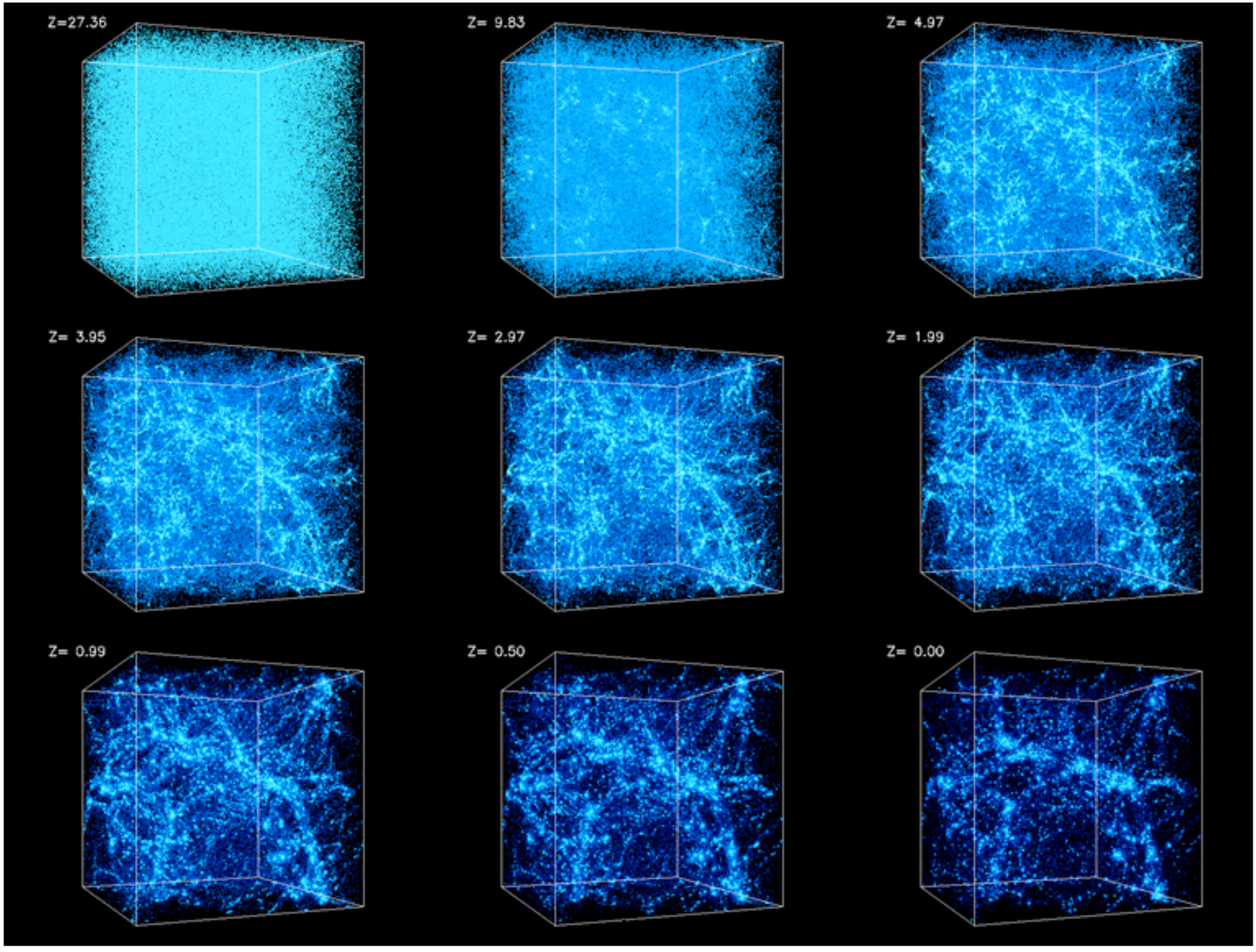

# 우주배경복사의 관측

Monopole
Dipole

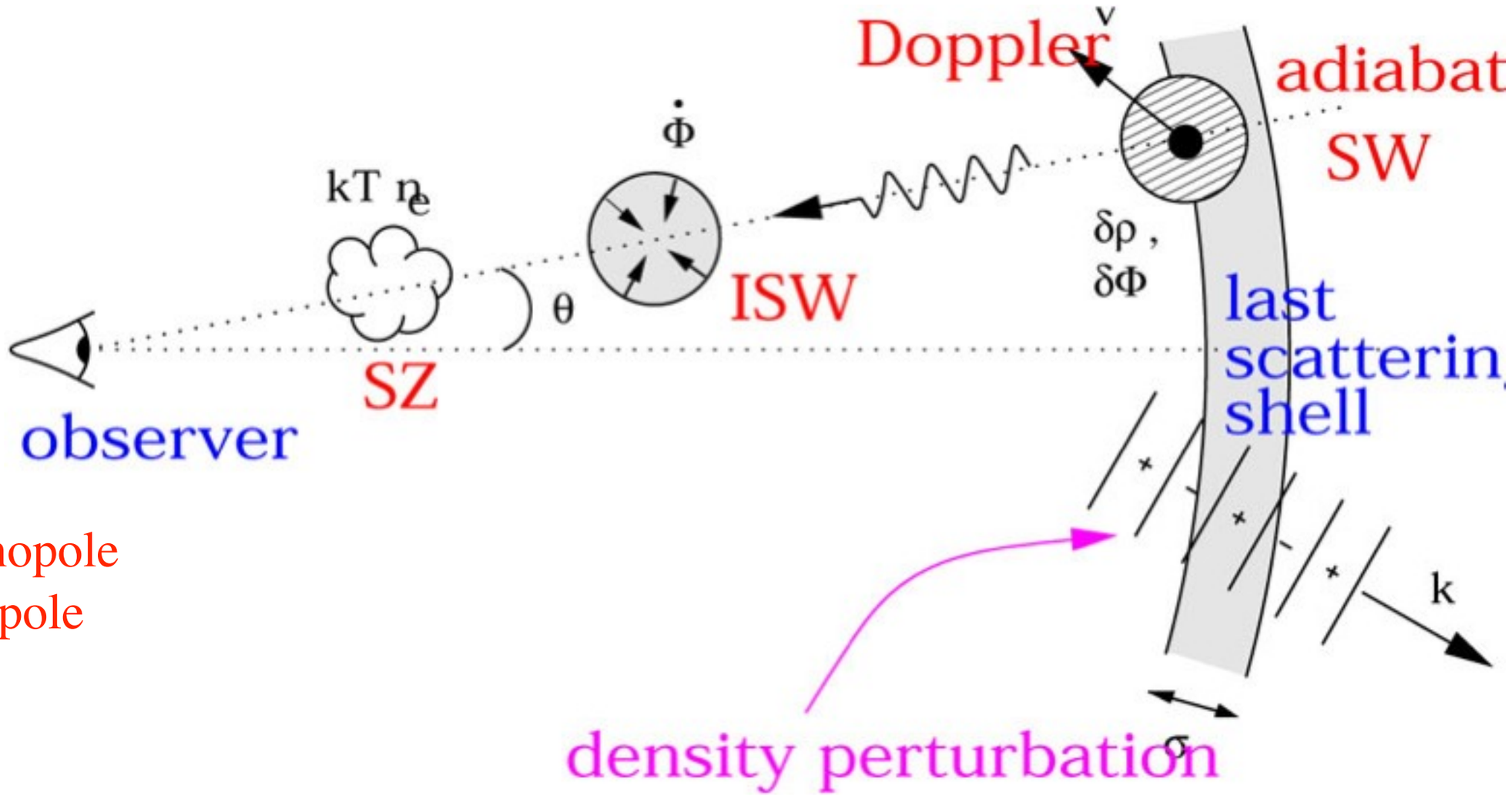

The decoupled photons makes the cosmic microwave background.

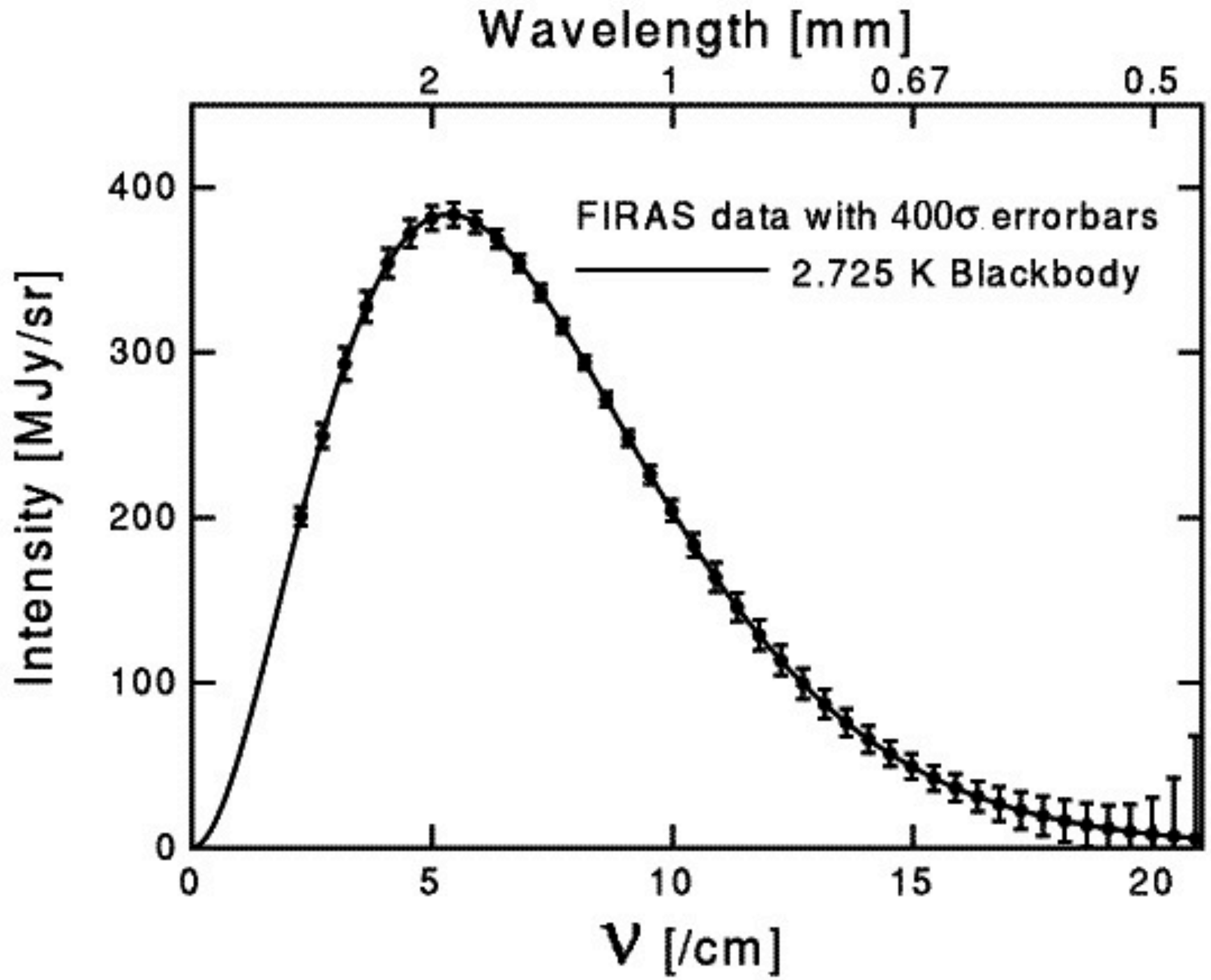

## Anisotropy of CMB

The motion of Earth, scattering of photons by intergalactic electrons in clusters of galaxies, and primordial anisotropy.

## Dipole anisotropy

The photon phase space distribution function is

$$f_\gamma(\mathbf{p}) = \frac{1}{\exp(|\mathbf{p}|/T) - 1}$$

to an observer at rest in the radiation background.

In a frame with velocity with a momentum $\mathbf{p}'$ what is the shape of the distribution function?

For Lorentz transformation, the phase space volume and the number of photons are Lorentz invariant, so

$$f_\gamma(\mathbf{p}') = f_\gamma(\mathbf{p})$$

For example,
moving to first direction, the Lorentz transformation is

$$\begin{pmatrix} |\mathbf{p}| \\ p_1 \\ p_2 \\ p_3 \end{pmatrix} = \begin{pmatrix} \gamma & \beta\gamma & 0 & 0 \\ \beta\gamma & \gamma & 0 & 0 \\ 0 & 0 & 1 & 0 \\ 0 & 0 & 0 & 1 \end{pmatrix} \begin{pmatrix} |\mathbf{p}|' \\ p_1' \\ p_2' \\ p_3' \end{pmatrix} \qquad \gamma \equiv (1-\beta^2)^{-1/2}$$

With angle between $\mathbf{p}'$ and the first axis,

$$|\mathbf{p}| = \gamma \left(1 + \beta \cos\theta\right) |\mathbf{p}'|$$

Then $$f_\gamma(\mathbf{p}') = f_\gamma(\mathbf{p}) = \frac{1}{\exp(|\mathbf{p}|/T) - 1} = \frac{1}{\exp(\gamma(1+\beta\cos\theta)|\mathbf{p}|'/T) - 1}$$
$$= \frac{1}{\exp(|\mathbf{p}'|/T') - 1}$$

where the temperature is a function of the angle between the direction of the photon and the velocity of the earth

$$\boxed{T' = \frac{T}{\gamma(1+\beta\cos\theta)}}$$

$$T' = \frac{T}{\gamma(1+\beta\cos\theta)}$$

The peculiar velocity of galaxy is typically hundred km/sec, so

$\beta \simeq 10^{-3}$ and $\gamma \simeq 1$

The apparent temperature is greatest for $\cos\theta = -1$ and the lowest for opposite direction.

This effect was first seen in 1969 with a ground-based radiometer in the earth equatorial plane. The full velocity was measured in 1977 by Berkeley group by U2 aircraft. COBE satellite improved this greatly. Now the WMAP and Planck satellite gives maximum temperature increase of $3.346 \pm 0.017\,\mathrm{mK}$ in the direction

$$\ell = 263^\circ.85 \pm 0^\circ.1, b = 48^\circ.25 \pm 0^\circ.04.$$

This corresponds to the velocity 370 km/sec.

Expanding in powers of $\beta$ the temperature shift can be expressed as Legendre Polynomials

$$\Delta T \equiv T' - T = T\left[-\frac{\beta^2}{6} - \beta P_1(\cos\theta) + \frac{2\beta^2}{3}P_2(\cos\theta) + \ldots\right]$$

$$P_1(x) = x$$

$$P_2(x) = \frac{1}{2}(3x^2 - 1)$$

Because $\beta = 370 \text{ km/sec}/c = 0.0013$ is small, the temperature shift is primarily dipole and there is small quadrupole contribution.

• Sunyaev-Zeldovich effect : depends on the density of the gas and size (S) of the cluster

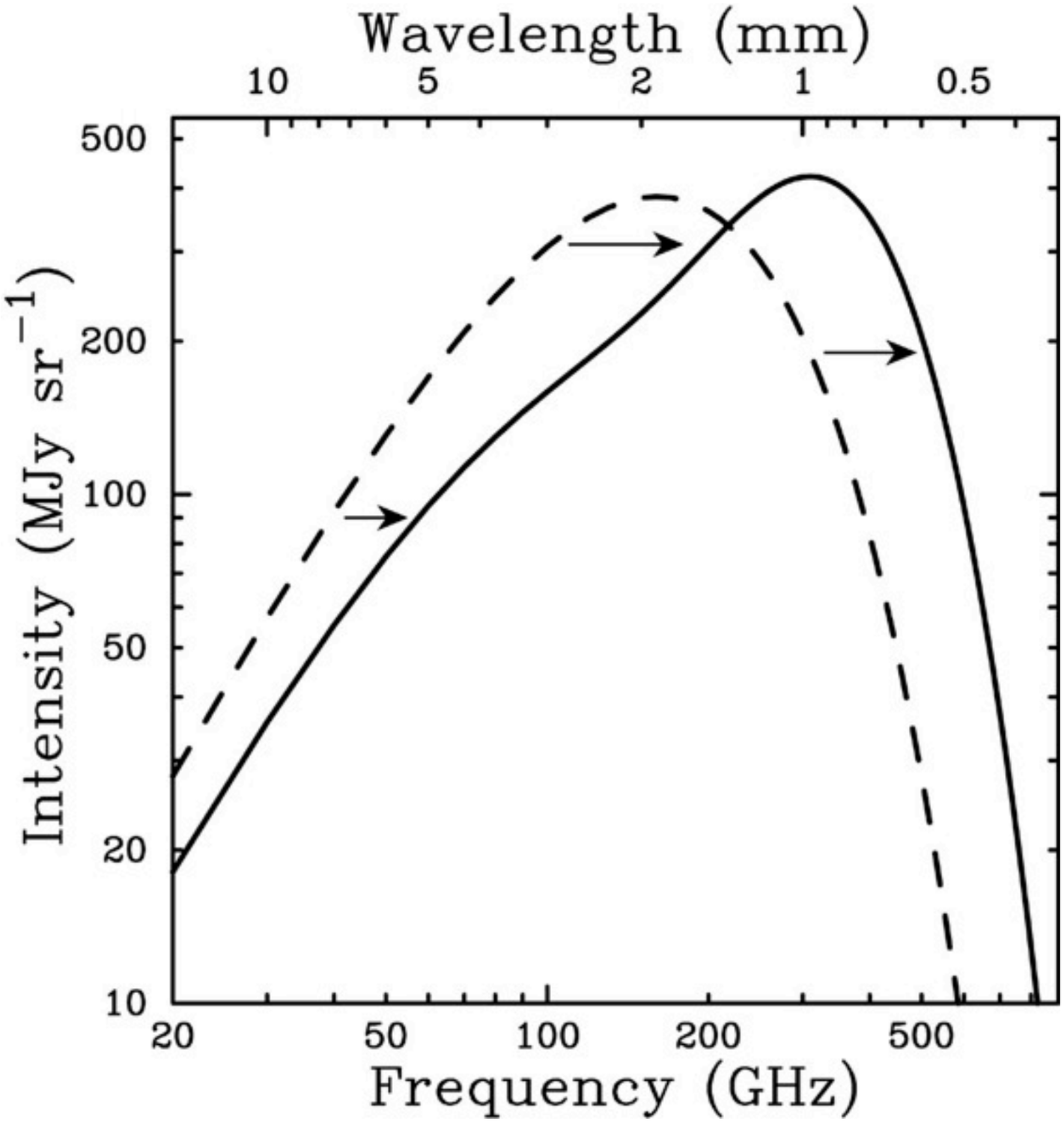


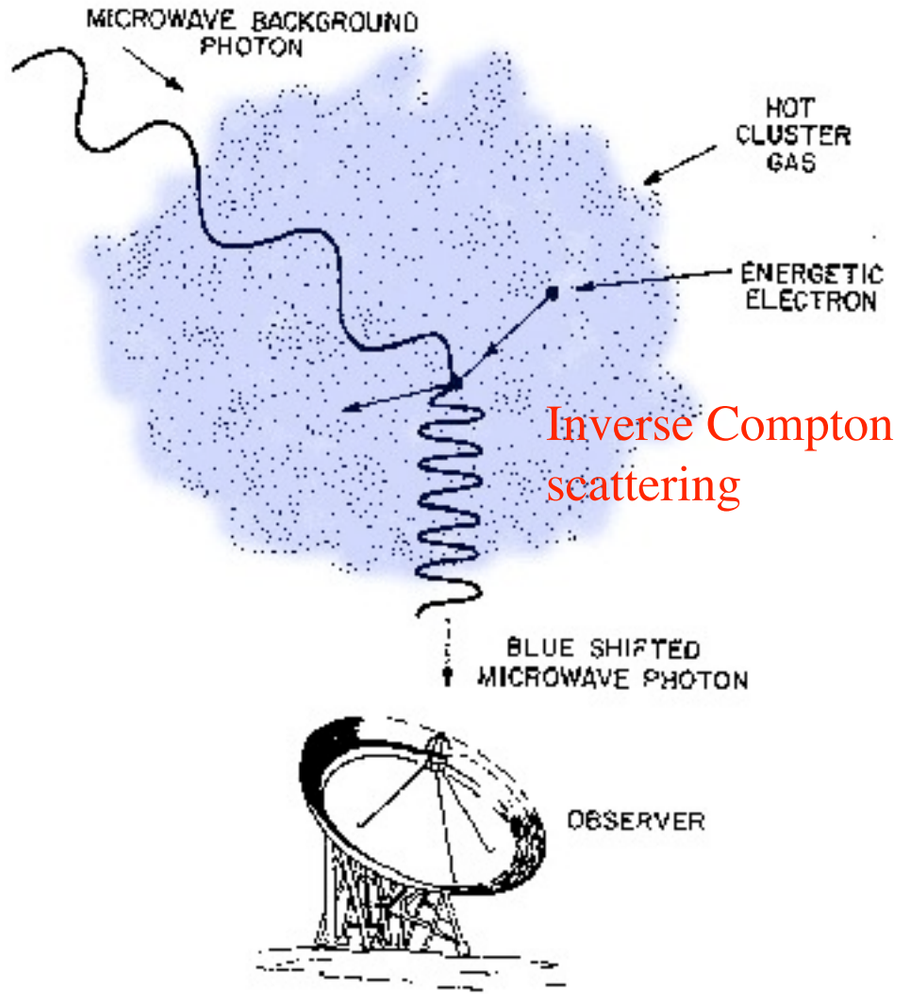


Angular diameter distance :

$$D = \frac{S}{\theta}$$

$S$: cluster size

$\theta$: angular size

# Planck SZ sources

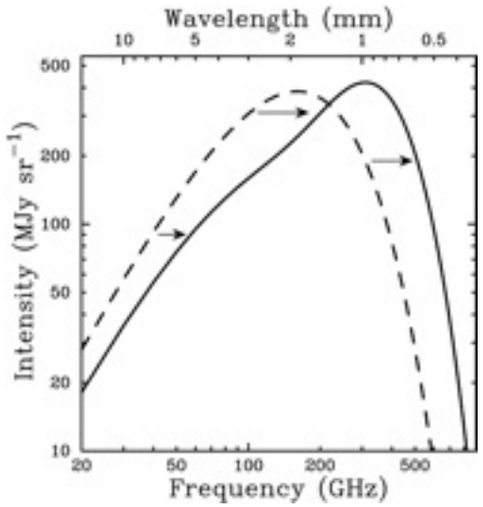


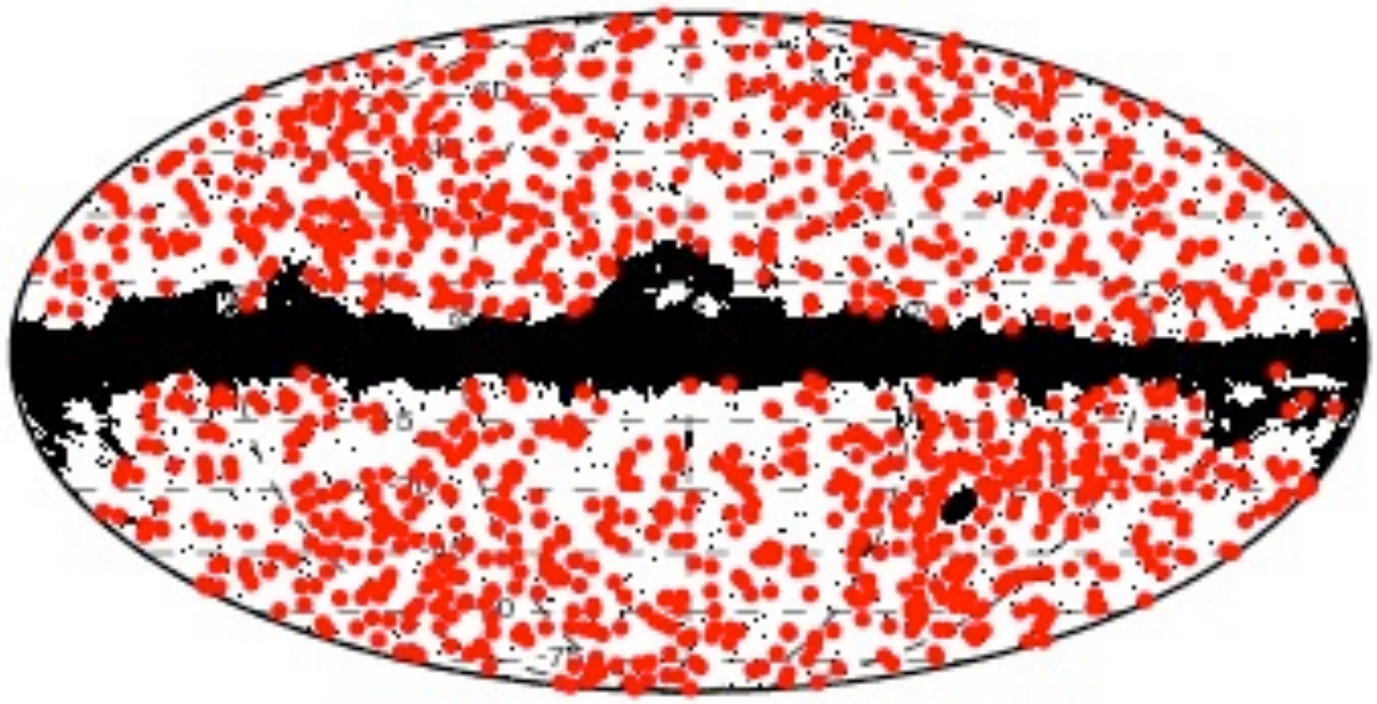

The distribution, shown in Mollweide projection with the Galactic plane horizontal and the Milky Way centre in the middle, of the 1227 \Planck\ clusters and candidates across the sky (red thick dots). The masked point-sources (black thin dots), the Magellanic clouds (large black areas) and the Galactic mask, covering a total of 16.3\% of the sky and used by the SZ-finder algorithms to detect SZ sources, are also shown.

Electromagnetic wave: amplitude and polarization

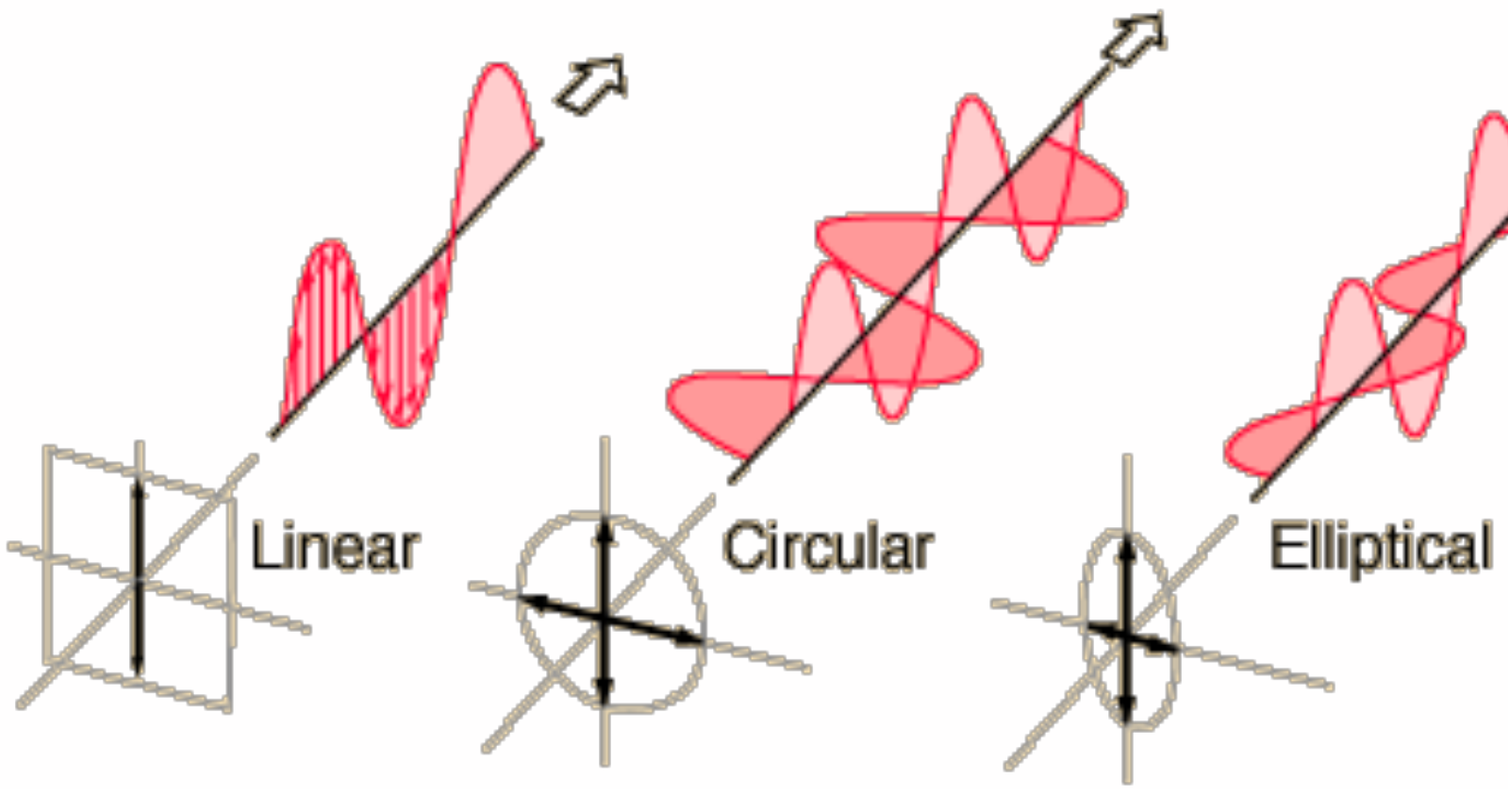

# What they observe?

- Perturbations in the CMB

✦ Temperature perturbation expanded in spherical harmonics

$$\frac{T(\theta,\phi)-T_0}{T_0}=\sum_{l,m} a_{lm}Y^l_m(\theta,\phi)$$

- Radiation power spectrum

$$C_l=\langle|a_{lm}|^2\rangle_{ensemble}$$

- depends on all the cosmological parameters, and can be used to constrain them

✦ Polarization perturbation

- Three additional power spectrum

- Two independent modes of polarization and the cross-correlation between temperature anisotropies and one polarization mode

# CMB temperature shows almost Gaussian distribution

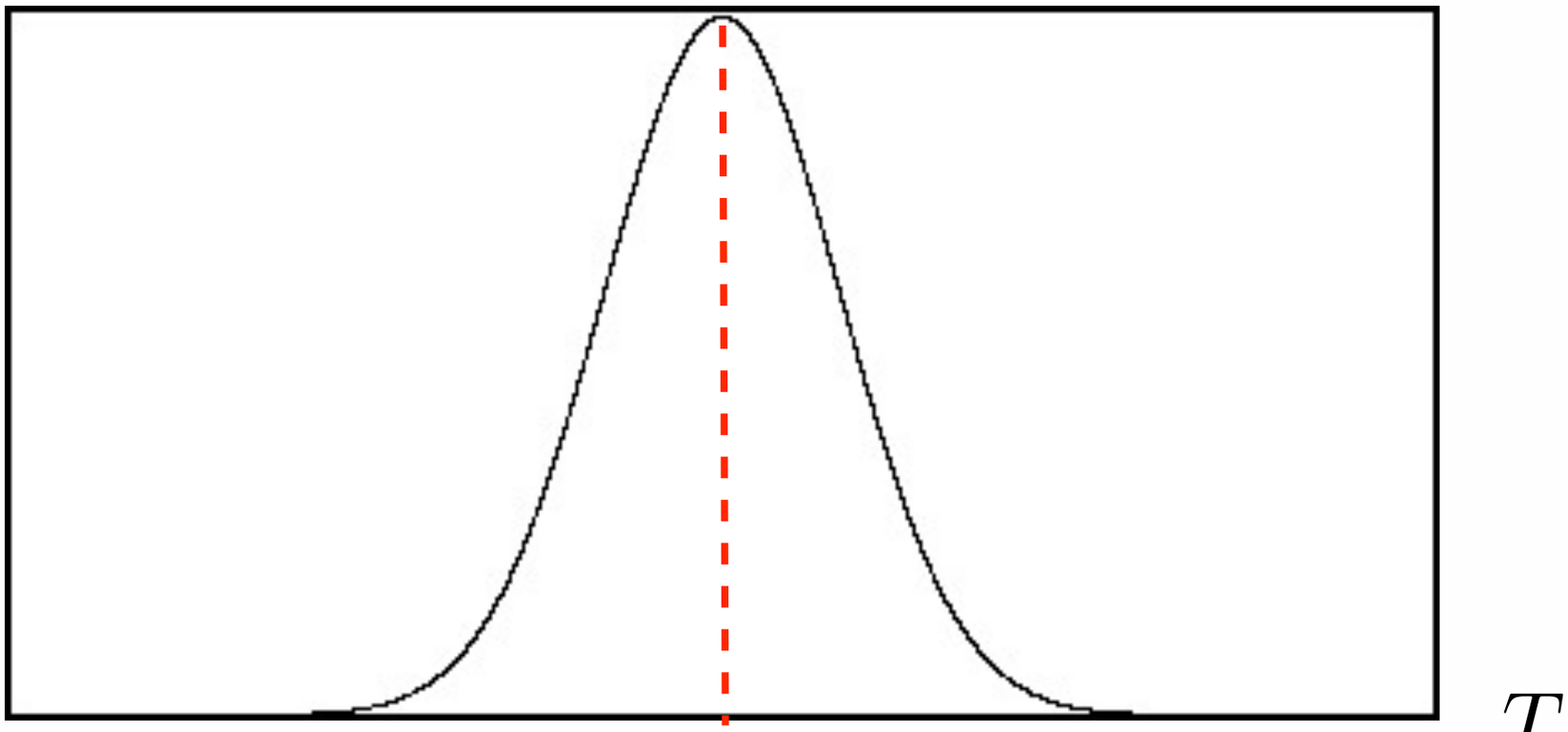


$$\mathrm{T} = 2.725\,\mathrm{K}$$

$$f(x) = \frac{1}{2\pi\sigma^2}\exp\left[-\frac{(x-\langle x\rangle)^2}{2\sigma^2}\right]$$

$\langle x\rangle$ : average, $\sigma^2$ : variance

The temperature anisotropy can be expanded in spherical harmonics:

$$\boxed{\delta T(\theta,\phi) \equiv \sum_{l,m} a_{lm} Y_l^m(\theta,\phi)}$$

where $\delta T(\theta,\phi) \equiv T(\theta,\phi) - T_0, \quad T_0 \equiv \frac{1}{4\pi}\int T(\theta,\phi) d\Omega$

and since $\delta T(\theta,\phi)$ is real, $a^*_{\ell m} = a_{\ell\ -m}$ .

The earth's motion gives dipole contribution. For z-axis along the earth's movement, this dipole contributes to l=1, m=0.

We are concerned only about the averages.

Averages $\langle \cdots \rangle$

1. the average over the possible positions from which the radiation could be observed
2. the average over the historical accidents that produced a particular pattern of fluctuations

Ergodic theorem says these two kinds of the averages are the same.

$\langle \Delta T(\hat{n}) \rangle$

Due to the rotational invariance, the average is angle independent.

By definition, $\int \Delta T(\hat{n}) d^2\hat{n}/4\pi$ vanishes.

Therefore $\int \langle \Delta T(\hat{n}) \rangle d^2\hat{n} = 0$ and $\langle \Delta T(\hat{n}) \rangle = 0$

$\langle \Delta T(\hat{n}) \Delta T(\hat{n}') \rangle$

The rotational invariance requires $\langle a_{\ell m} a_{\ell' m'} \rangle = \delta_{\ell\ell'} \delta_{m\,-m'} C_\ell$

Thus

$$\langle \Delta T(\hat{n}) \Delta T(\hat{n}') \rangle = \sum_{\ell m} C_\ell \, Y_\ell^m(\hat{n}) \, Y_\ell^{-m}(\hat{n}') = \sum_\ell C_\ell \left( \frac{2\ell+1}{4\pi} \right) P_\ell(\hat{n} \cdot \hat{n}') \ ,$$

Legendre polynomial

$$\int_{-1}^{1} P_m(x) P_n(x)\, dx = \frac{2}{2n+1} \delta_{mn}$$

By inverting Legendre transformation,

$$C_\ell = \frac{1}{4\pi} \int d^2\hat{n}\, d^2\hat{n}' \, P_\ell(\hat{n} \cdot \hat{n}') \langle \Delta T(\hat{n}) \Delta T(\hat{n}') \rangle \ .$$

For Gaussian distribution of temperature,

$C_\ell$ tells about all the higher averages of $\Delta T$s.

However we cannot average over the positions, what is actually observed is a quantity averaged over m but not position,

$$C_\ell^{\rm obs} \equiv \frac{1}{2\ell+1}\sum_m a_{\ell\,m}\,a_{\ell\,-m} = \frac{1}{4\pi}\int d^2\hat{n}\,d^2\hat{n}'\,P_\ell(\hat{n}\cdot\hat{n}')\Delta T(\hat{n})\Delta T(\hat{n}')\ .$$

$$\int_{\theta=0}^{\pi}\int_{\varphi=0}^{2\pi} Y_\ell^m\,Y_{\ell'}^{m'*}\,d\Omega = \delta_{\ell\ell'}\,\delta_{mm'},$$

$$a_{lm} = \int d^2\hat{n} Y_l^{m*}\Delta T(\hat{n})$$

$$P_\ell(\mathbf{x}\cdot\mathbf{y}) = \frac{4\pi}{2\ell+1}\sum_{m=-\ell}^{\ell} Y_{\ell m}^*(\theta',\varphi')\,Y_{\ell m}(\theta,\varphi).$$

The fractional difference between $C_\ell$ and $C_\ell^{\rm obs}$ is called cosmic variance.

$$\left\langle\left(\frac{C_\ell - C_\ell^{\rm obs}}{C_\ell}\right)^2\right\rangle = 1 - 2 + \frac{1}{(2\ell+1)^2 C_\ell^2}\sum_{m\,m'}\left\langle a_{\ell\,m}\,a_{\ell\,-m}\,a_{\ell\,m'}\,a_{\ell\,-m'}\right\rangle \ = \frac{2}{2\ell+1}\ .$$

for Gaussian distribution. $P(F)\,dF = \frac{1}{\sqrt{2\pi\langle F^2\rangle}}\exp\left(-\frac{F^2}{2\langle F^2\rangle}\right)\,dF$

$$\langle F_1F_2F_3F_4\rangle = \langle F_1F_2\rangle\langle F_3F_4\rangle + \langle F_1F_3\rangle\langle F_2F_4\rangle + \langle F_1F_4\rangle\langle F_2F_3\rangle$$

$$\left\langle a_{\ell\, m}\, a_{\ell\, -m}\, a_{\ell\, m'}\, a_{\ell\, -m'} \right\rangle = \left\langle a_{\ell\, m}\, a_{\ell\, -m} \right\rangle \left\langle a_{\ell\, m'}\, a_{\ell\, -m'} \right\rangle + \left\langle a_{\ell\, m}\, a_{\ell\, m'} \right\rangle \left\langle a_{\ell\, -m}\, a_{\ell\, -m'} \right\rangle + \left\langle a_{\ell\, m}\, a_{\ell\, -m'} \right\rangle \left\langle a_{\ell\, -m}\, a_{\ell\, m'} \right\rangle$$

Acoustic peaks

$\Delta\theta \simeq \pi/l.$

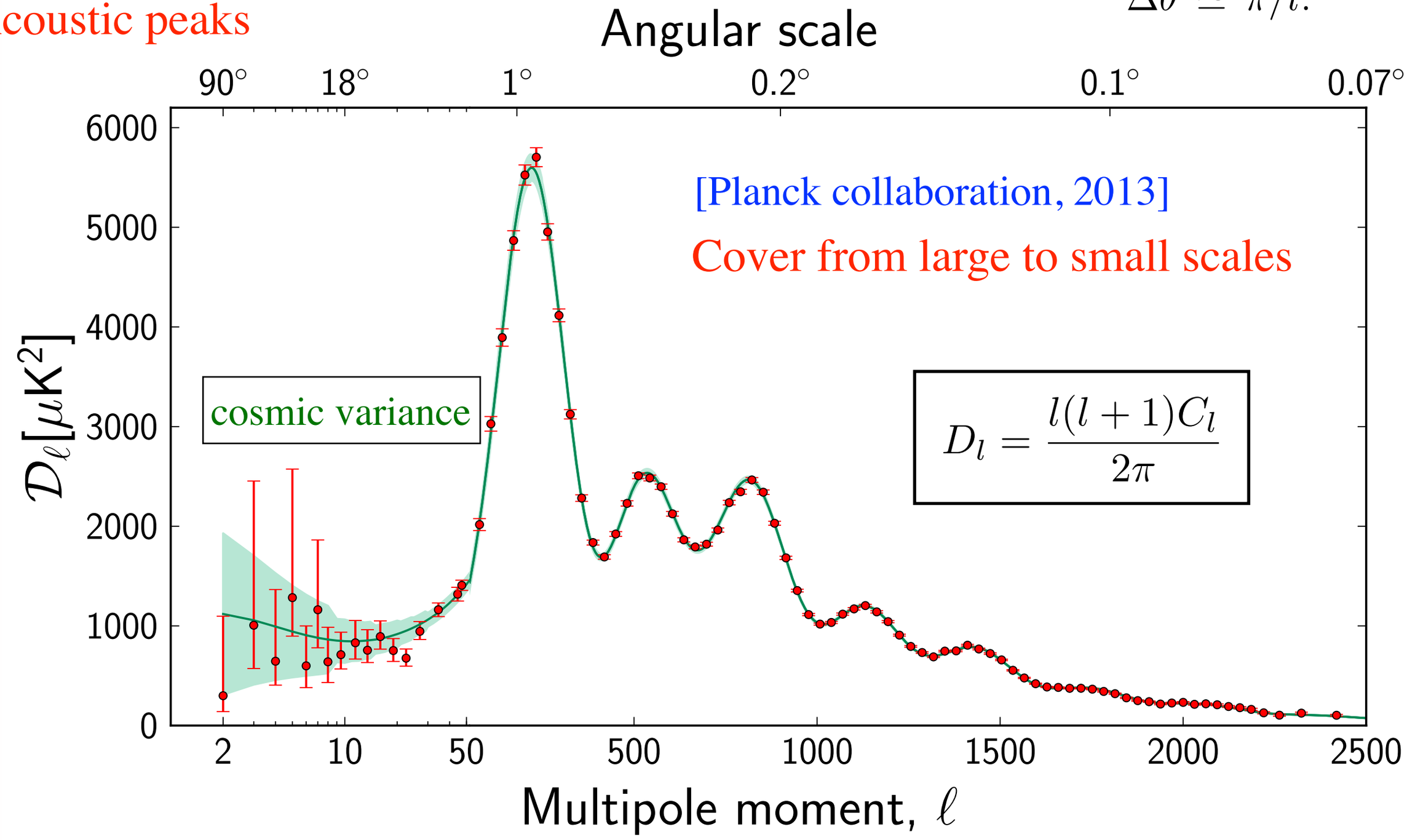


**Fig. 19.** The temperature angular power spectrum of the primary CMB from *Planck*, showing a precise measurement of seven acoustic peaks, that are well fit by a simple six-parameter ΛCDM theoretical model (the model plotted is the one labelled [Planck+WP+highL] in Planck Collaboration XVI (2013)). The shaded area around the best-fit curve represents cosmic variance, including the sky cut used. The error bars on individual points also include cosmic variance. The horizontal axis is logarithmic up to $\ell = 50$, and linear beyond. The vertical scale is $\ell(\ell+1)C_l/2\pi$. The measured spectrum shown here is exactly the same as the one shown in Fig. 1 of Planck Collaboration XVI (2013), but it has been rebinned to show better the low-$\ell$ region.

## How do the acoustic peaks generated?

1. We can solve the perturbation equation of photon until the last scattering of photons.

2. From the last scattering, the photons travel to the observer.

# 2. From the last scattering, the photons travel to the observer.

Conformal Newtonian gauge

$$ds^2 = (1+2\Phi)dt^2 - a^2(t)(1+2\Psi)d\mathbf{x}^2,$$

The observed temperature perturbation of the CMB photons coming to us along the direction n from the point x where they have scattered is given by

$$\frac{\delta T}{T} = \frac{1}{4}\frac{\delta\rho_\gamma}{\rho_\gamma}(\mathbf{x}) + \Phi(\mathbf{x}) + \mathbf{n}\cdot\mathbf{v}_\gamma(\mathbf{x}) + \int_{t_r}^{t_0} dt\ (\dot{\Phi} - \dot{\Psi}),$$

Integrates Sachs-Wolfe effect due to the time-dep. gravitational potential (early ISW, ISW)

Doppler effect due to the velocity of the baryon-photon plasma

red(blue)-shift when they escape form the gravitational potential

temperature perturbation from the density perturbation of photons at last scattering

Sachs-Wolfe effect

Sachs-Wolfe effect come from the perturbations in the baryon-photon plasma and dark matter, and this is the dominant source. The other Doppler and ISW effects are numerically rather small.

[Challinor, 2004]

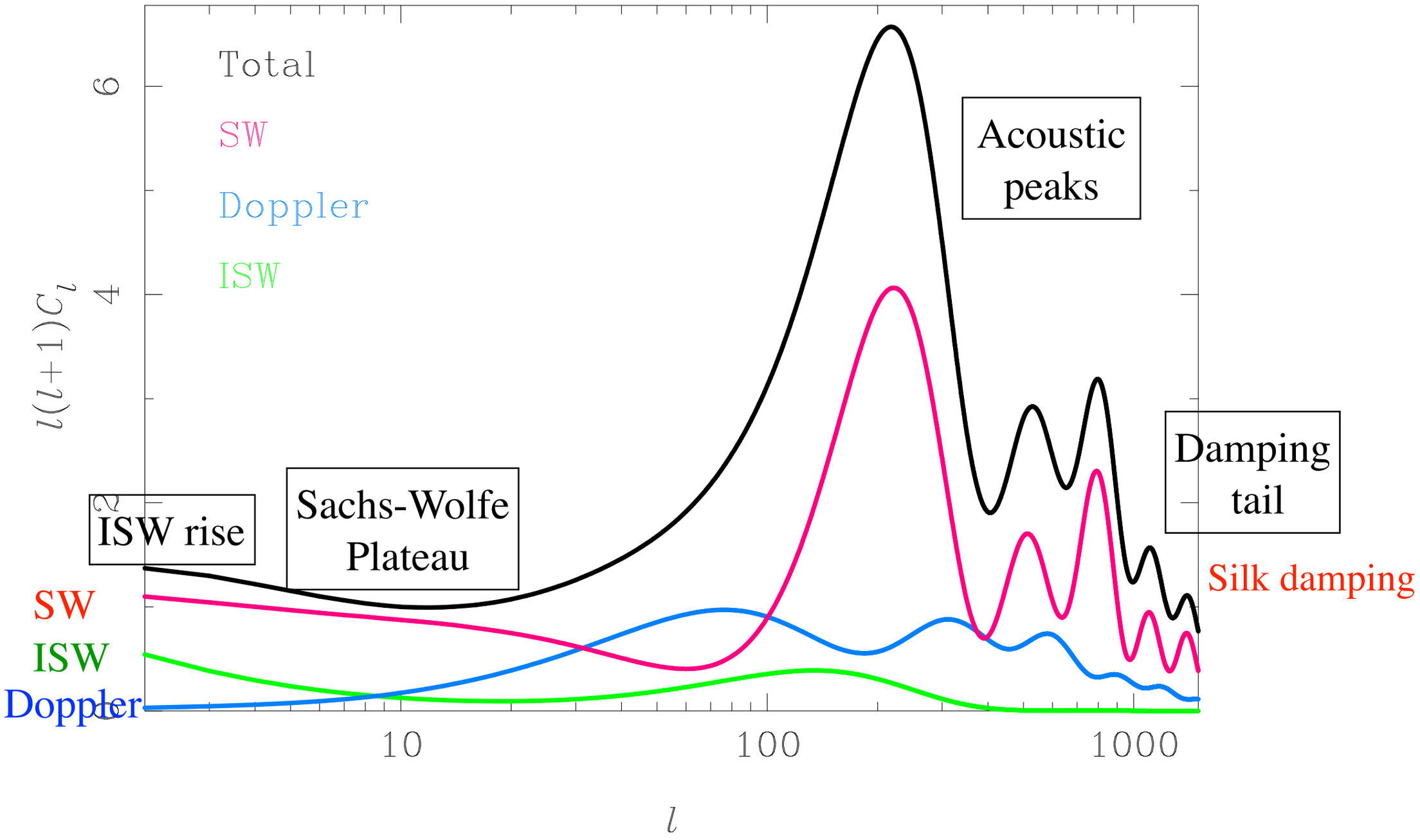

Baryon-photon plasma and cold dark matter

## Baryon-photon plasma and cold dark matter

Before recombination, baryons are tightly coupled to the photons and we consider this as a single fluid, baryon-photon plasma.

At the same time, there is a dark matter component, which is decoupled from the baryon-photon plasma but interact only with gravity.

Much before the matter-radiation equality, the baryon density and DM density are negligible to the radiation. Thus photon's contribution is dominant, however around matter-radiation equality the dark matter and baryon's contribution becomes important.

The sound speed of baryon-photon plasma is also affected by the baryon fraction and changes around recombination.

We want to derive the photon density perturbation at last scattering moment (recombination).

# The approximate solutions at recombination epoch for different scales.

## 1. The scale which enters the horizon after equality, still outside horizon at recombination

$$k^{-1} \gg \eta_r$$

$$\Phi = \frac{9}{10}\Phi^0 , \qquad \delta_\gamma = -\frac{8}{3}\Phi = -\frac{12}{5}\Phi^0 , \qquad \delta_d = -2\Phi = -\frac{9}{5}\Phi^0$$

## 2. The scale which enters the horizon between the equality and recombination

$$\eta_r \gg k^{-1} \gg \eta_{eq}$$

$$\Phi = \frac{9}{10}\Phi^0 , \qquad \delta_\gamma(\eta) = \left[ -\frac{4}{3c_s^2} + \frac{4\sqrt{c_s}}{3^{3/4}} \cos\left( k \int_0^\eta c_s d\tilde{\eta} \right) e^{-(k/k_D)^2} \right] \left( \frac{9}{10}\Phi_k^0 \right)$$

## 3. The scale which enters the horizon before equality

$$\eta_{eq} \gg k^{-1}$$

$$\Phi_k(\eta > \eta_{eq}) \simeq \frac{\ln(0.15 k\eta_{eq})}{(0.27 k\eta_{eq})^2}\Phi_k^0 ,$$

$$\delta_\gamma \simeq \left[ -\frac{4}{3c_s^2}\frac{\ln(0.15 k\eta_{eq})}{(0.27 k\eta_{eq})^2} + 3^{5/4}\sqrt{4c_s} \cos\left( k \int_0^\eta c_s d\eta \right) e^{-(k/k_D)^2} \right] \Phi_k^0$$

Sachs-Wolfe plateau $k^{-1} \gg \eta_r \qquad (\theta \gg 1^\circ) \quad \text{or} \cdot\, l \ll 200.$

At large scales, the mode which is superhorizon at the recombination epoch, the first and second term dominate.

$$\left(\frac{\delta T}{T}\right) \simeq \left(\frac{1}{4}\frac{\delta\rho_\gamma}{\rho_\gamma} + \Phi\right)(\eta_r) \simeq \frac{1}{3}\Phi(\eta_r) = \frac{3}{10}\Phi^0 = -\frac{1}{8}\delta_\gamma(\eta_r)$$

The observed anisotropy of overdense region is underdense at recombination due to the potential well. Also note the factor 1/8 from density perturbation.

Actually $C_l$ is a weighted sum over all k including near horizon and subhorizon scales. This give a good approximation for $l > 20$, and the neglected effects become essential.

---

1. The scale which enters the horizon after equality, still outside horizon at recombination $k^{-1} \gg \eta_r$

$$\Phi = \frac{9}{10}\Phi^0\,, \qquad \delta_\gamma = -\frac{8}{3}\Phi = -\frac{12}{5}\Phi^0\,, \qquad \delta_d = -2\Phi = -\frac{9}{5}\Phi^0$$

$$\delta_k'(\eta_r) \simeq 0$$

$\Delta\theta \simeq \pi/l.$

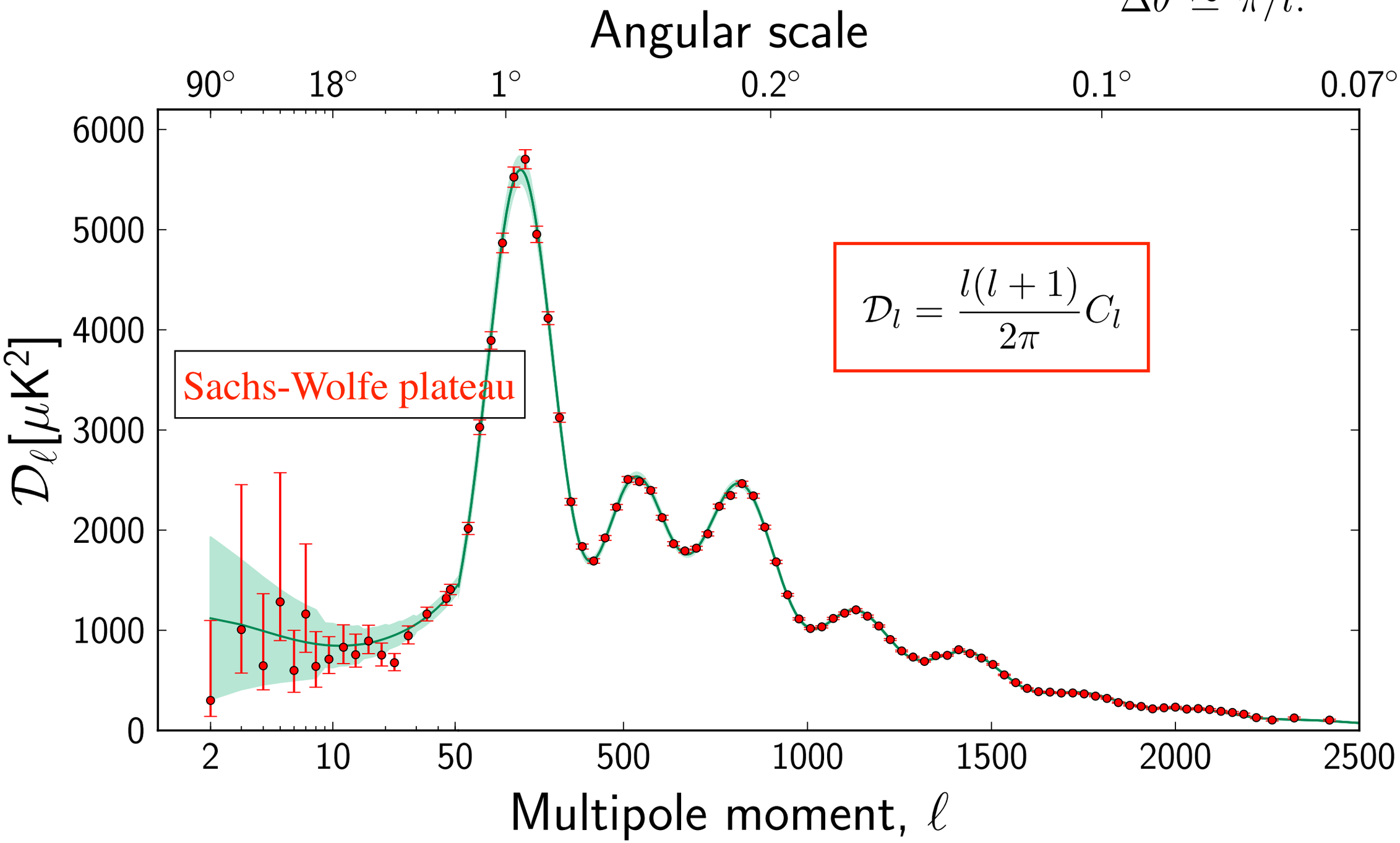


**Fig. 19.** The temperature angular power spectrum of the primary CMB from *Planck*, showing a precise measurement of seven acoustic peaks, that are well fit by a simple six-parameter ΛCDM theoretical model (the model plotted is the one labelled [Planck+WP+highL] in Planck Collaboration XVI (2013)). The shaded area around the best-fit curve represents cosmic variance, including the sky cut used. The error bars on individual points also include cosmic variance. The horizontal axis is logarithmic up to $\ell = 50$, and linear beyond. The vertical scale is $\ell(\ell+1)C_l/2\pi$. The measured spectrum shown here is exactly the same as the one shown in Fig. 1 of Planck Collaboration XVI (2013), but it has been rebinned to show better the low-$\ell$ region.

Planck 2013

The European Space Agency's *Planck* satellite.


# New results from Planck

Planck was launched on 14 May 2009

9 bands (30 - 857 GHz)

Angular resolution ~ 7 arcminutes

accuracy around 10^{-6} in temperature fluctuation

21st March, 2013 first release of data

15.5 months data

Temperature data only (Polarization next year)

29 papers at

http://www.sciops.esa.int/index.php?project=PLANCK&page=Planck_Published_Papers

In 2014, full temperature and polarization date will be released

# Lagrangian point

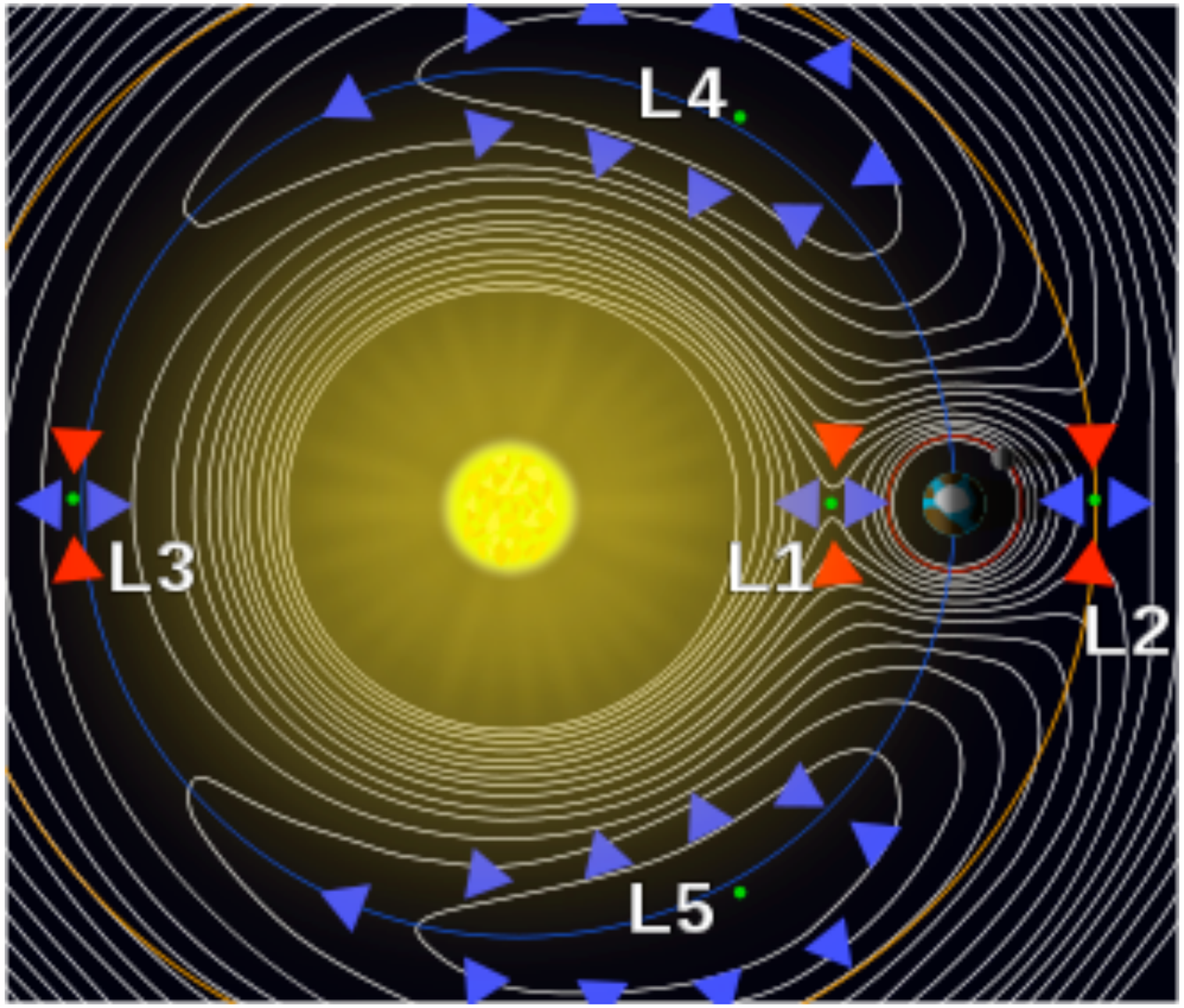


A contour plot of the effective potential due to gravity and the centrifugal force of a two-body system in a rotating frame of reference. The arrows indicate the gradients of the potential around the five Lagrange points — downhill toward them (red) or away from them (blue). Counterintuitively, the $L_4$ and $L_5$ points are the high points of the potential. At the points themselves these forces are balanced.

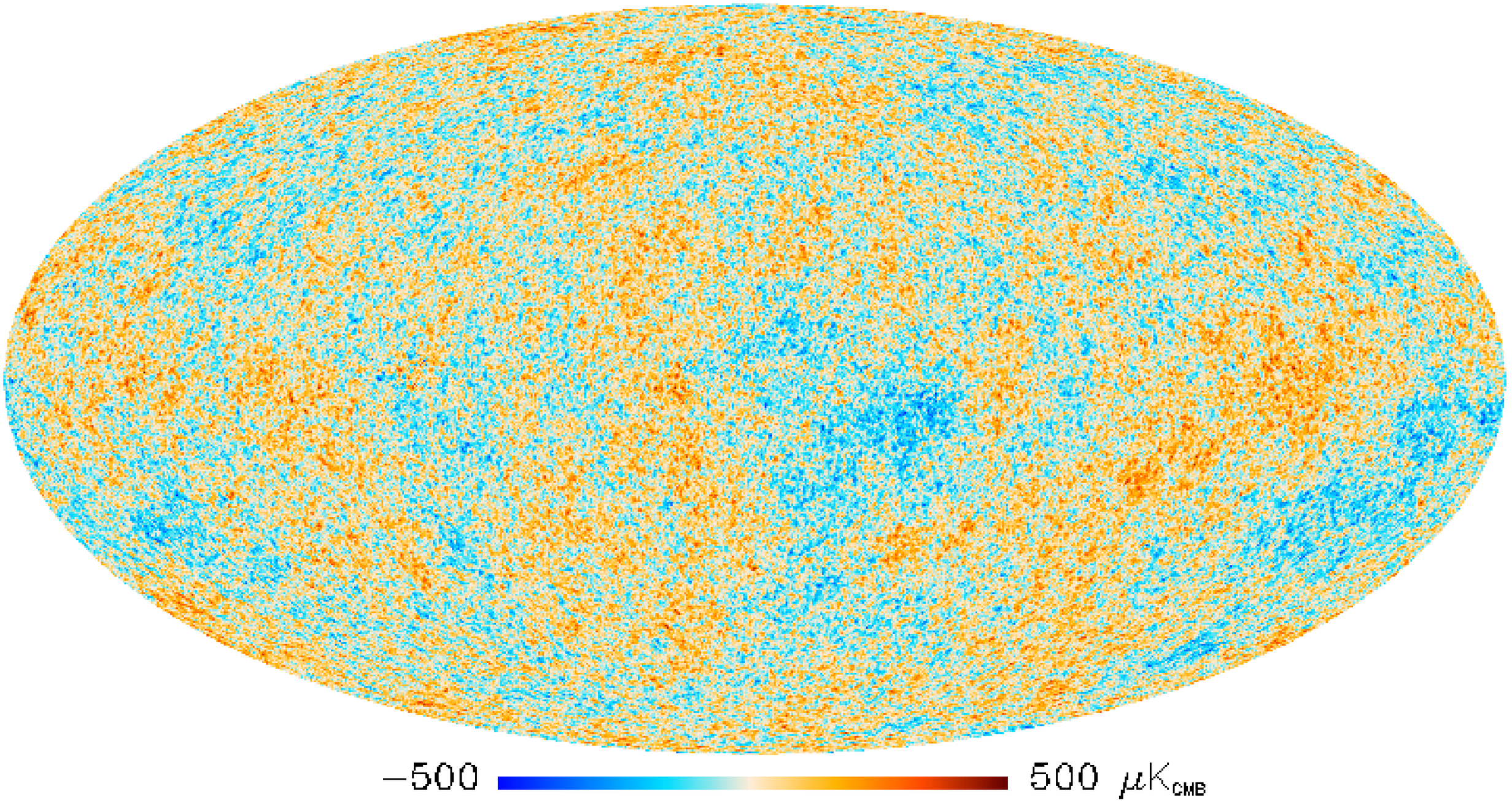
−500
500 $\mu K_{CMB}$

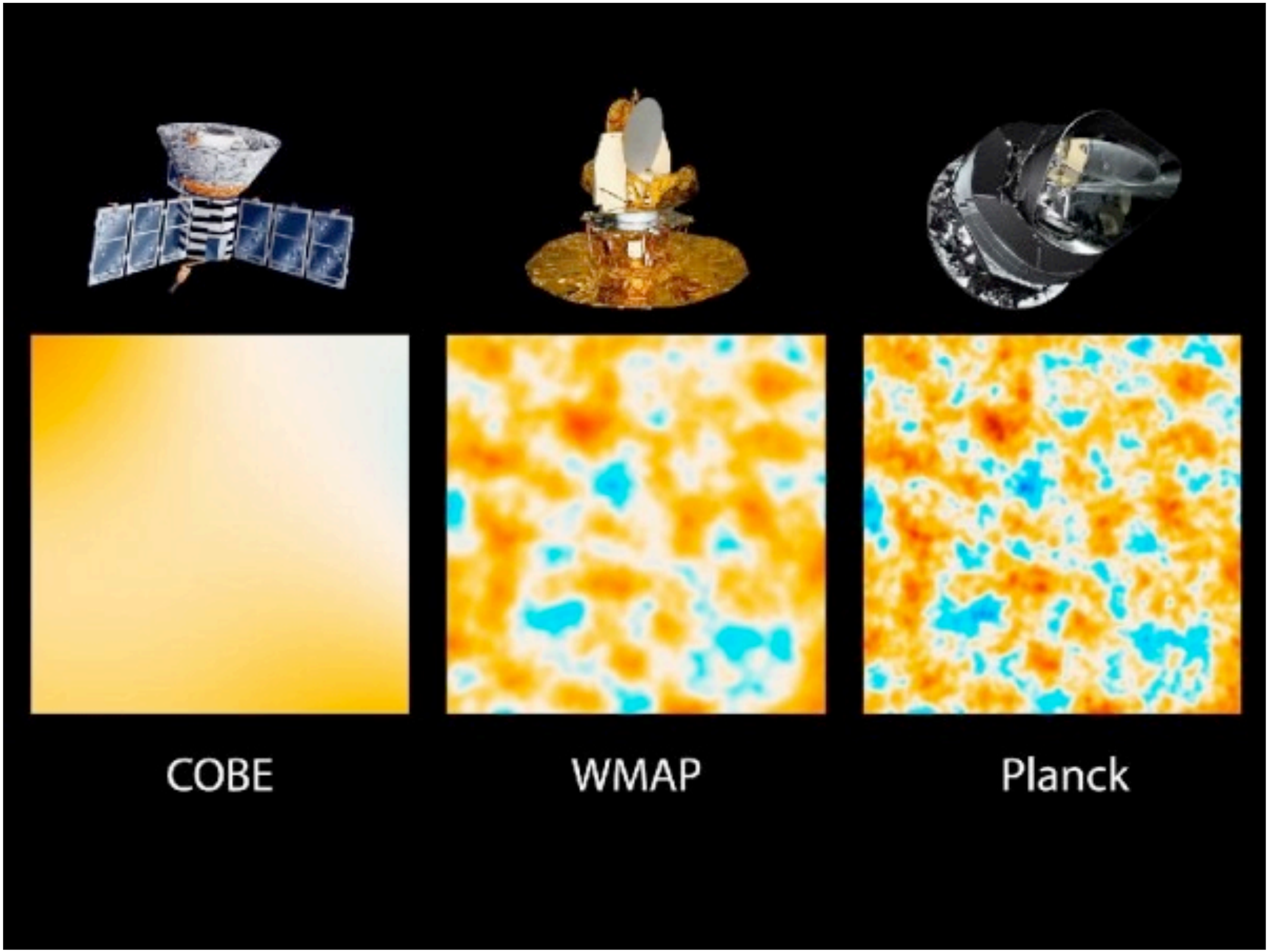
COBE
WMAP
Planck

# Cosmic Microwave Background Radiation

Atacama Cosmology Telescope (ACT),
6m, Atacama desert, Chile

[1301.0824]

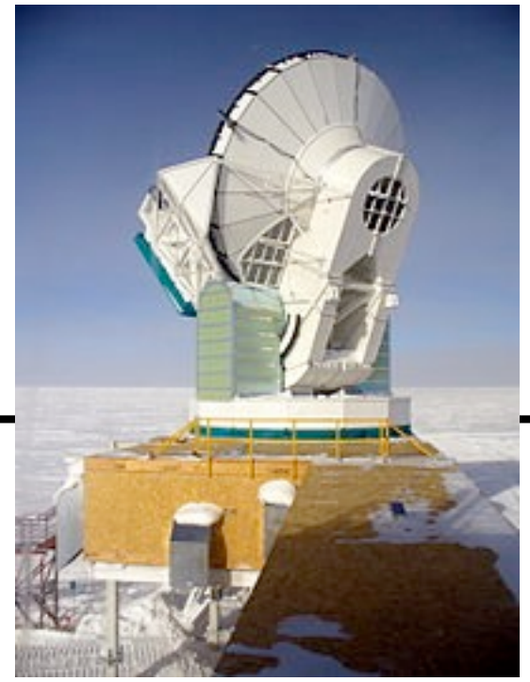

South Pole Telescope
10m (SPT)

[1212.6267]

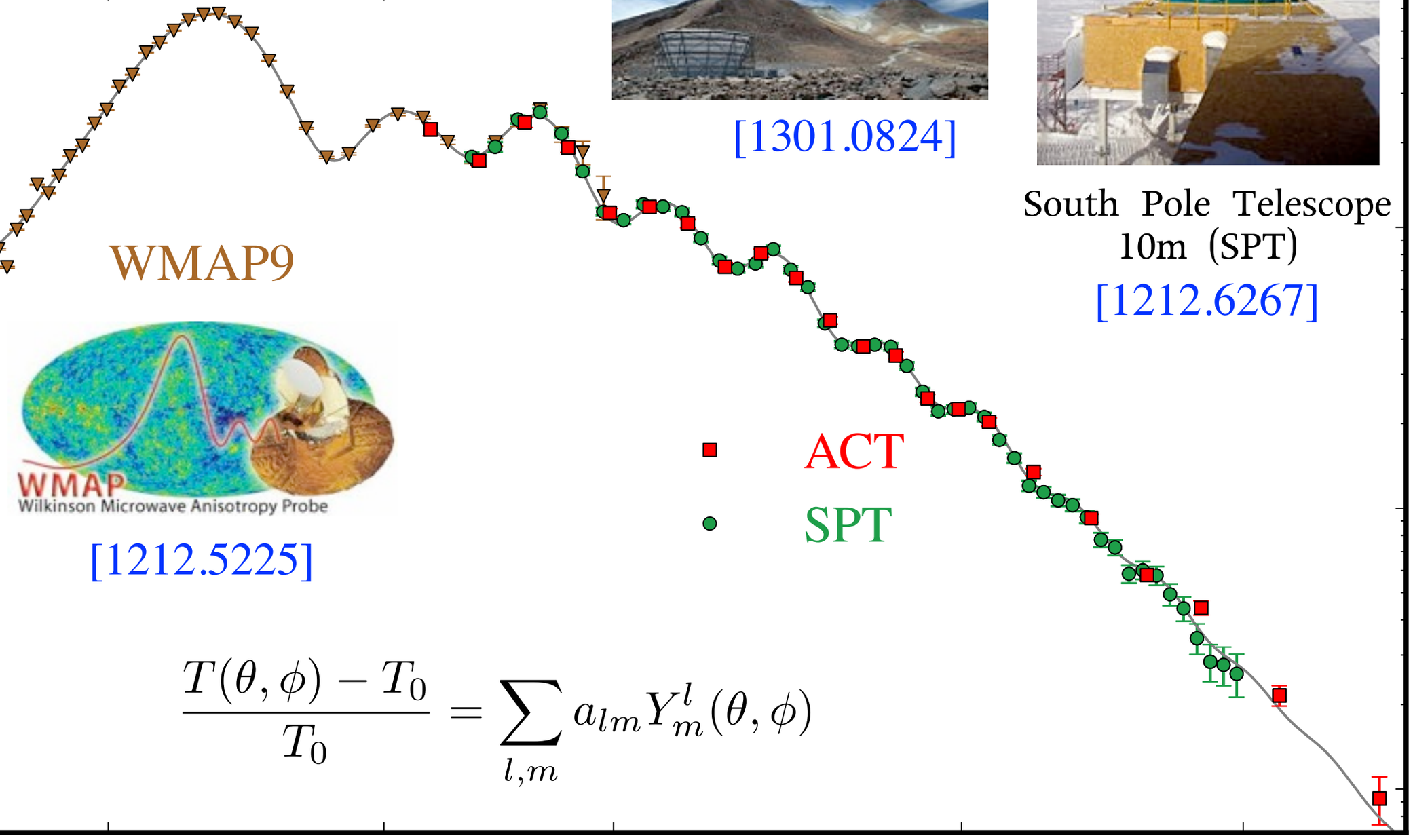





[1212.5225]

$$\frac{T(\theta,\phi)-T_0}{T_0}=\sum_{l,m} a_{lm} Y^l_m(\theta,\phi)$$

$$\Delta\theta \simeq \pi/l.$$

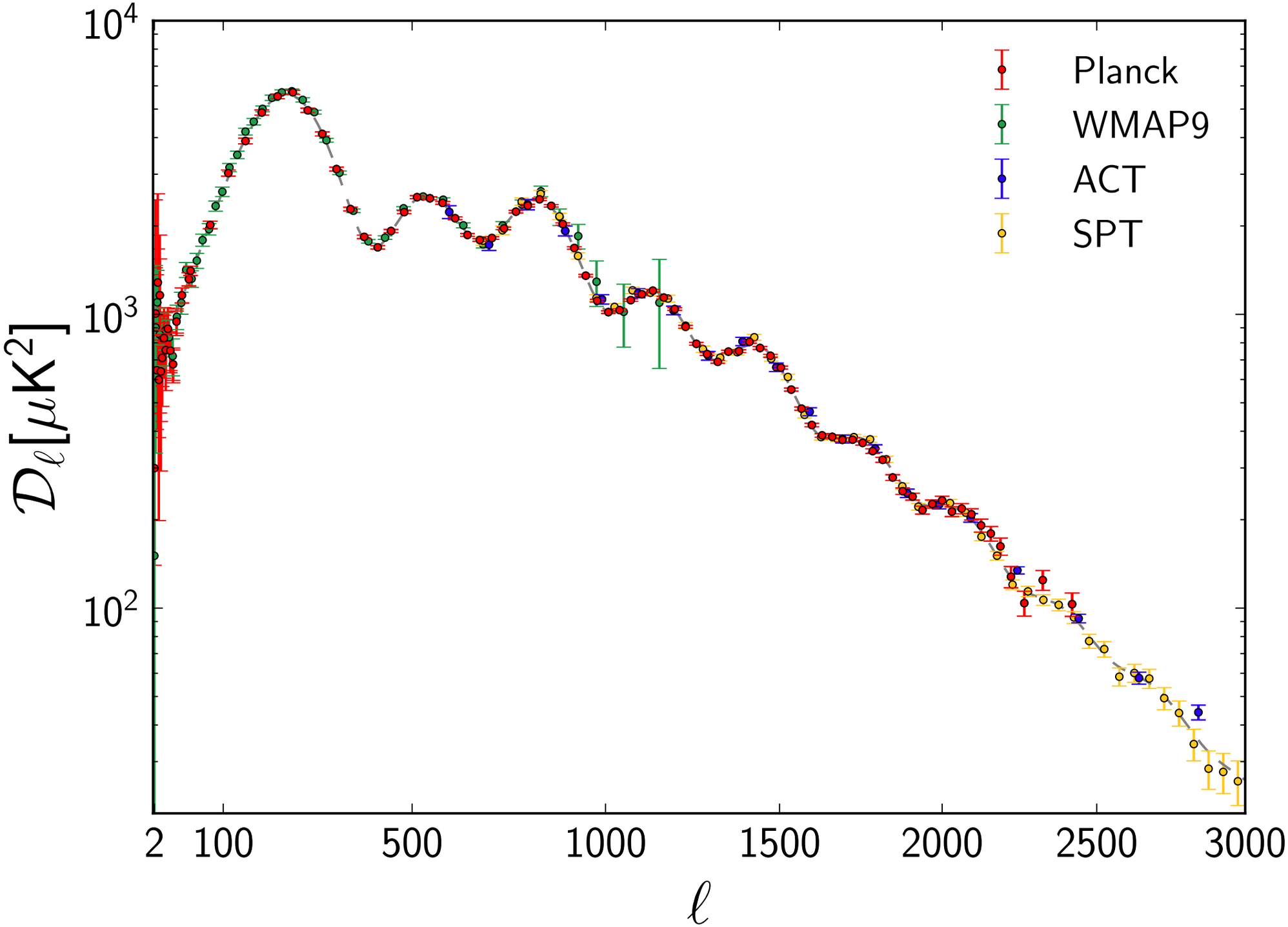


**Fig. 25.** Measured angular power spectra of *Planck*, WMAP9, ACT, and SPT. The model plotted is *Planck*'s best-fit model including *Planck* temperature, WMAP polarization, ACT, and SPT (the model is labelled [Planck+WP+HighL] in Planck Collaboration XVI (2013)). Error bars include cosmic variance. The horizontal axis is $\ell^{0.8}$.

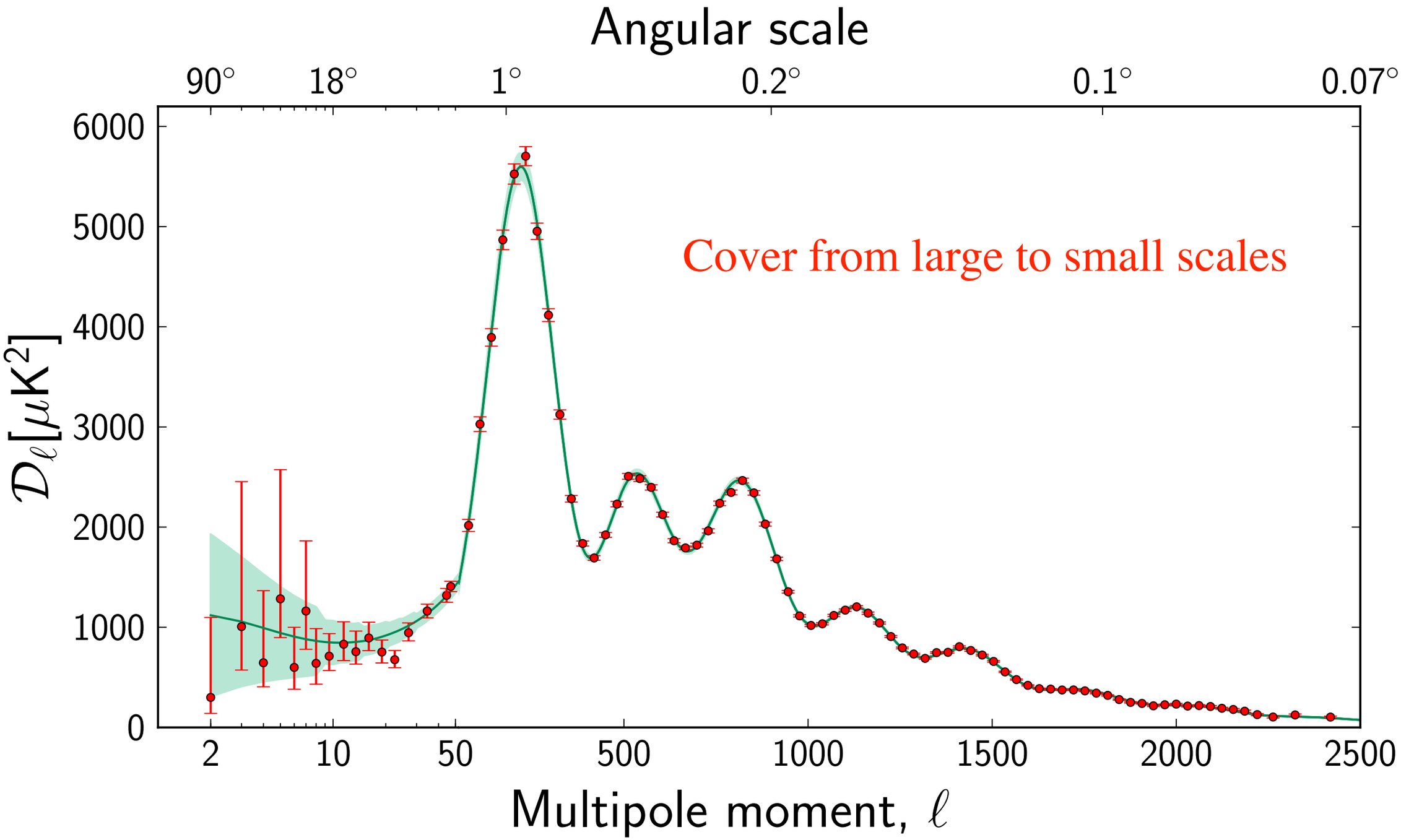


**Fig. 19.** The temperature angular power spectrum of the primary CMB from *Planck*, showing a precise measurement of seven acoustic peaks, that are well fit by a simple six-parameter ΛCDM theoretical model (the model plotted is the one labelled [Planck+WP+highL] in Planck Collaboration XVI (2013)). The shaded area around the best-fit curve represents cosmic variance, including the sky cut used. The error bars on individual points also include cosmic variance. The horizontal axis is logarithmic up to $\ell = 50$, and linear beyond. The vertical scale is $\ell(\ell+1)C_l/2\pi$. The measured spectrum shown here is exactly the same as the one shown in Fig. 1 of Planck Collaboration XVI (2013), but it has been rebinned to show better the low-$\ell$ region.

# Base Lambda-CDM model

# Lambda-CDM model

## Angular size of Acoustic scale $\theta_* = r_s/D_A$

$$\theta_* = (1.04148 \pm 0.00066) \times 10^{-2} = 0.596724^\circ \pm 0.00038^\circ.$$

## Hubble parameter, DE, Matter densities

Baryon $\Omega_b h^2 = 0.02207 \pm 0.00033$ (68%; *Planck*).

Cold dark matter $\Omega_c h^2 = 0.1196 \pm 0.0031$ (68%; *Planck*).

Hubble constant $H_0 = (67.4 \pm 1.4)\,\mathrm{km\,s^{-1}\,Mpc^{-1}}$ (68%; *Planck*).

Dark energy $\Omega_\Lambda = 0.686 \pm 0.020$ (68%; *Planck*),

Matter $\Omega_m h^2 = 0.1423 \pm 0.0029$ (68%; *Planck*).

: Dark Energy 68.3%, Dark Matter 26.8%, Baryon 4.9%

## Optical depth $\tau = 0.089 \pm 0.032$ (68%; *Planck*+lensing).

## Amplitude $\ln(10^{10} A_s) = 3.103 \pm 0.072$

## Spectral index $n_s = 0.9616 \pm 0.0094$ (68%; *Planck*).

## Early Universe Physics

$$\mathcal{P}_{\mathcal{R}}(k) = A_{\rm s}\left(\frac{k}{k_0}\right)^{n_{\rm s}-1+(1/2)(dn_{\rm s}/d\ln k)\ln(k/k_0)},$$

### Scale dependence

$$n_{\rm s} = 0.9603 \pm 0.0073 \qquad \textit{Planck}+\text{WP} \quad k_* = 0.002\ \text{Mpc}^{-1}$$

: 5-sigma departures form scale invariance, rule out HZ spectrum

: robust to change in the underlying theoretical model

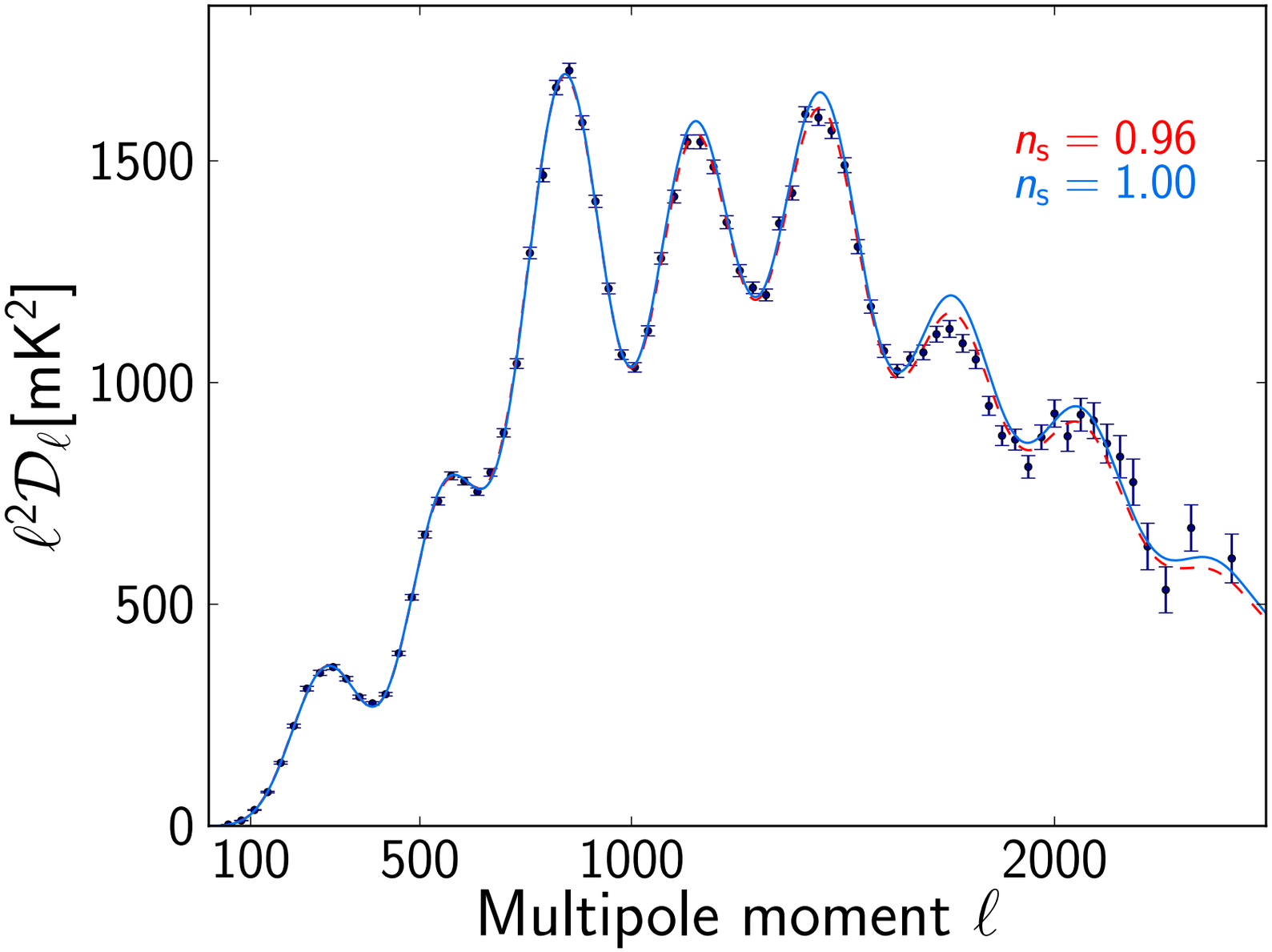

- The properties of the primordial curvature perturbation [Planck, 2013]

- Power spectrum $\langle \zeta_{\mathbf{k_1}} \zeta_{\mathbf{k_2}} \rangle \equiv (2\pi)^3 \delta^3(\mathbf{k_1} + \mathbf{k_2}) \frac{2\pi^2}{k^3} \mathcal{P}_\zeta(k)$ $\mathcal{P}_\zeta = (2.198 \pm 0.056) \times 10^{-9}$

: small perturbation

- Spectral index $n_\zeta - 1 \equiv \frac{d \log \mathcal{P}_\zeta}{d \log k}$ $n_\zeta = 0.959 \pm 0.007$

: almost scale-invariant

- Tensor-to-scalar ratio $r \equiv \frac{\mathcal{P}_T}{\mathcal{P}_\zeta}$

$$\mathcal{P}_T = 8 \left( \frac{H_*}{2\pi} \right)^2$$

*Planck*+WP+highL likelihood we find

$r_{0.002} < 0.11$ (95%; no running),

$r_{0.002} < 0.26$ (95%; including running).

: unobserved yet

- primordial tensor perturbation determines the initial amplitude of gravitational waves, whose oscillation begins at horizon entry

- Non-Gaussianity

: No evidence of non-G yet

| $f_{\rm NL}$ | | |
|---|---|---|
| Local | Equilateral | Orthogonal |
| $2.7 \pm 5.8$ | $-42 \pm 75$ | $-25 \pm 39$ |

✦ Polarization perturbation

# E and B modes

## ✦ Polarization perturbation

Two flavors of CMB polarization:

Density perturbations: curl-free, "E-mode"
Gravity waves: curl, "B-mode"

E-mode

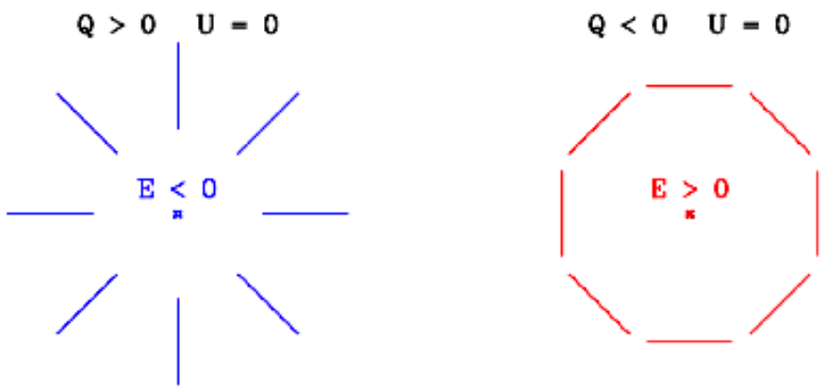


B-mode

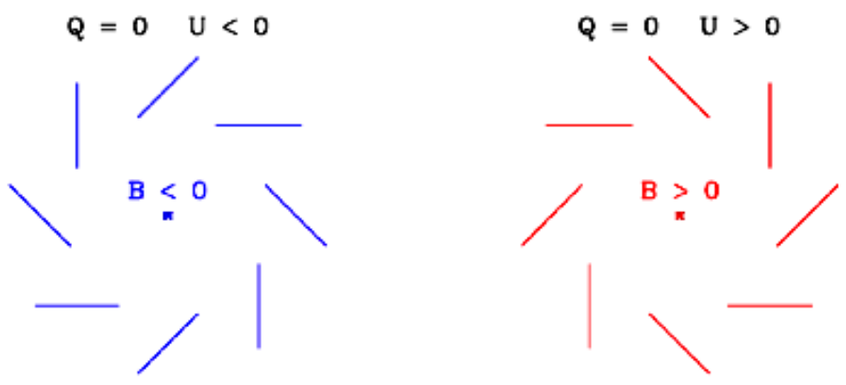


- We can break down the polarization field into two components which we call E and B modes. This is the spin-2 analog of the gradient/curl decomposition of a vector field.
- E modes are generated by density (scalar) perturbations via Thomson scattering.
- Additional vector modes are created by vortical motion of the matter at recombination – this is small
- B modes are generated by gravity waves (tensor perturbations) at last scattering or by gravitational lensing (which transforms E modes into B modes along the line of sight to us) later on.

# What is the origin of the polarization?

In the uniform Universe in thermal equilibrium, it is unpolarized.

Density perturbation → T-perturbation

E-mode

Tensor perturbation → T-perturbation

E-mode

B-mode

* E-mode —Gravitational lensing→ B-mode

# Quadrupole + Thomson scattering

E-mode

Polarization is induced by Thomson scattering, either at decoupling or during a later epoch of reionization.
(No circular polarization, i.e. V=0)

$$P(\theta,\phi) \propto 1-\cos^2\theta$$

$$\frac{d\sigma}{d\Omega} = \left(\frac{e^2}{4\pi m c^2}\right)^2 |\hat{\epsilon}\cdot\hat{\epsilon}'|^2$$

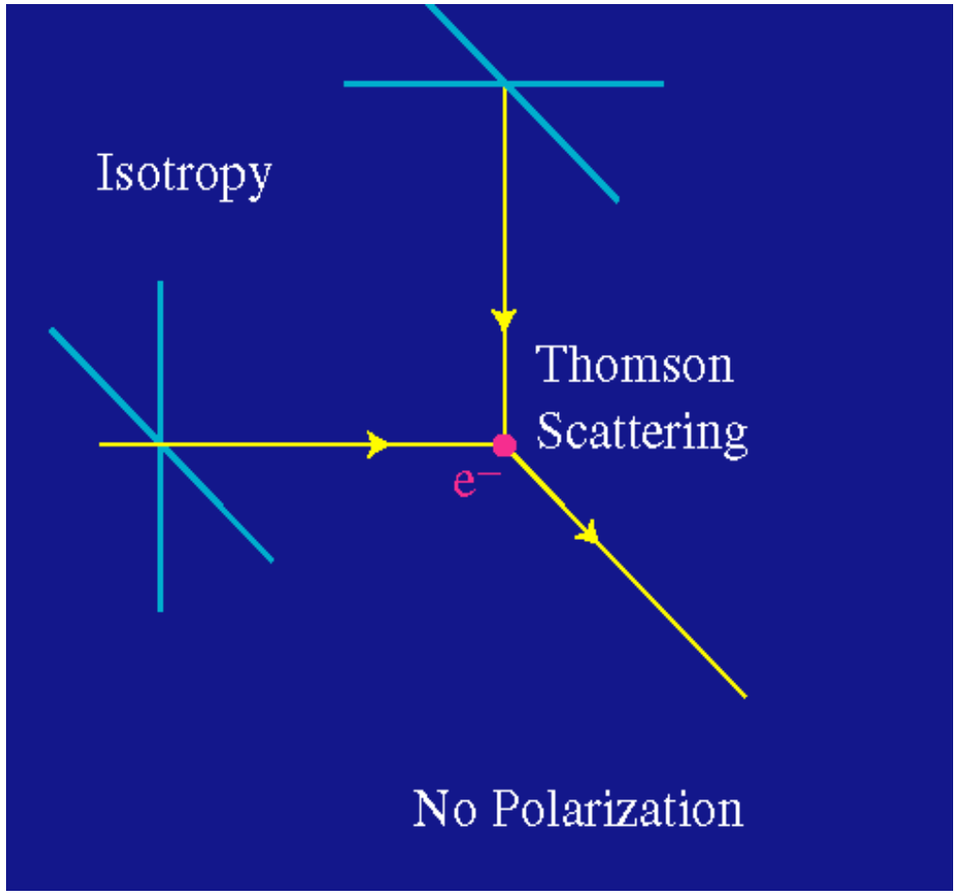


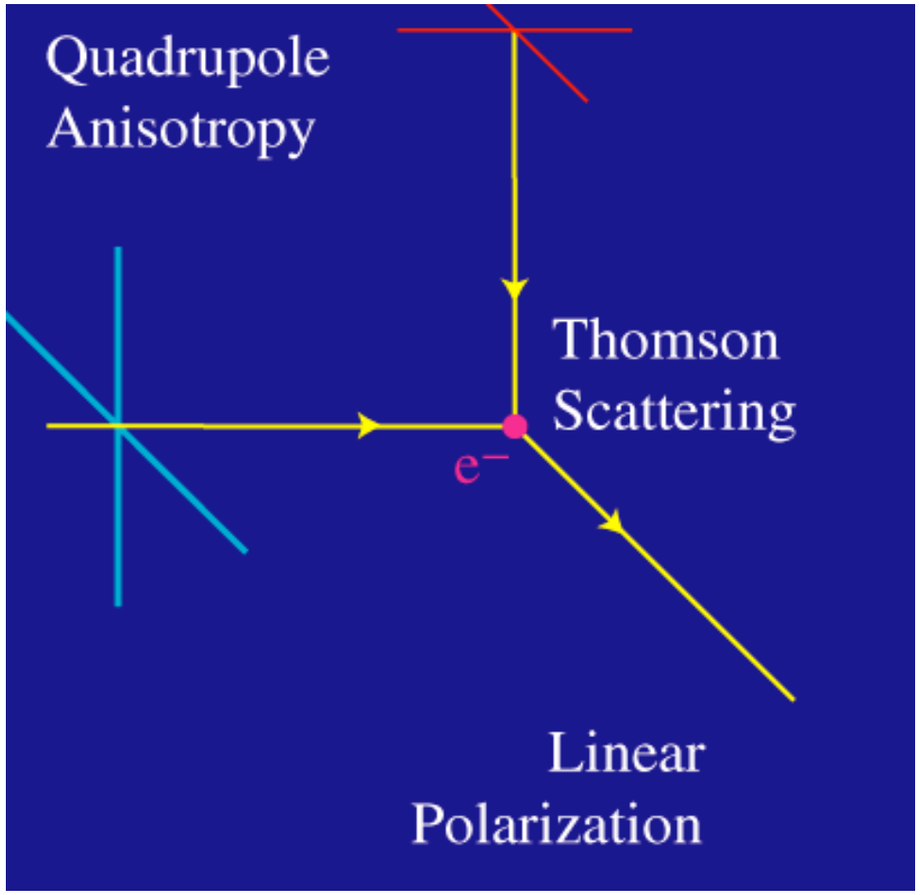

Density perturbation

$\zeta$

Tensor perturbation

$h_{ij}$

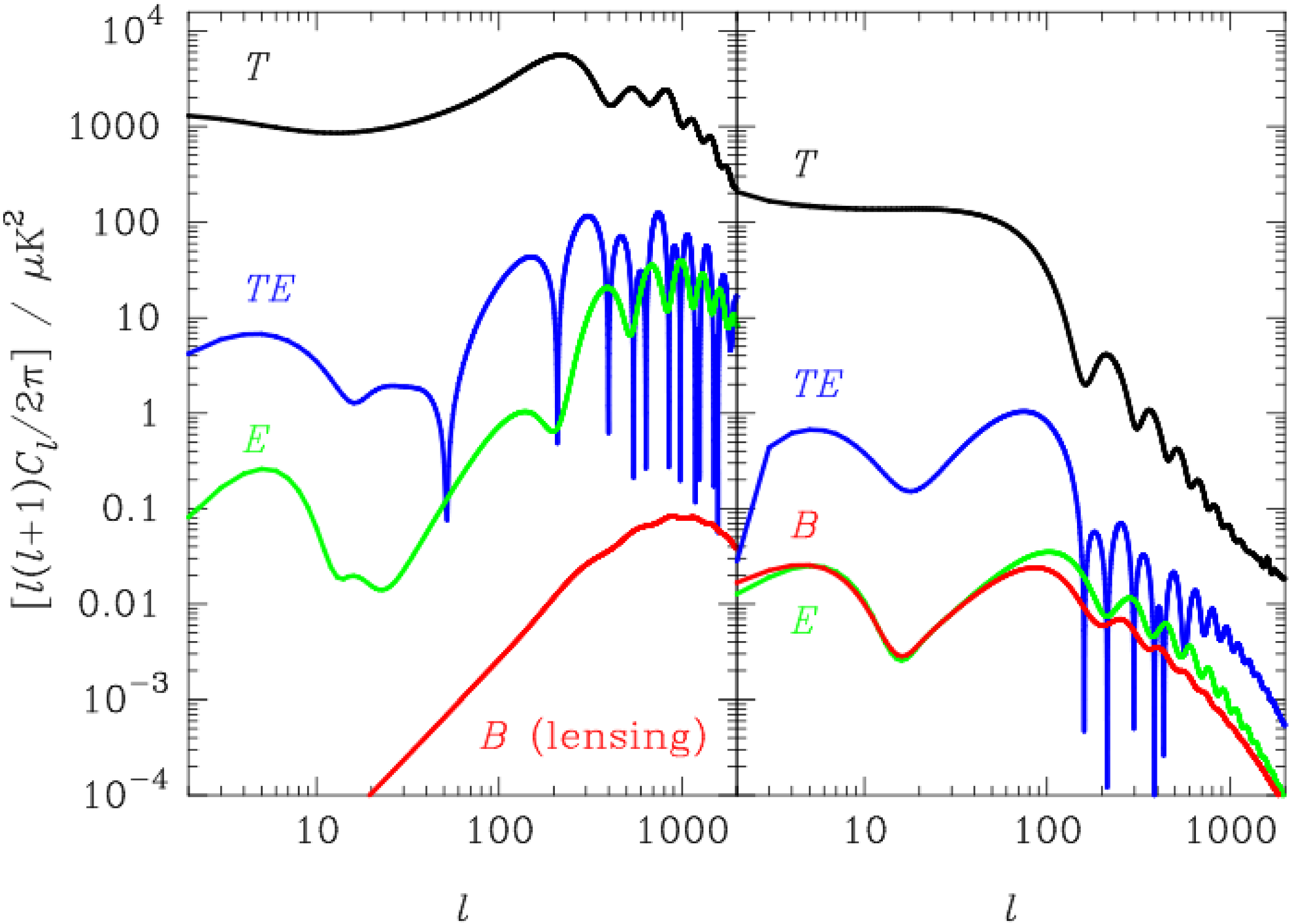

# Tensor fluctuations [Planck, 2013]

Tensor spectrum $\mathcal{P}_{\rm t}(k) = A_{\rm t}\left(\frac{k}{k_0}\right)^{n_{\rm t}}$ $n_{\rm t} = -r_{0.05}/8,$

: polarization data (B-mode) in 2014 December?

: temperature alone can constrain the amplitude of tensor modes indirectly

: constrain the energy scale of inflation

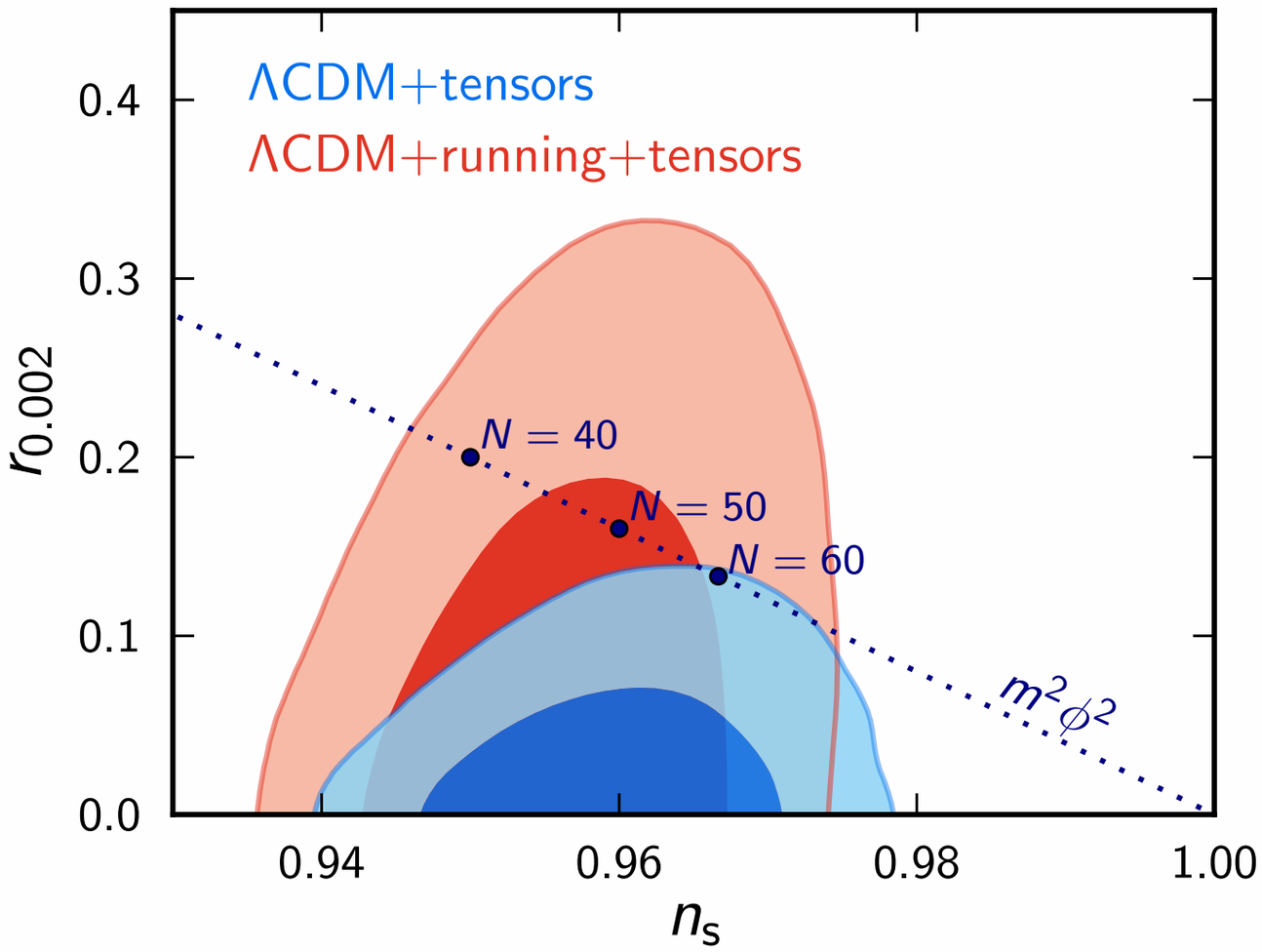


*Planck*+WP+highL likelihood we find

$r_{0.002} < 0.11$ (95%; no running),

$r_{0.002} < 0.26$ (95%; including running).

upper bound on energy scale of inflation

$$V_* = \frac{3\pi^2 A_{\rm s}}{2}\, r\, M_{\rm pl}^4 = (1.94\times 10^{16}\ {\rm GeV})^4 \frac{r_*}{0.12}\,,$$

with tensor

$$n_{\rm s} = 0.9624 \pm 0.0075.$$

| Model | Parameter | *Planck*+WP | *Planck*+WP+lensing | *Planck* + WP+high-$\ell$ | *Planck*+WP+BAO |
|---|---|---|---|---|---|
| ΛCDM + tensor | $n_{\rm s}$ | 0.9624 ± 0.0075 | 0.9653 ± 0.0069 | 0.9600 ± 0.0071 | 0.9643 + 0.0059 |
| | $r_{0.002}$ | < 0.12 | < 0.13 | < 0.11 | < 0.12 |
| | $-2\Delta \ln \mathcal{L}_{\rm max}$ | 0 | 0 | 0 | -0.31 |

# Detection of B-mode with BICEP2 ???

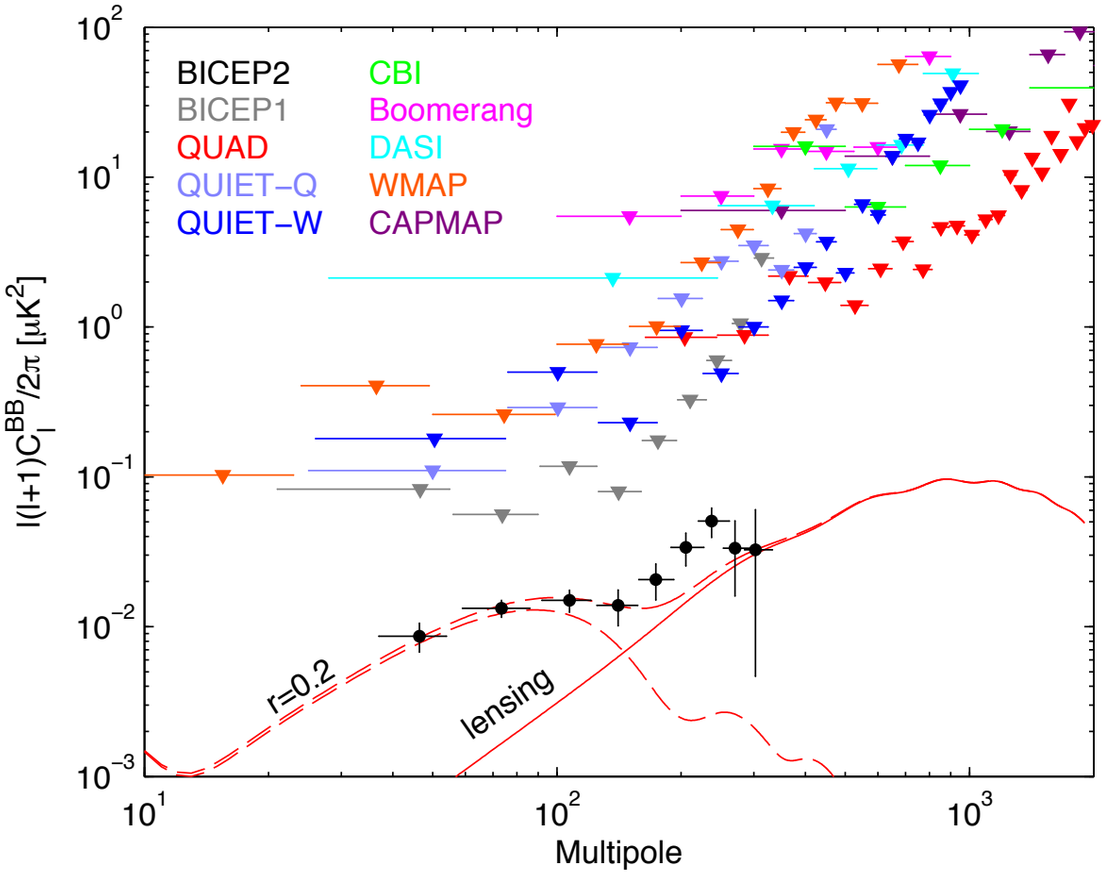


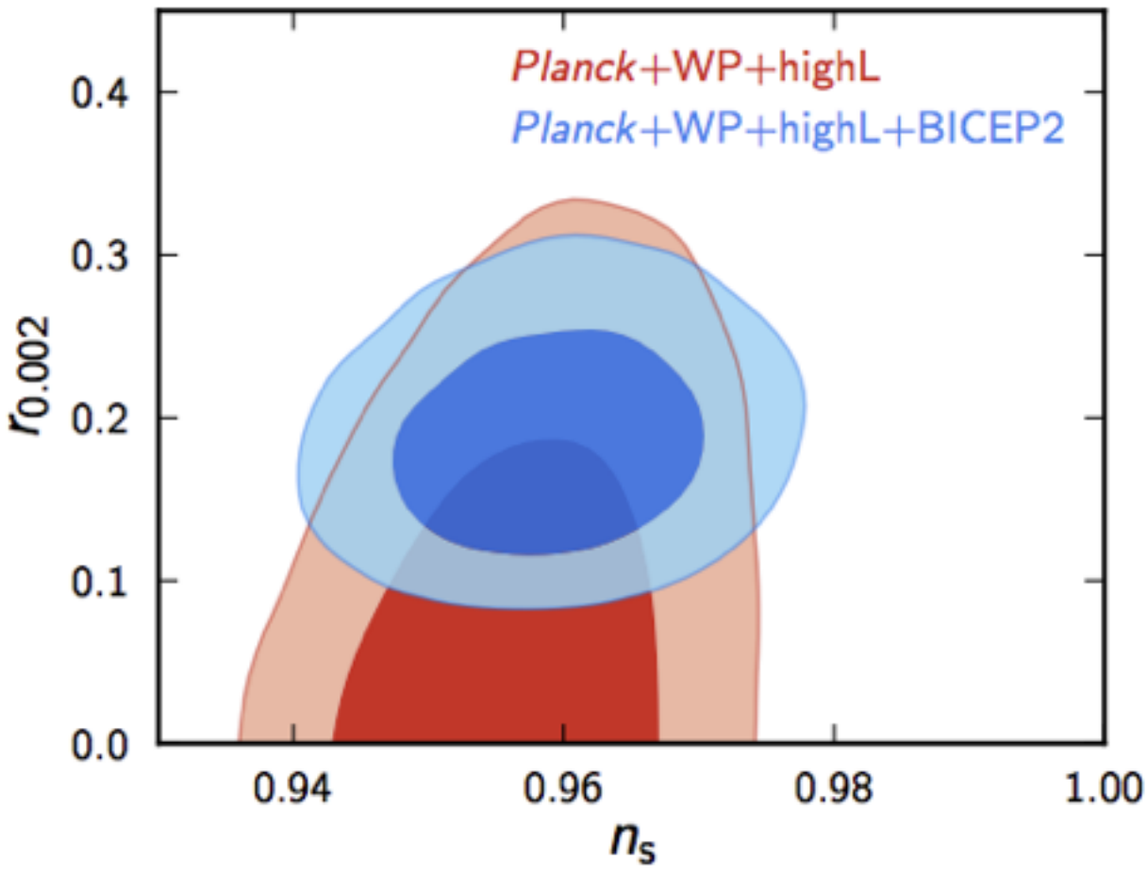

New report : 2014 March 17

# BICEP2 I: DETECTION OF *B*-mode POLARIZATION AT DEGREE ANGULAR SCALES

BICEP2 COLLABORATION - P. A. R. ADE[1], R. W. AIKIN[2], D. BARKATS[3], S. J. BENTON[4], C. A. BISCHOFF[5], J. J. BOCK[2,6], J. A. BREVIK[2], I. BUDER[5], E. BULLOCK[7], C. D. DOWELL[6], L. DUBAND[8], J. P. FILIPPINI[2], S. FLIESCHER[9], S. R. GOLWALA[2], M. HALPERN[10], M. HASSELFIELD[10], S. R. HILDEBRANDT[2,6], G. C. HILTON[11], V. V. HRISTOV[2], K. D. IRWIN[12,13,11], K. S. KARKARE[5], J. P. KAUFMAN[14], B. G. KEATING[14], S. A. KERNASOVSKIY[12], J. M. KOVAC[5,16], C. L. KUO[12,13], E. M. LEITCH[15], M. LUEKER[2], P. MASON[2], C. B. NETTERFIELD[4], H. T. NGUYEN[6], R. O'BRIENT[6], R. W. OGBURN IV[12,13], A. ORLANDO[14], C. PRYKE[9,7,16], C. D. REINTSEMA[11], S. RICHTER[5], R. SCHWARZ[9], C. D. SHEEHY[9,15], Z. K. STANISZEWSKI[2,6], R. V. SUDIWALA[1], G. P. TEPLY[2], J. E. TOLAN[12], A. D. TURNER[6], A. G. VIEREGG[5,15], C. L. WONG[5], AND K. W. YOON[12,13]

*to be submitted to a journal TBD*

## ABSTRACT

We report results from the BICEP2 experiment, a Cosmic Microwave Background (CMB) polarimeter specifically designed to search for the signal of inflationary gravitational waves in the *B*-mode power spectrum around $\ell \sim 80$. The telescope comprised a 26 cm aperture all-cold refracting optical system equipped with a focal plane of 512 antenna coupled transition edge sensor (TES) 150 GHz bolometers each with temperature sensitivity of $\approx 300\ \mu\mathrm{K}_{\mathrm{CMB}}\sqrt{\mathrm{s}}$. BICEP2 observed from the South Pole for three seasons from 2010 to 2012. A low-foreground region of sky with an effective area of 380 square degrees was observed to a depth of 87 nK-degrees in Stokes $Q$ and $U$. In this paper we describe the observations, data reduction, maps, simulations and results. We find an excess of *B*-mode power over the base lensed-$\Lambda$CDM expectation in the range $30 < \ell < 150$, inconsistent with the null hypothesis at a significance of $> 5\sigma$. Through jackknife tests and simulations based on detailed calibration measurements we show that systematic contamination is much smaller than the observed excess. We also estimate potential foreground signals and find that available models predict these to be considerably smaller than the observed signal. These foreground models possess no significant cross-correlation with our maps. Additionally, cross-correlating BICEP2 against 100 GHz maps from the BICEP1 experiment, the excess signal is confirmed with $3\sigma$ significance and its spectral index is found to be consistent with that of the CMB, disfavoring synchrotron or dust at $2.3\sigma$ and $2.2\sigma$, respectively. The observed *B*-mode power spectrum is well-fit by a lensed-$\Lambda$CDM + tensor theoretical model with tensor/scalar ratio $r = 0.20^{+0.07}_{-0.05}$, with $r = 0$ disfavored at $7.0\sigma$. Subtracting the best available estimate for foreground dust modifies the likelihood slightly so that $r = 0$ is disfavored at $5.9\sigma$.

*Subject headings:* cosmic background radiation — cosmology: observations — gravitational waves — inflation — polarization

# Detection of B-mode Polarization at Degree Scales using BICEP2

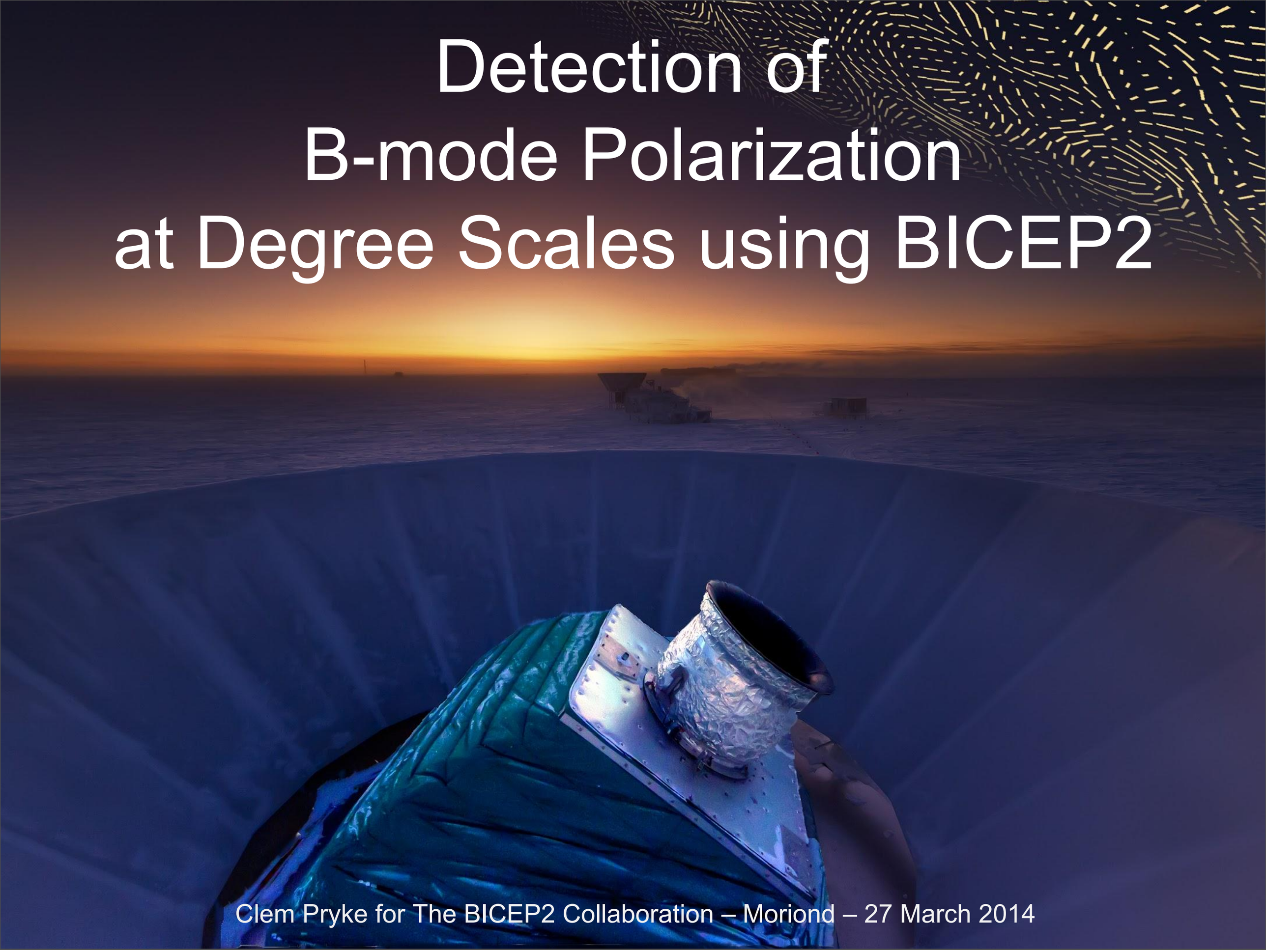

Clem Pryke for The BICEP2 Collaboration – Moriond – 27 March 2014

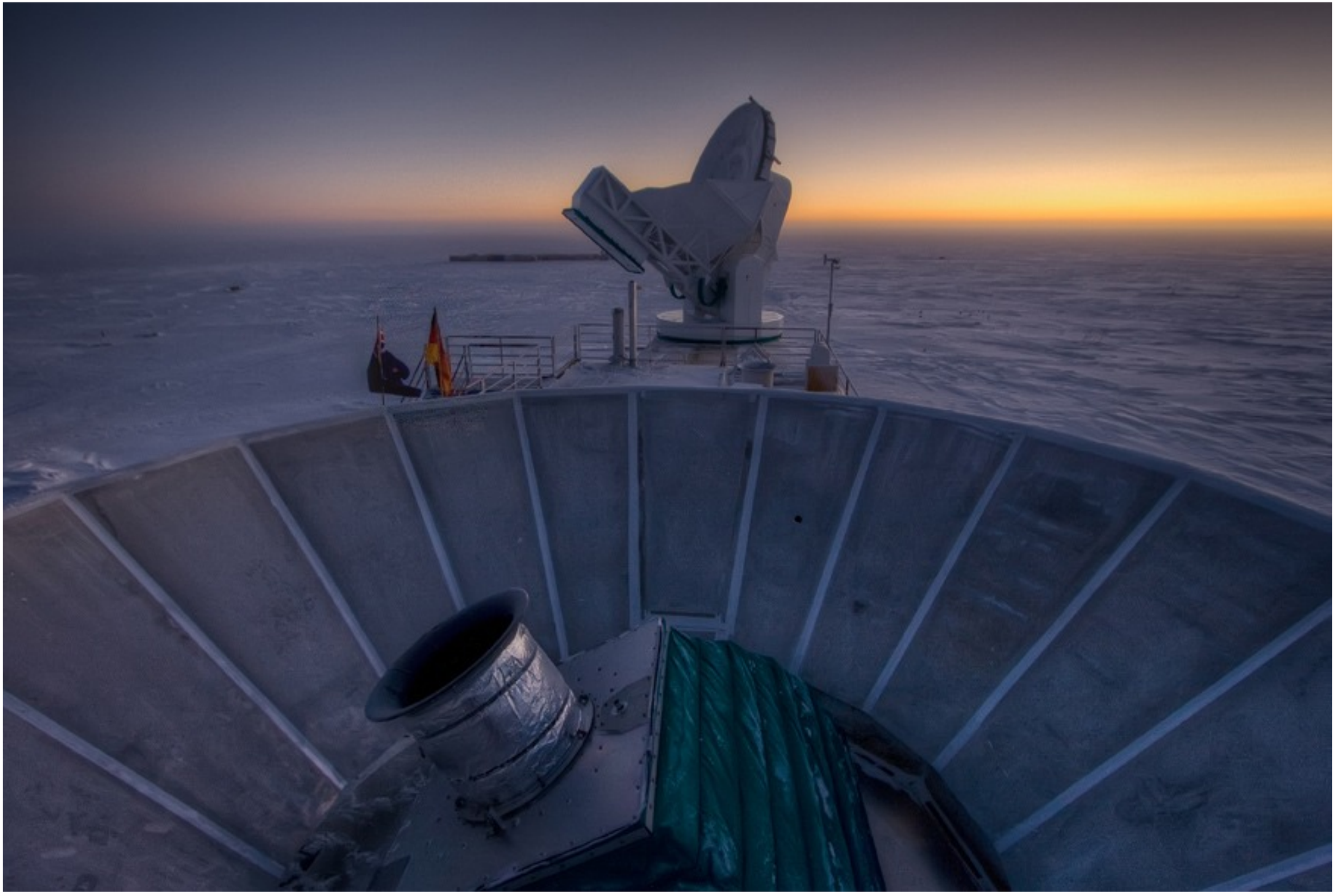

# South Pole CMB telescopes


NSF's South Pole Station:
A popular place with CMB Experimentalists!

Super dry atmosphere and 24h coverage of "Southern Hole".

Also power, LHe, $LN_2$, 200 GB/day, 3 square meals, Open Mic Night...

| BICEP1 (2006-2008) | BICEP2 (2010-2012) | Keck Array (2011-2016) | BICEP3 (2015-2016) |
|---|---|---|---|
| 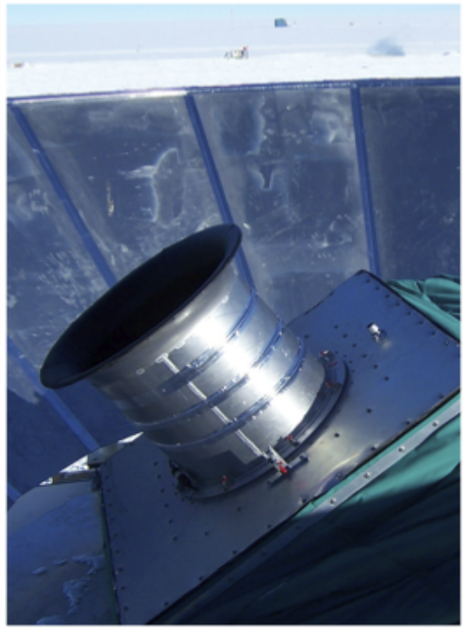 |   |   | 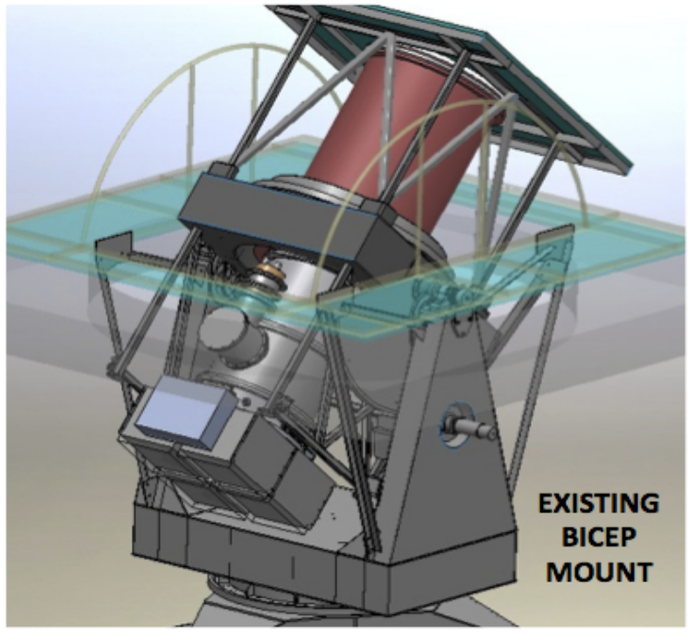  |
| 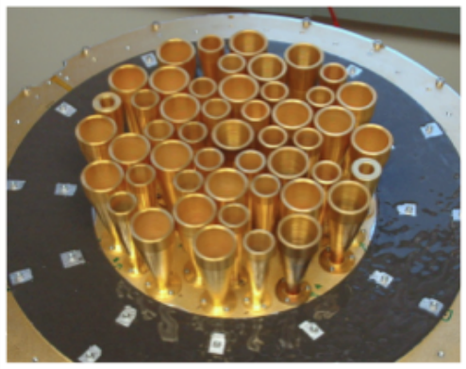 | 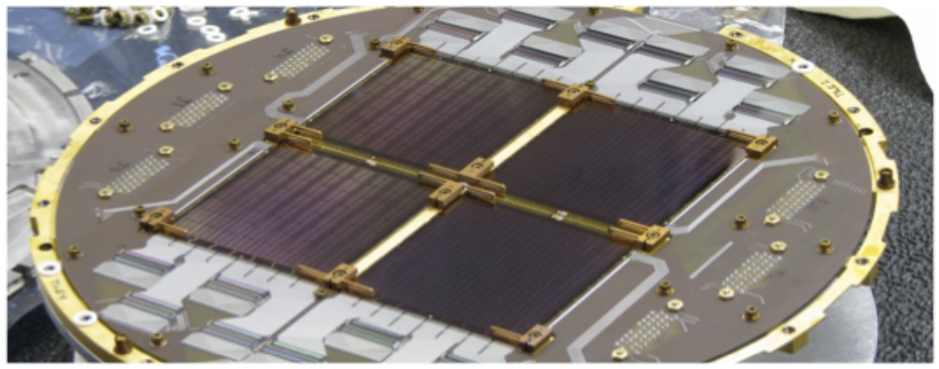 | | 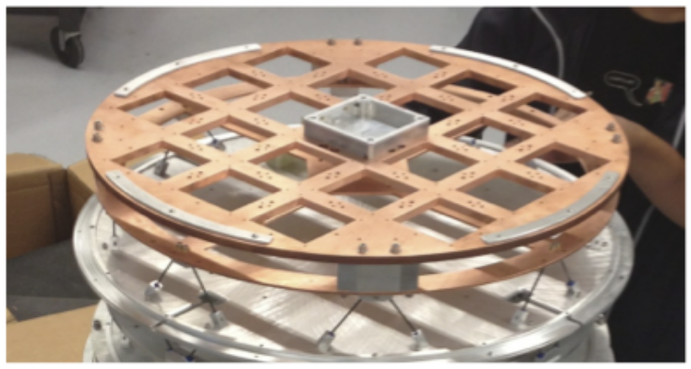 |
| 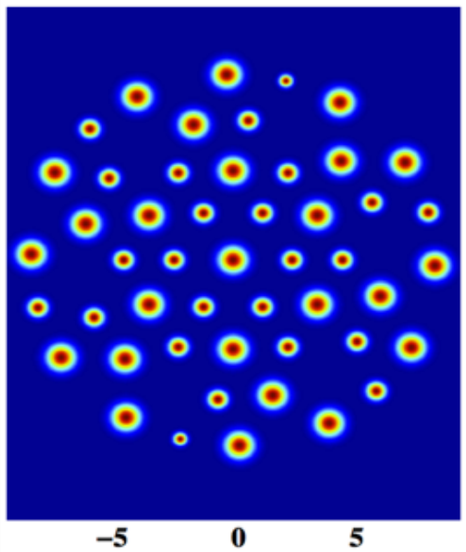  | 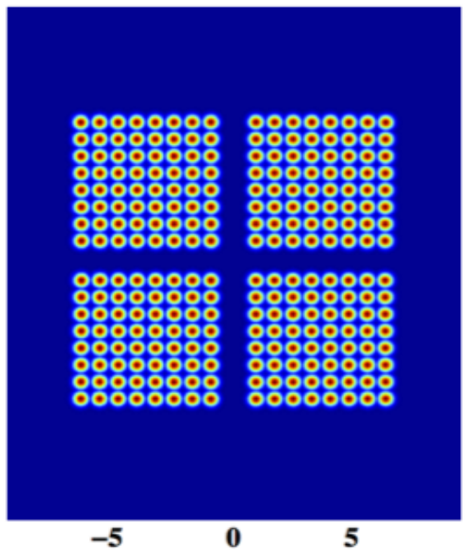  | 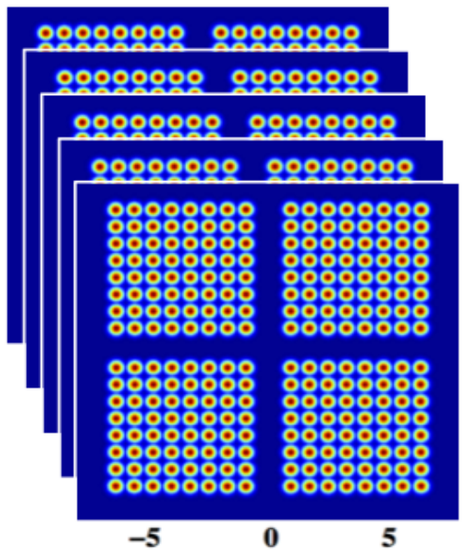  | 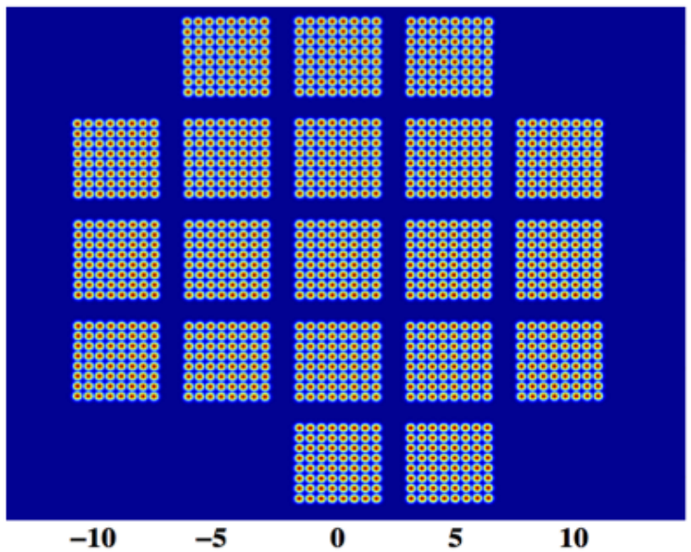  |
| 98 NTDs (95/150 GHz) | 512 TESs (150 GHz) | 2560 TESs (150 GHz) | 2560 TESs (95 GHz) |
| 0.93°/0.60° FWHM | 0.52° FWHM | | 0.37° FWHM |
| 18° FOV | 17° FOV | | 26° FOV |
| 44 $m^2$ $deg^2$ AΩ | 44 $m^2$ $deg^2$ AΩ | 222 $m^2$ $deg^2$ AΩ | 502 $m^2$ $deg^2$ AΩ optical throughput |

# BICEP2 Observational Strategy

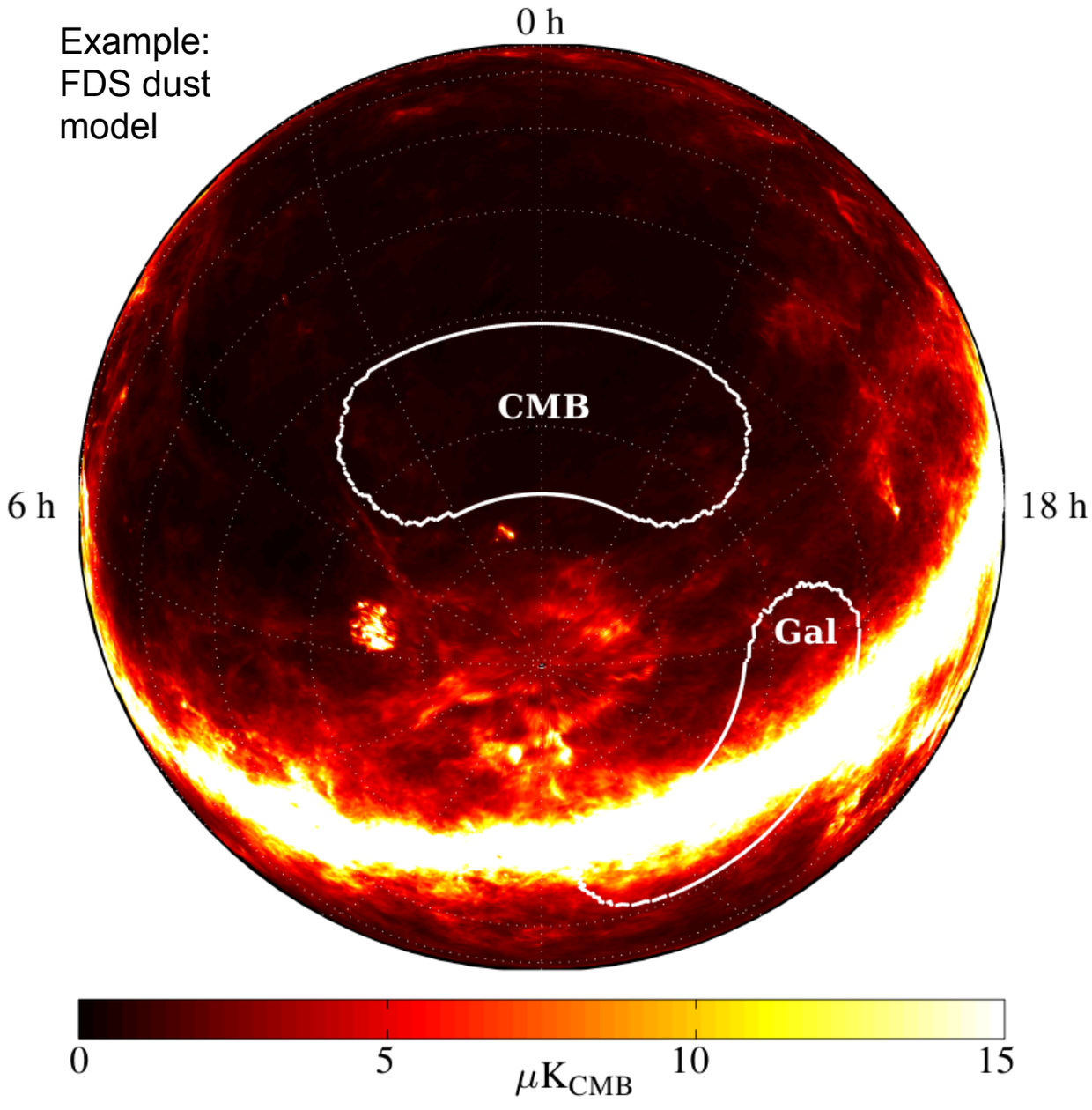


Target the “Southern Hole” - a region of the sky exceptionally free of dust and synchrotron foregrounds.

Detectors tuned to 150 GHz, near the peak of the CMB’s 2.7 K blackbody spectrum.

At 150 GHz the combined dust and synchrotron spectrum is predicted to be at a minimum in the Southern Hole.

Clem Pryke for The Bicep2 Collaboration

# Planck's Polarization Fraction

Polarization Fraction

Apparent polarization fraction (p) at 353 GHz, 1° resolution

Not CIB subtracted

$$p = \frac{\sqrt{Q^2 + U^2}}{I}$$

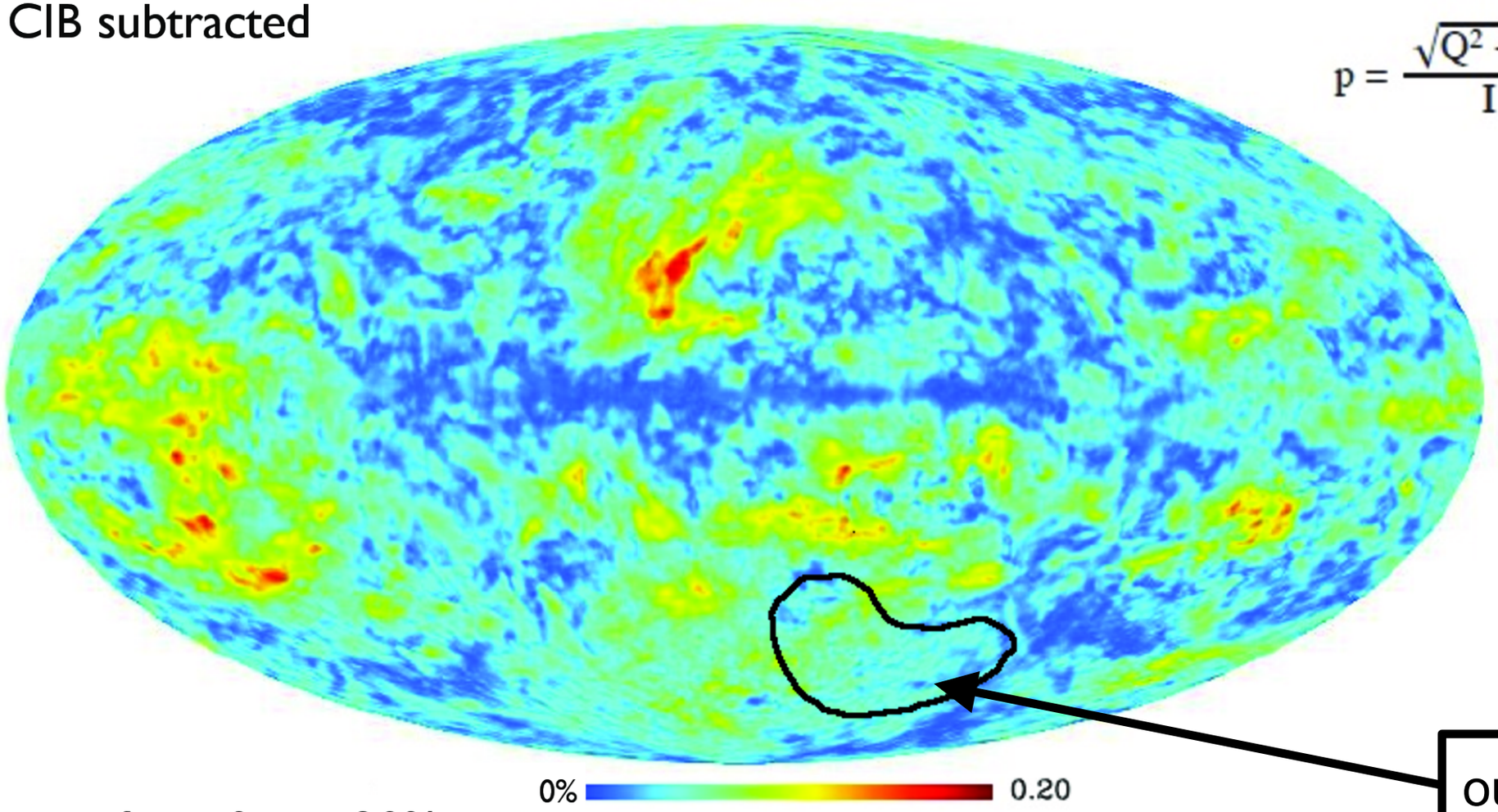


our field

p ranges from 0 to ~20%

Low p values in inner MW plane. Consistent with unpolarized CIB

Large p values in outer plane and intermediate latitudes

*Bernard J.Ph., ESLAB 2013* 6

mercredi 3 avril 13

http://www.rssd.esa.int/SA/PLANCK/docs/eslab47/Session07_Galactic_Science/

Clem Pryke for The Bicep2 Collaboration

# Detection of polarization

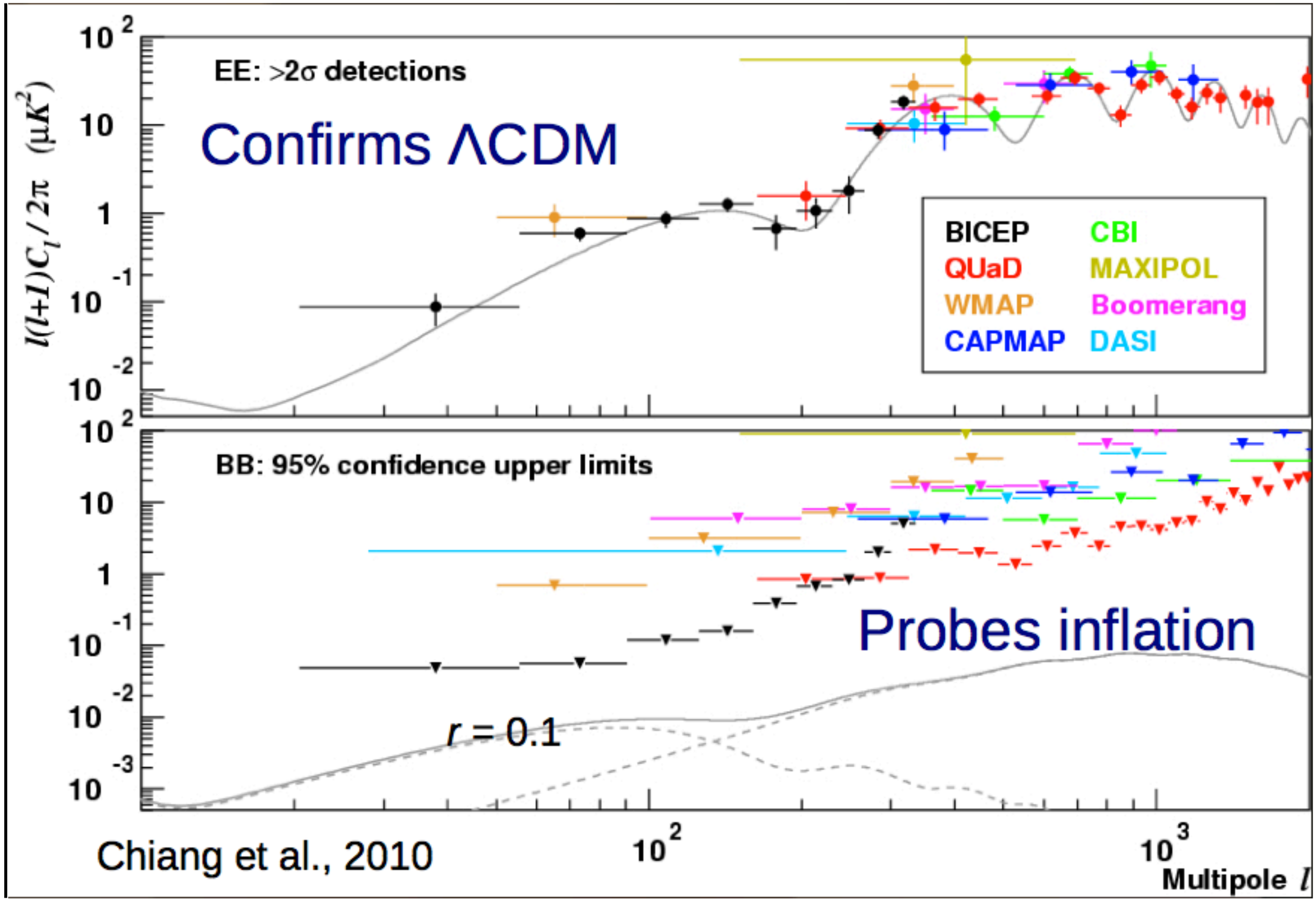

# BICEP2 Collaborating Institutions

- Caltech
- JPL
- UC San Diego
- Harvard
- NIST Boulder
- Stanford
- University of British Columbia
- University of Chicago
- University of Minnesota
- University of Toronto
- University of Wales Cardiff

**John M. Kovac**

Faculty of Havard U.
PI of BICEP

First discovery of the CMB polarisation by DASI,
It was PhD thesis of Kovac.

Density (scalar, inflaton) perturbations produce only E-mode polarization, whereas gravitational wave (tensor) perturbations produce B-mode polarization as well as E-modes.

with other various backgrounds, such as B-mode from lensing, dust, synchrotron, foreground sources etc.

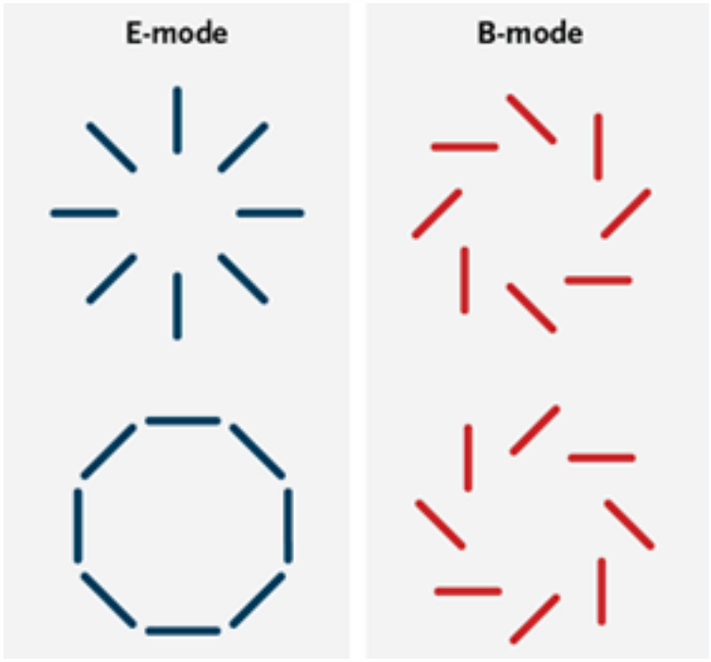

# Polarized foregrounds

(CMB Task Force Report)

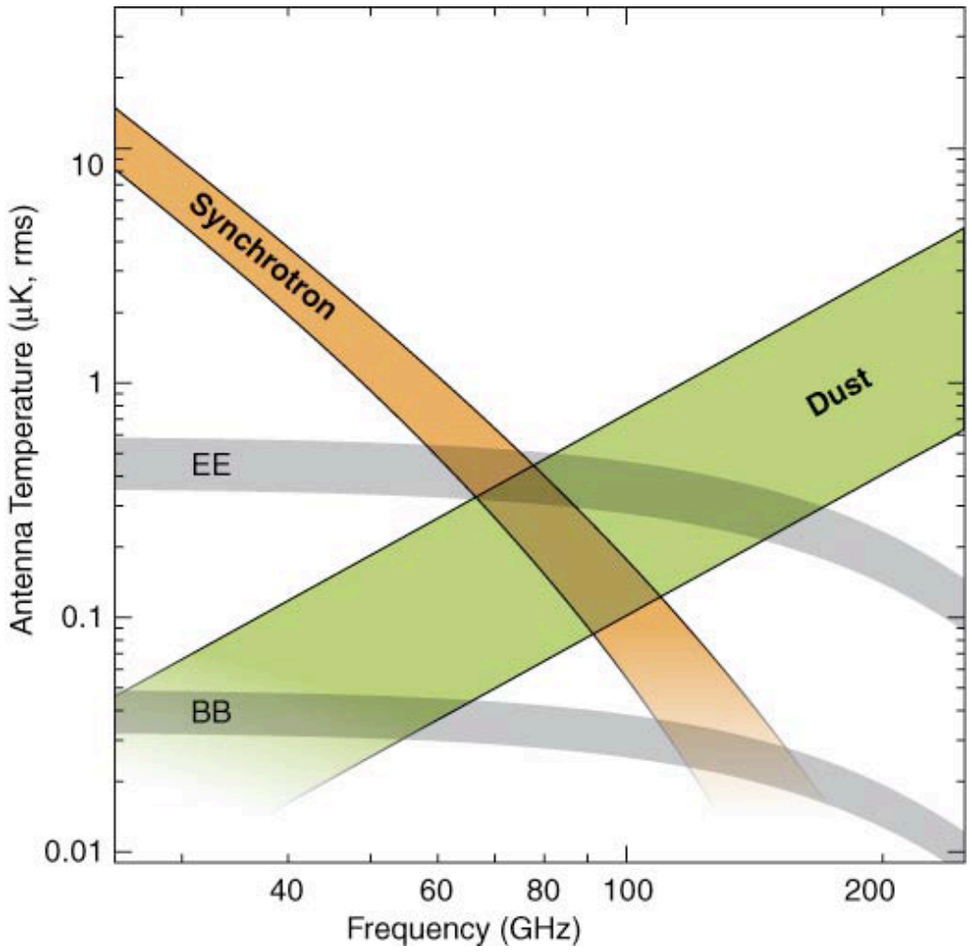


RMS fluctuations in the polarized CMB and foreground signals as function of frequency

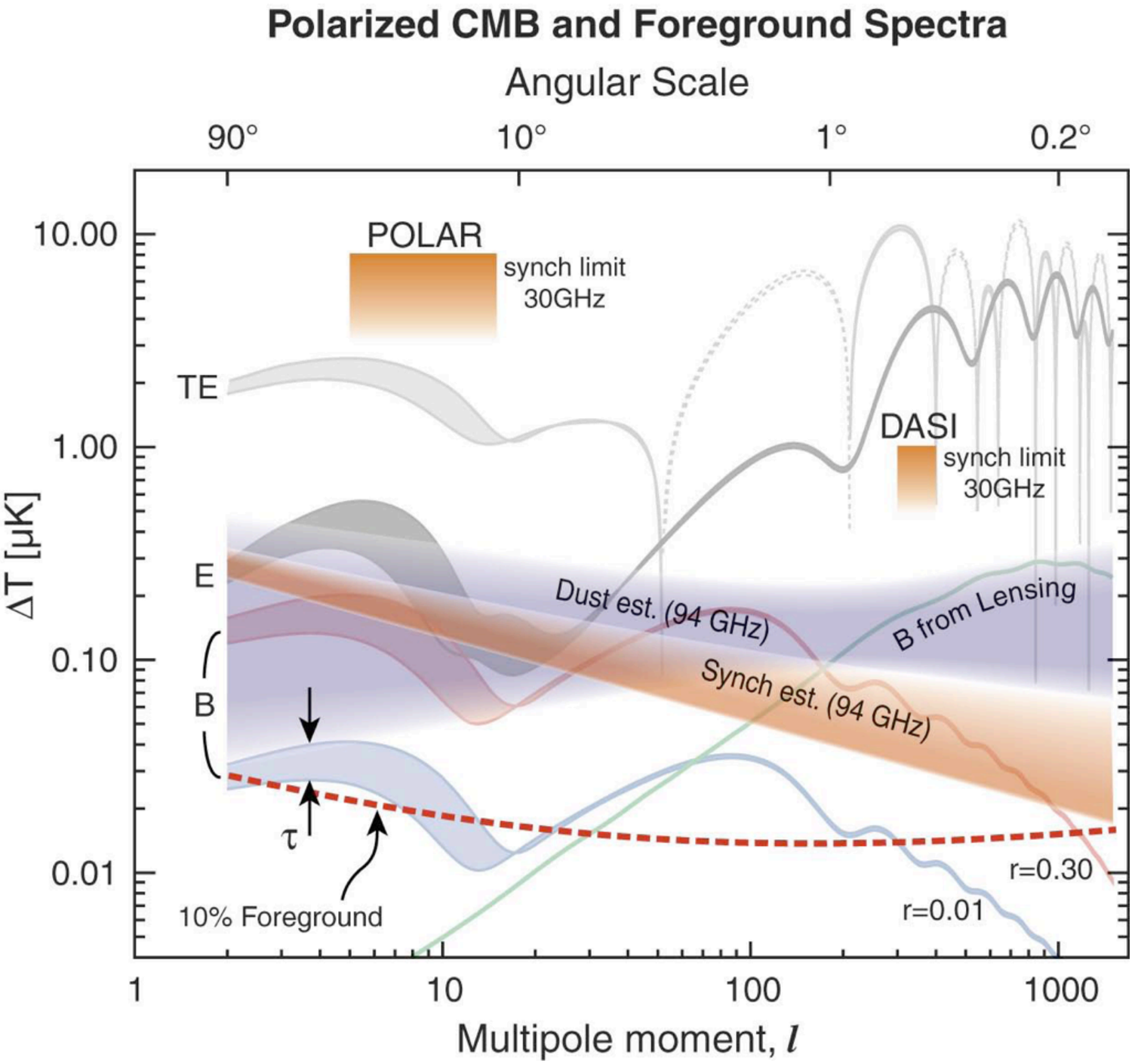

# Polarized Dust Foreground Projections

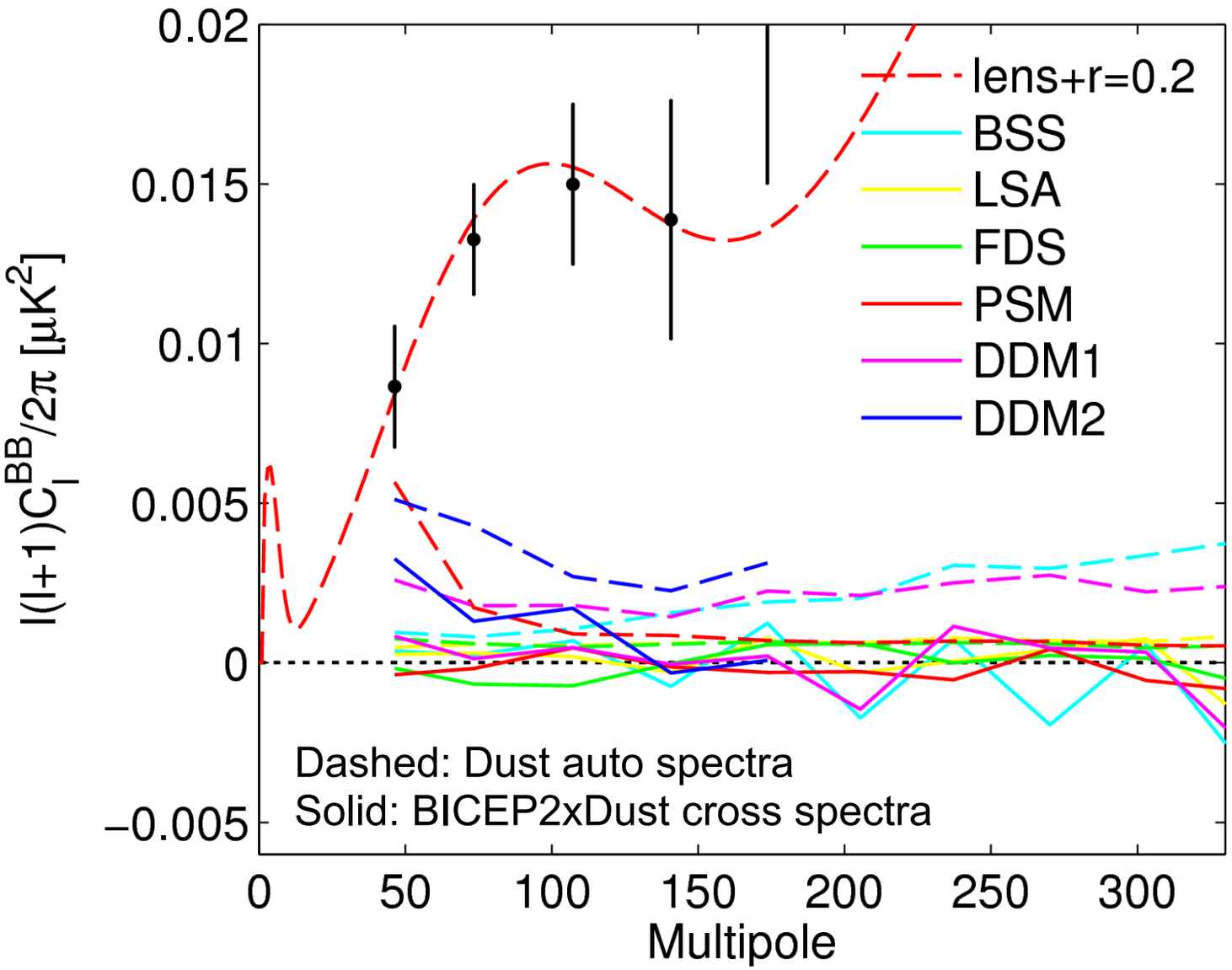


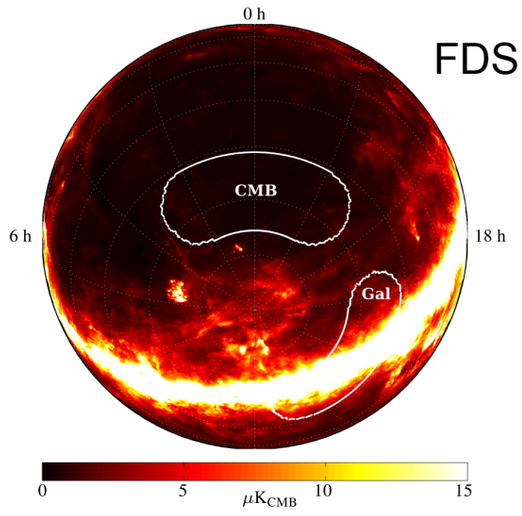


FDS Model

The BICEP2 region is chosen to have extremely low foreground emission.

Use various models of polarized dust emission to estimate foregrounds.

**All dust auto spectra well below observed signal level.**

Cross spectra consistent with zero.

Clem Pryke for The Bicep2 Collaboration

# BICEP2 B-mode Power Spectrum

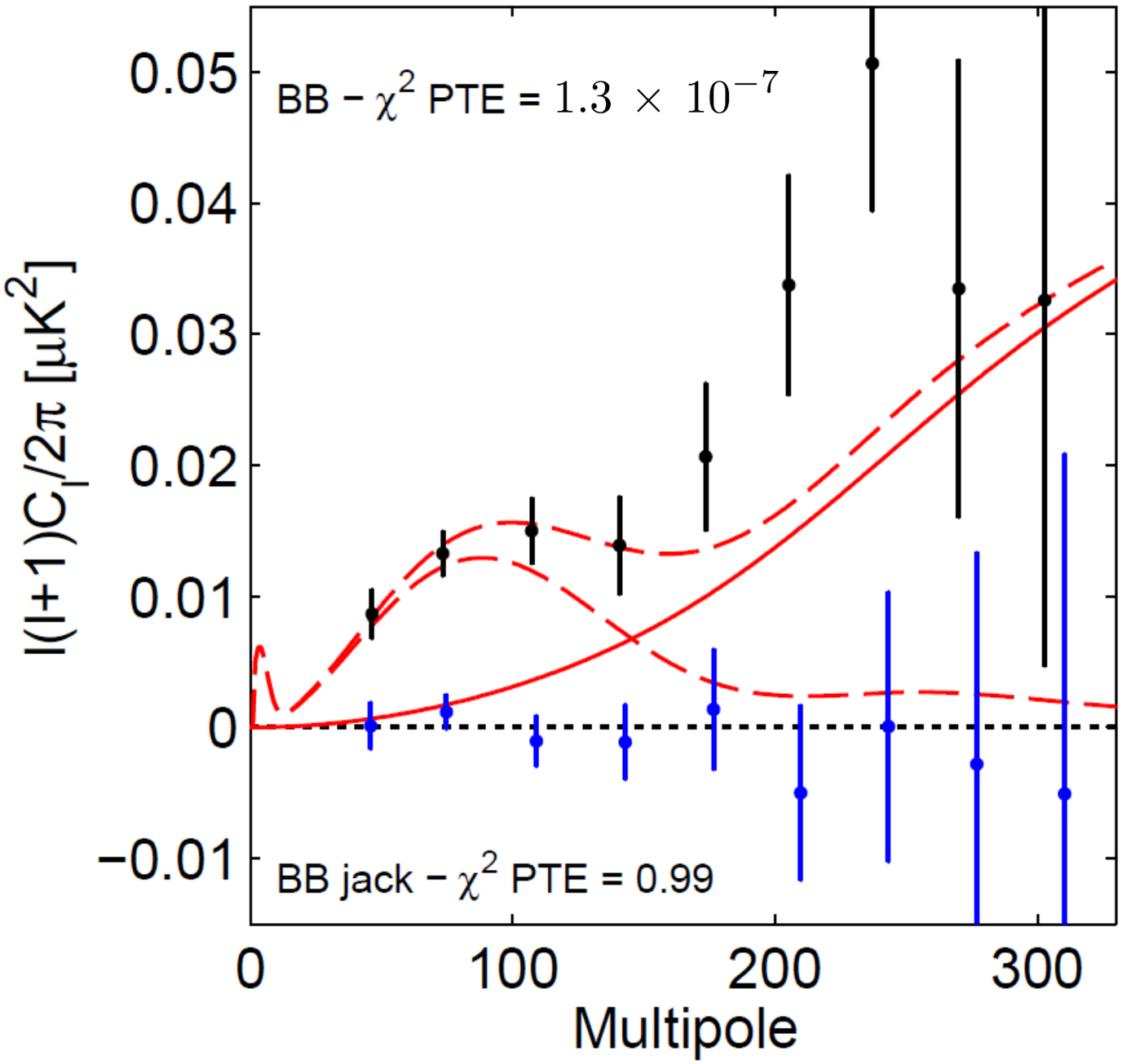


B-mode power spectrum
temporal split jackknife
lensed-ΛCDM
r=0.2

B-mode power spectrum estimated from Q&U maps, including map based "purification" to avoid E→B mixing

Consistent with lensing expectation at higher l. (yes – a few points are high but not excessively…)

At low l excess over lensed-ΛCDM with high signal-to-noise.

For the hypothesis that the measured band powers come from lensed-ΛCDM we find:

| | |
|---|---|
| $\chi^2$ PTE | $1.3 \times 10^{-7}$ |
| significance | $5.3\,\sigma$ |

Clem Pryke for The Bicep2 Collaboration

# BICEP2 B-mode Map vs. Simulation

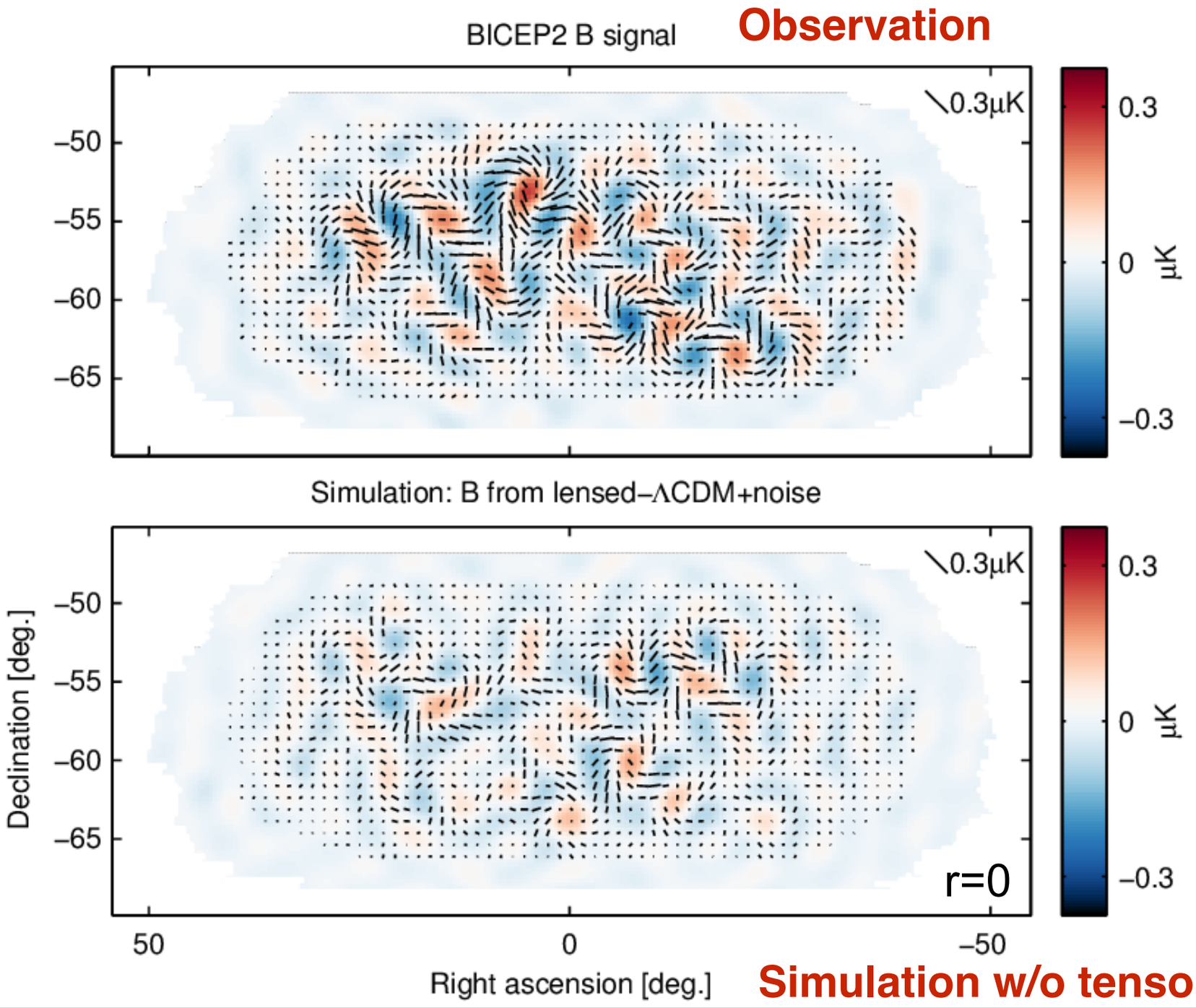


Analysis “calibrated” using lensed-ΛCDM+noise simulations.

The simulations repeat the full observation at the timestream level - including all filtering operations.

We perform various filtering operations: Use the sims to correct for these

Also use the sims to derive the final uncertainties (error bars)

Clem Pryke for The Bicep2 Collaboration

# Constraint on Tensor-to-scalar Ratio r

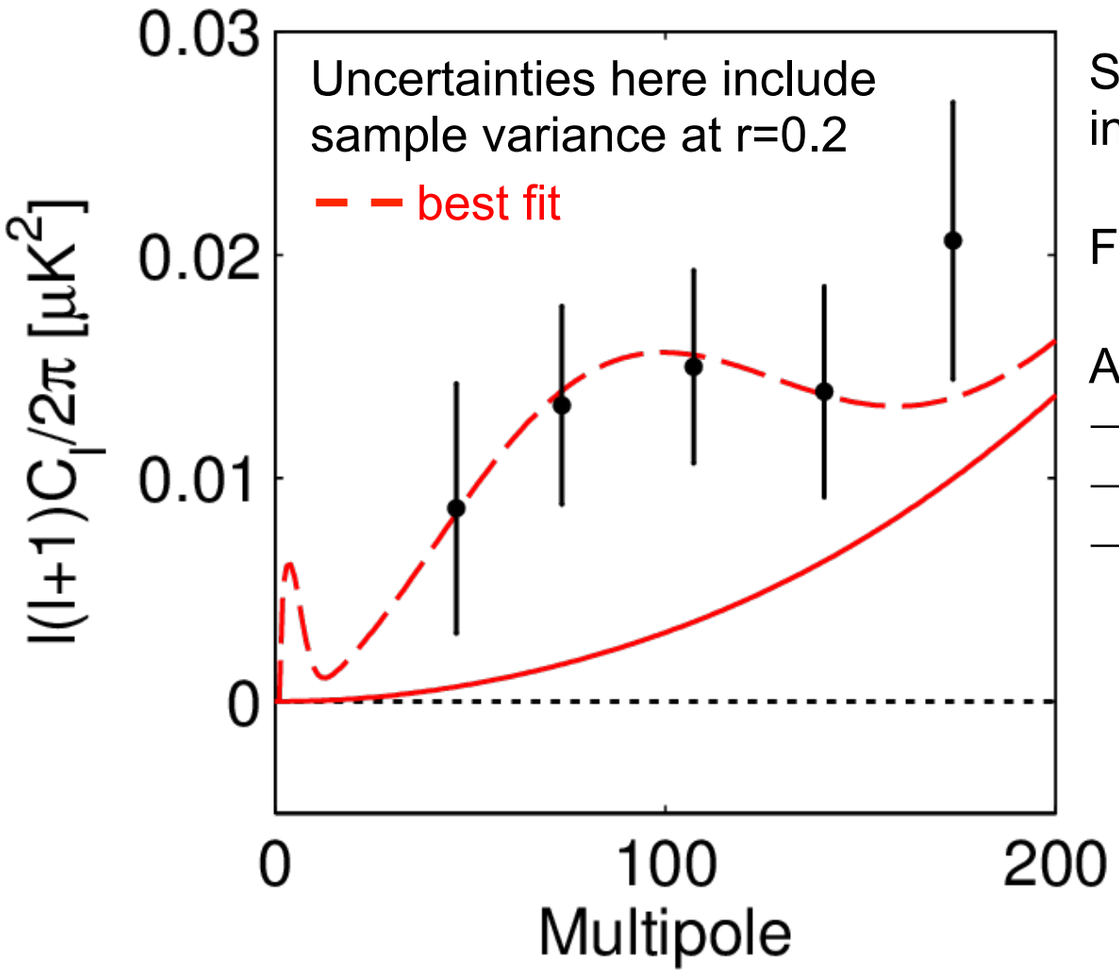


Substantial excess power in the region where the inflationary gravitational wave signal is expected to peak

Find the most likely value of the tensor-to-scalar ratio r

Apply "direct likelihood" method, uses:

→ lensed-ΛCDM + noise simulations

→ weighted version of the 5 bandpowers

→ B-mode sims scaled to various levels of r ($n_T$=0)

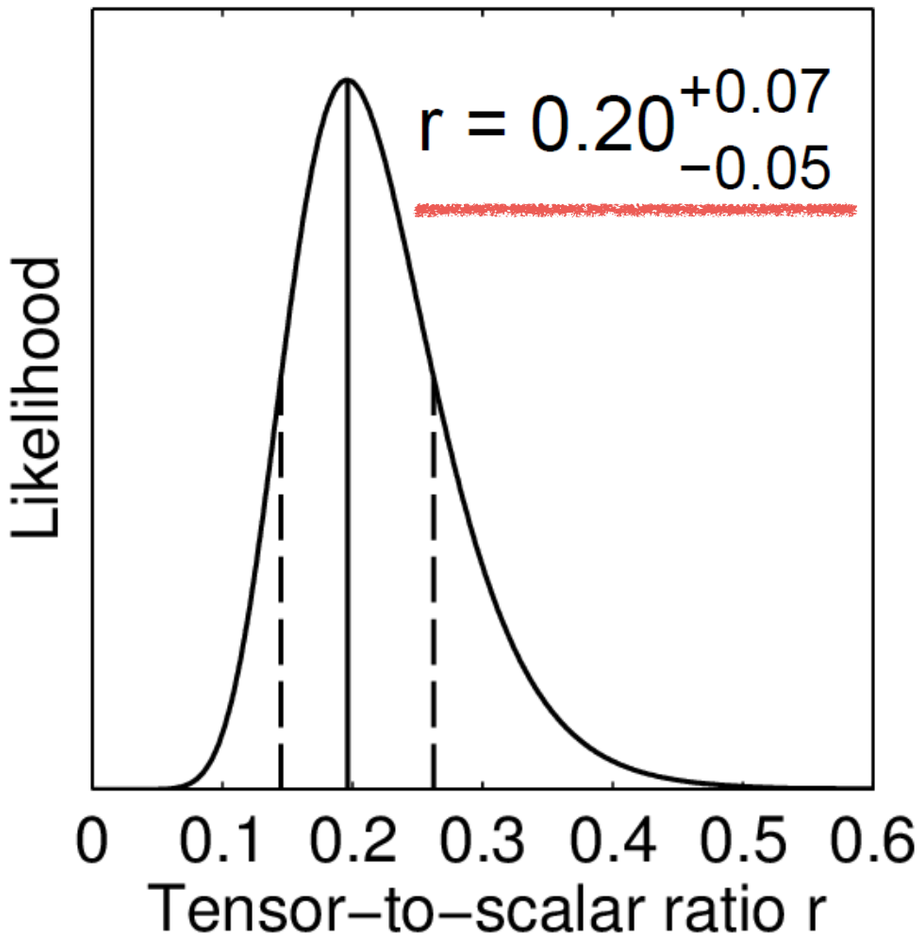


Within this simplistic model we find:

r = 0.2 with uncertainties dominated by sample variance

PTE of fit to data: 0.9
→ model is perfectly acceptable fit to the data

r = 0 ruled out at 7.0σ

Clem Pryke for The Bicep2 Collaboration

# Conclusions

BICEP2 and upper limits from other experiments:

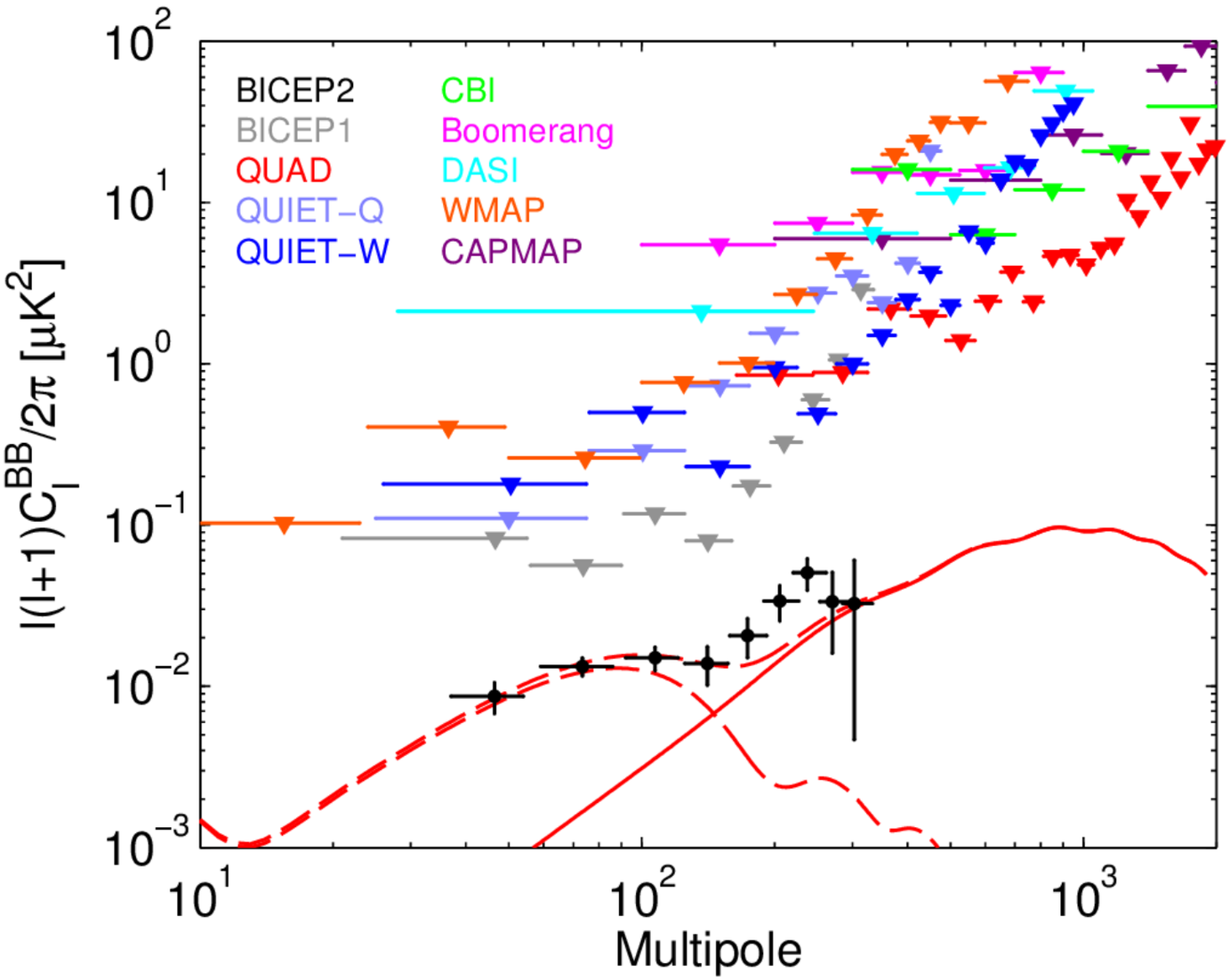


**http://www.bicepkeck.org**

Most sensitive polarization maps ever made

Power spectra perfectly consistent with lensed-ΛCDM except:
5.2σ excess in the B-mode spectrum at low multipoles!

Extensive studies and jackknife test strongly argue against systematics as the origin

Foregrounds do not appear to be a large fraction of the signal:
→ foreground projections
→ lack of cross correlations
→ CMB-like spectral index
→ shape of the B-mode spectrum

Constraint on tensor-to-scalar ratio r in simple inflationary gravitational wave model:

$$r = 0.20^{+0.07}_{-0.05}$$

r = 0 is ruled out at 7.0σ.

Clem Pryke for The Bicep2 Collaboration

# Compatibility with Indirect Limits on r

## BICEP2

Constraint on r *with running allowed*:

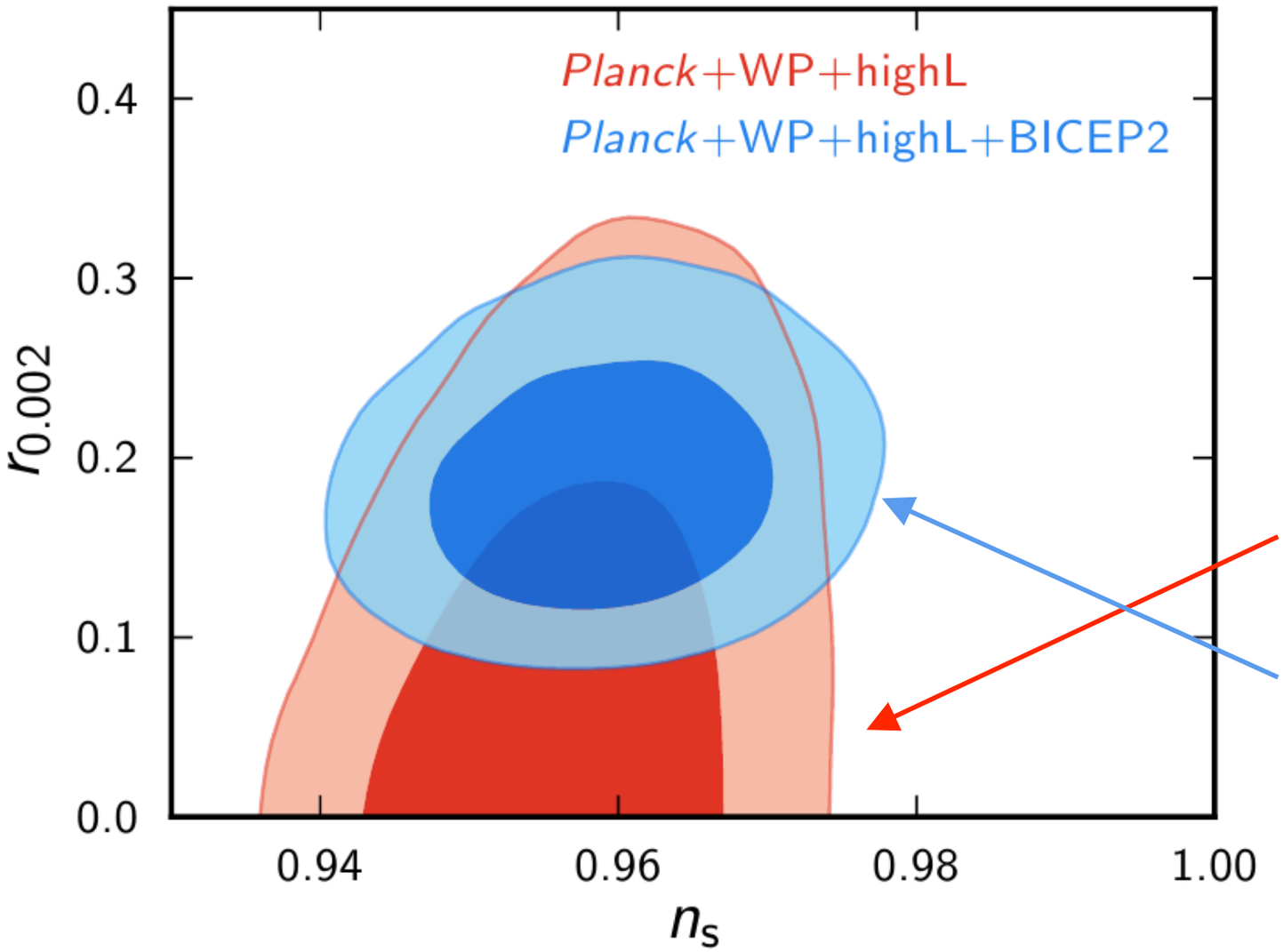


Indirect limit on r from combination of temperature data over a wide range of angular scales:

SPT+WMAP+BAO+$H_0$ : r < 0.11

Planck+SPT+ACT+$WMAP_{pol}$ : r < 0.11

This apparent tension can be relieved with various extensions to lensed ΛCDM.
**Example:** running of the spectral index

Planck likelihood chains for lensed ΛCDM + *tensors* + *running*

Same chains, importance sampled with the BICEP2 r likelihood

Other possibilities within ΛCDM?...

Clem Pryke for The Bicep2 Collaboration

# Planck & BICEP
# : Dust Contamination

- Planck (May. 06. 14) :
  @ 353 GHz, whole sky

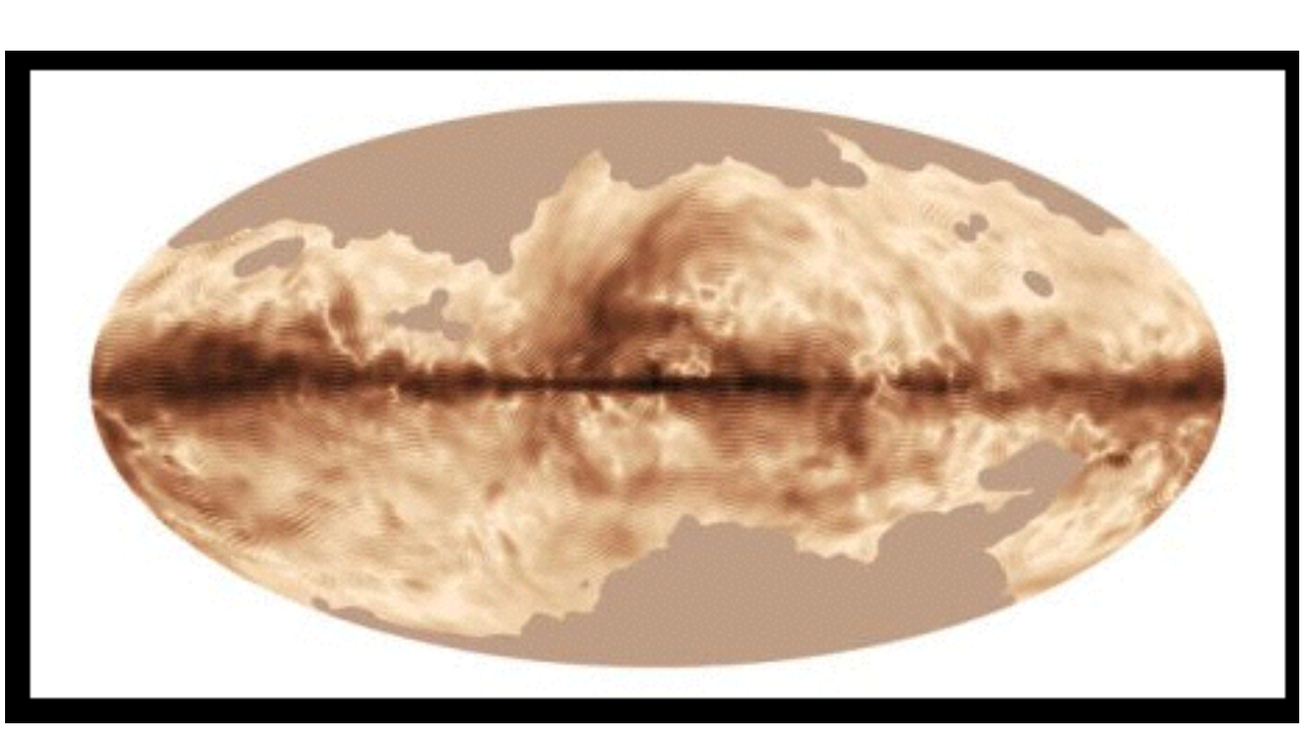

BICEP2 (Mar.17.14) :
@150 GHz, Part of sky

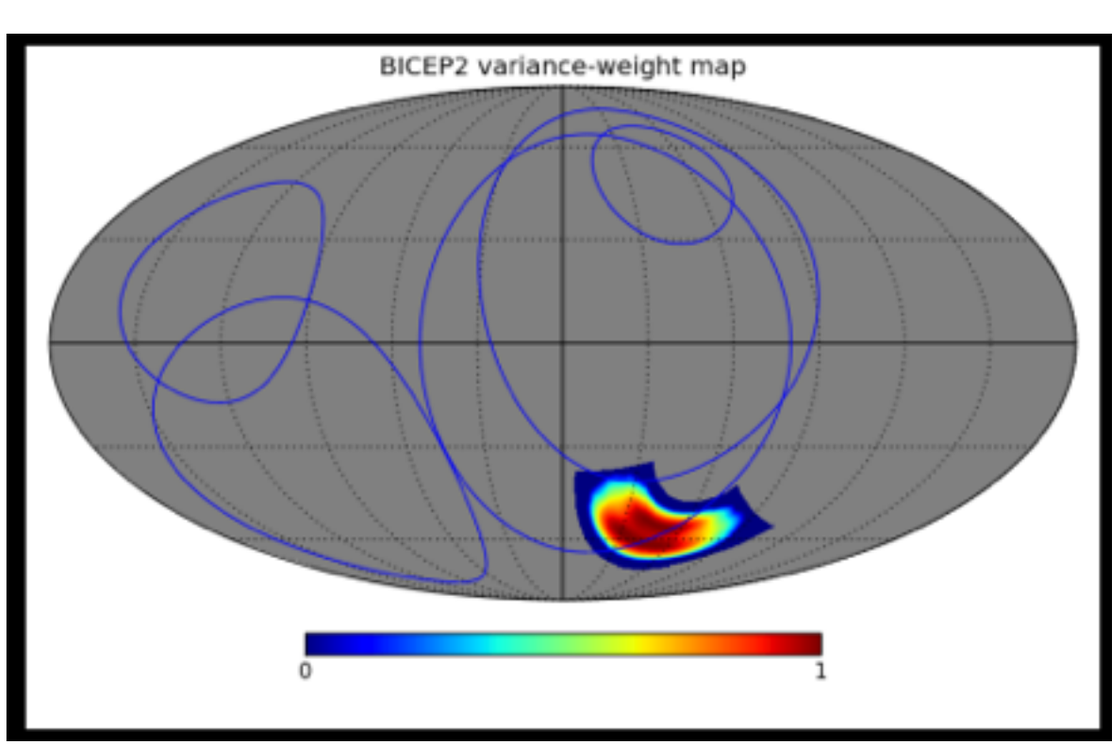

# Next .....

## Keck Array

The scientific objective is the same as BICEP2 – to attempt to measure B-mode polarization of the cosmic microwave background (CMB)

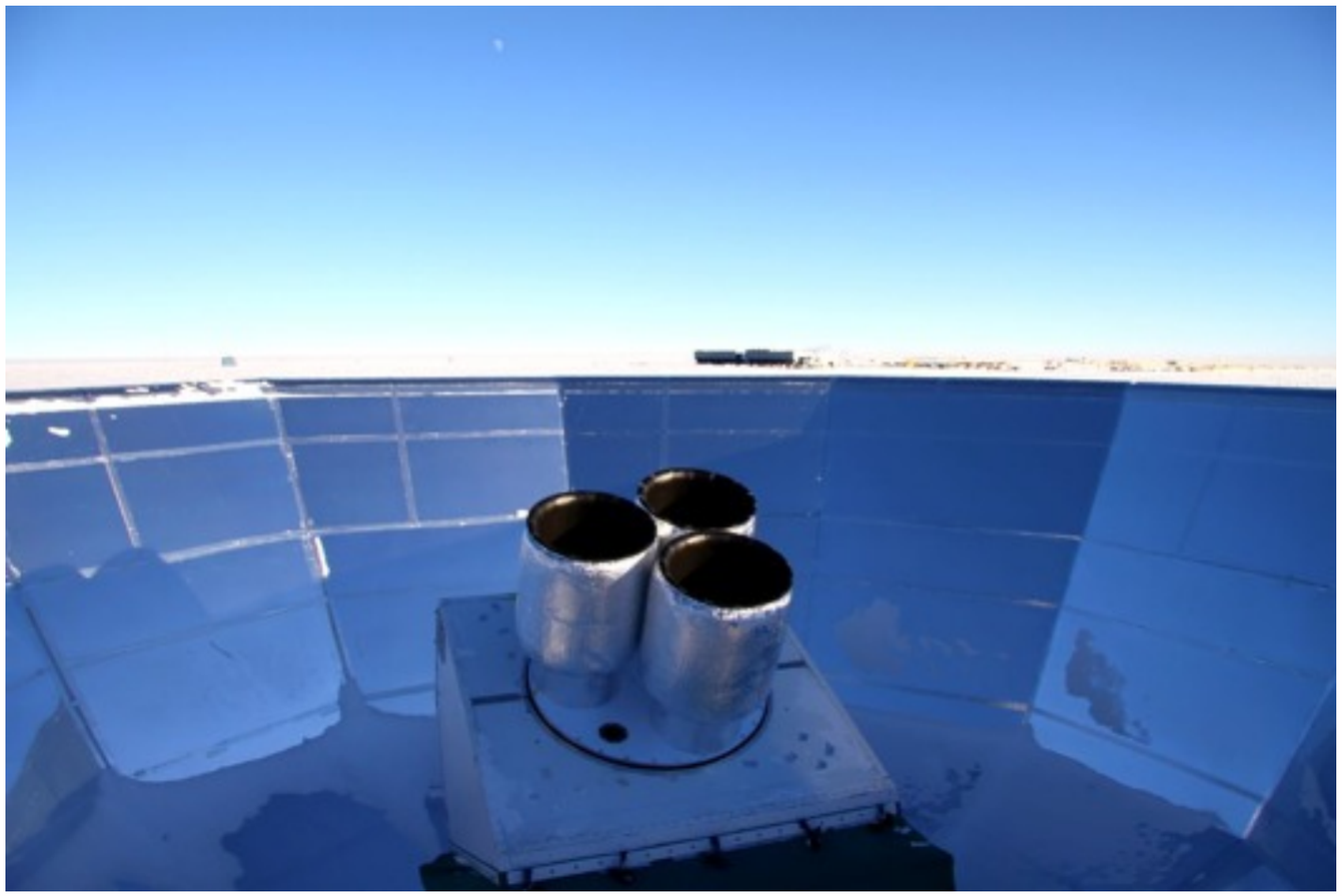

**Exterior view of Keck Array in its three-receiver configuration.**

## BICEP3

# Next ....

Planck

CMBpol

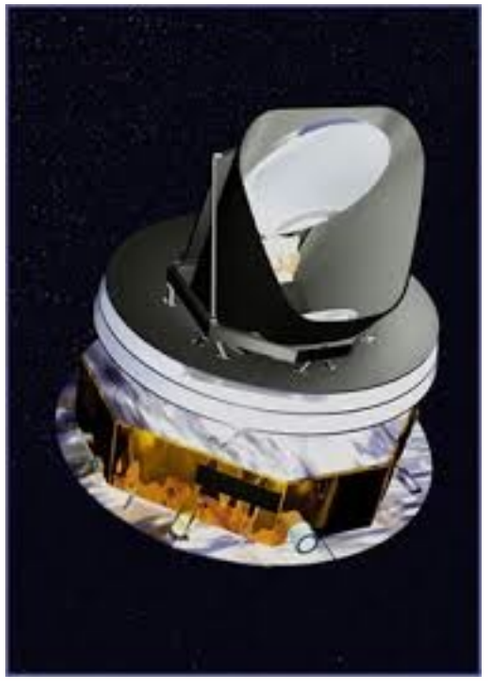

## Atacama Cosmology Telescope

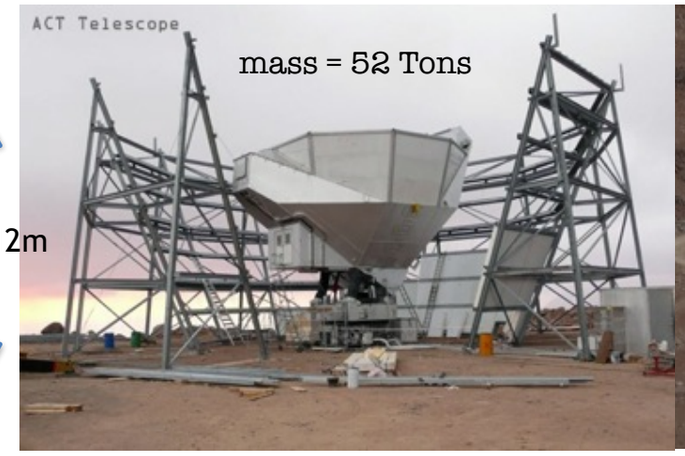



- Location: Atacama desert, Chile 17,030 ft (5190m)
  - low atmospheric attenuation and variability
- Finished construction in 2007
- Observed with temperature sensitive receiver from 2008 through 2010
- Observed 2013 season with ACTPol: upgraded receiver with polarization sensitivity.

## The South Pole Telescope (SPT)

- 10-meter sub-mm quality wavelength telescope

**2007: SPT-SZ**
960 detectors
100,150,220 GHz

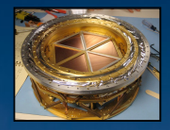

**2012: SPTpol**
1600 detectors
100,150 GHz
*+Polarization*

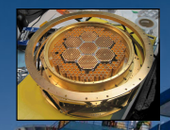

**2016: SPT-3G**
~15,200 detectors
100,150,220 GHz
*+Polarization*

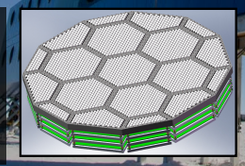

## The POLARBEAR experiment

- CMB polarization dedicated experiment in Atacama Desert
- Targeting both large and small scales
- 80% of the sky with *el* > 30 accessible
- First season: deep integration for sub-degree signal on 5x5 patches

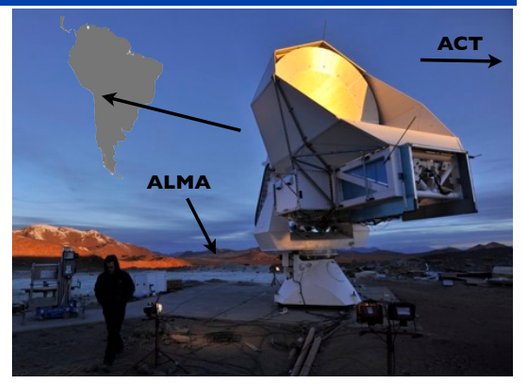


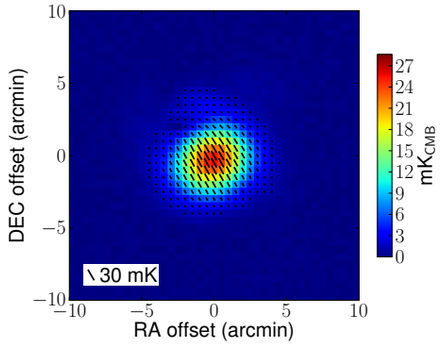


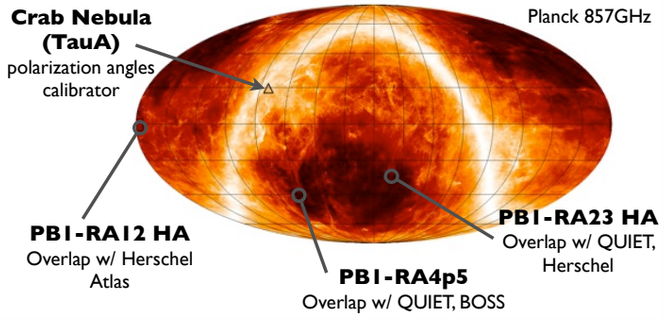

# Inflation

generates density (scalar) perturbation and tensor perturbation.

CMB Temp anisotropy  Gravitational Waves

$$V^{1/4} \simeq (r/.07)^{1/4} \times 1.8 \times 10^{16}\,\mathrm{GeV}$$ Height of potential

r=0.2 means V^1/4=2.34*10^16

$$H_I = 1.1 \times 10^{14}\ \mathrm{GeV}$$

## Lyth bound

$$\Delta\phi/m_{Pl} \simeq 4.6(r/6.9)^{1/2} = 0.46(r/.07)^{1/2}$$ field variation

If $r > 0.01$, the inflaton φ rolled by more than the Planck scale during inflation. That's not impossible — it's just provocative.

In Stringy inflation, large r is hard to get. Even axion monodromy inflation.

# Axion DM

[Baer, Choi, Kim, Roszkowski, 2014]

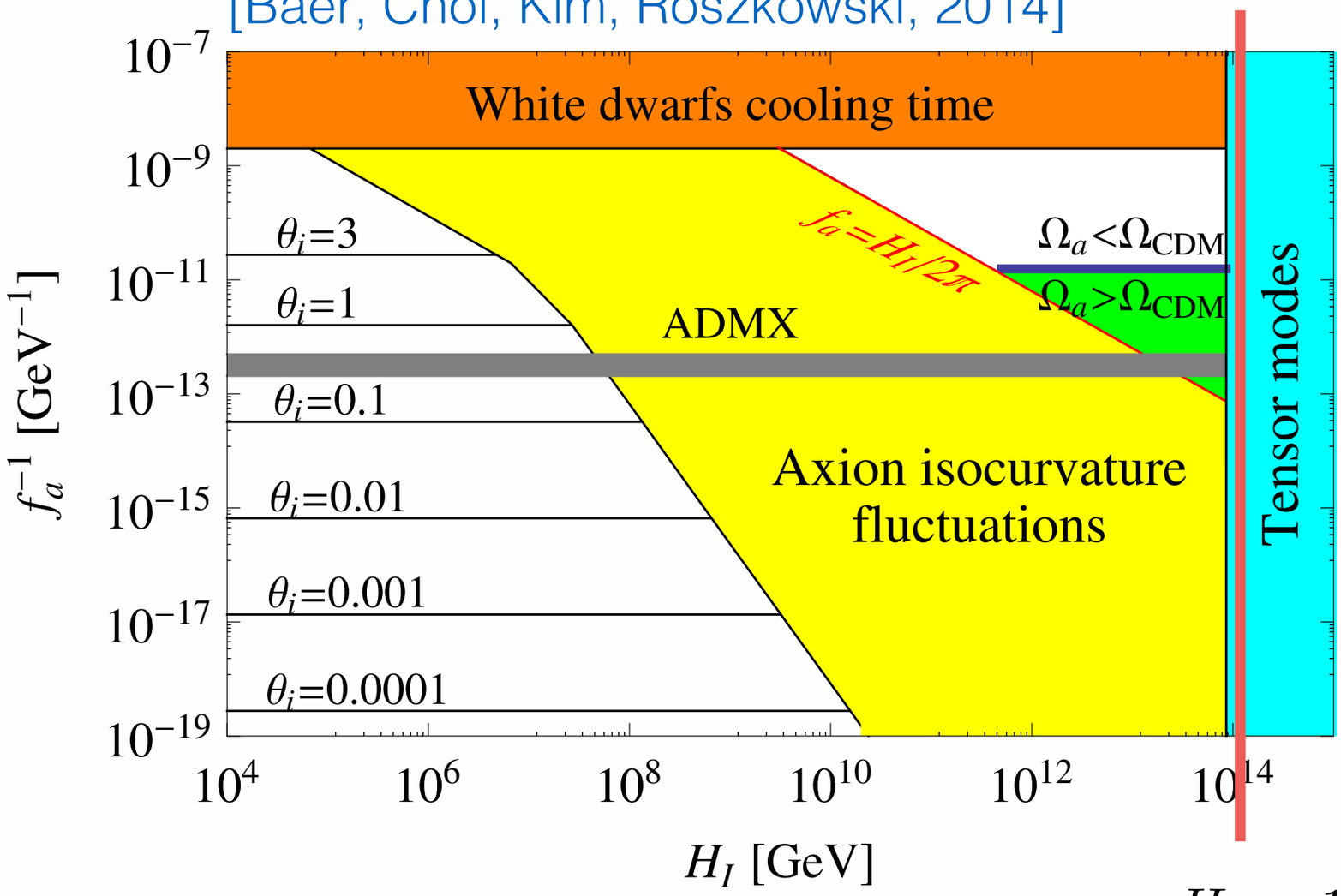


$$H_I = 1.1 \times 10^{14}\ \text{GeV}$$

[1403.3216, Marsh et.al.]

decay constant $f_a > H_I$ then isocurvature constraints effectively rule out the QCD axion as dark matter for $m_a \lesssim 0.06\mu$ eV, contributing only a fraction $\Omega_a/\Omega_d \lesssim 10^{-11}(f_a/10^{16}\ \text{GeV})^{5/6}$ (where $\Omega_i$

[1403.4186, Higaki, Jeong, Takahashi]

Heavy mass of axion during inflation

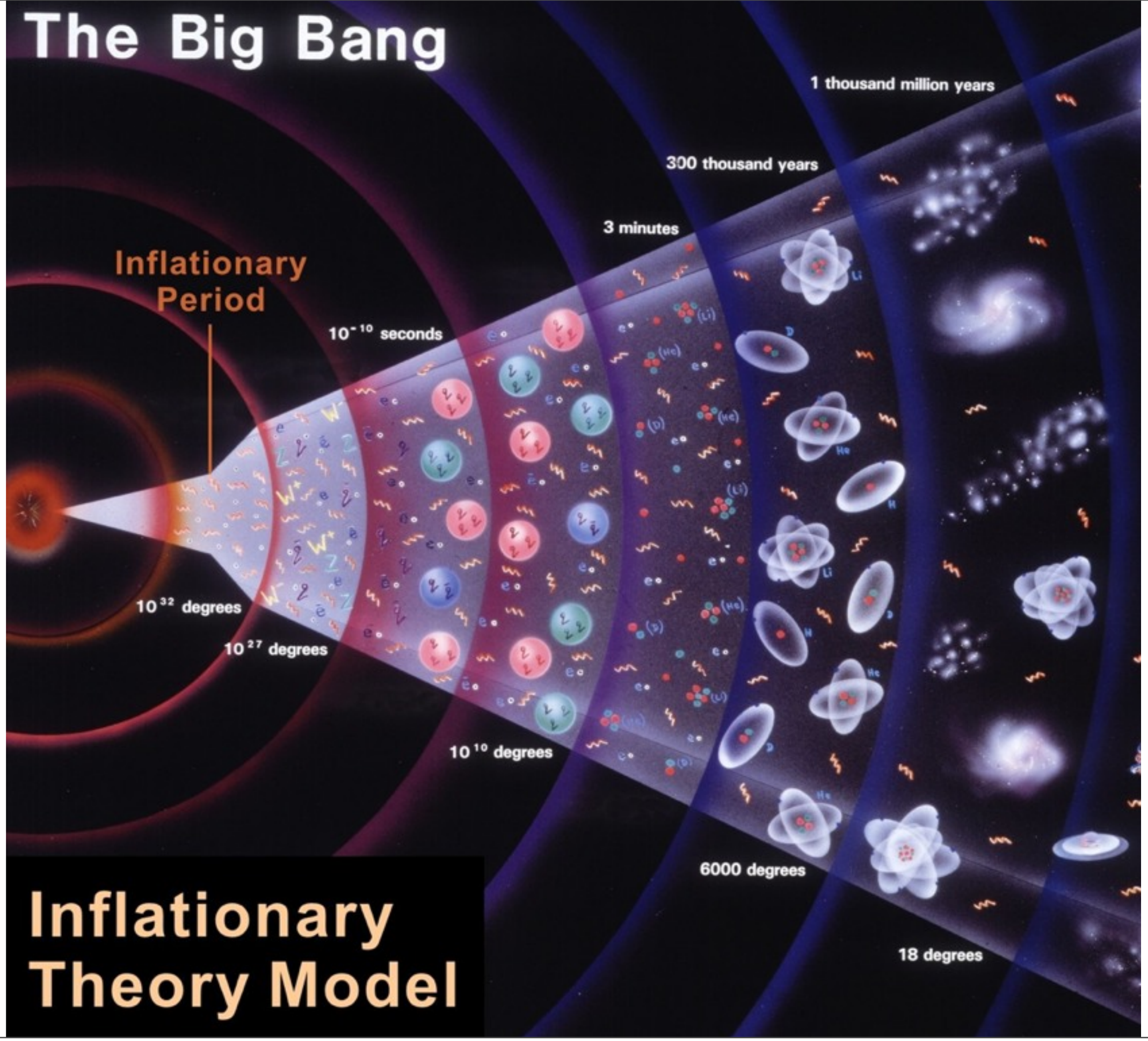
The Big Bang
1 thousand million years
300 thousand years
3 minutes
Inflationary Period
10⁻¹⁰ seconds
10³² degrees
10²⁷ degrees
10¹⁰ degrees
6000 degrees
18 degrees
Inflationary Theory Model

# 요 약

1. 우주는 팽창하고 있으며, 우주원리와 함께 아인슈타인 방정식에 의하여 잘 설명된다. - 빅뱅우주론: 우주팽창, 빅뱅핵합성, 우주배경복사

2. 인플레이션은 큰 규모에서 우주가 평탄하고 균일한 이유를 설명할 뿐만 아니라, 양자요동으로부터 물질밀도의 작은 섭동을 만들어낸다.

3. 작은 섭동은 우주배경복사에서의 온도차이만들고, 또한 우주거대구조를 만드는 씨앗의 역할을 한다.

4. 특히 우주배경복사의 정밀한 관측으로 우주의 물질밀도와 초기조건에 대한 여러가지 값들을 정확하게 정할 수 있었다. 또한 인플레이션에서 만들어진 중력파의 관측은 인플레이션 존재에 관하여 또 다른 검증이 될 것이다.

http://kcosmo.kasi.re.kr/TRP/TPLSSF.htm

# APCTP : Topical Research Program
# Theories and Practices in Large Scale Structure Formation

To subscribe the event, you can register at Mailing List

Year 2014

| Date | Place | |
|---|---|---|
| April 25 | KASI | Seminars |
| May 9 | APCTP Seoul branch | CMB polarization |
| July 4 | APCTP Seoul branch | Neutrinos in Cosmology |

NEXT lecture:

2014, September 26 (Friday) 14:00 - 18:00

about “statistical methods in cosmology” by Dr. Arman Shafieloo (APCTP)

# Thank You!